



Technische Universität München

Fakultät für Chemie

Werner Siemens-Lehrstuhl für Synthetische Biotechnologie

Enzymatic functionalization of bio based fatty acids and algae based triglycerides

Jan Lorenzen

Vollständiger Abdruck der von der Fakultät für Chemie der Technischen Universität München zur Erlangung des akademischen Grades eines

Doktors der Naturwissenschaften (Dr. rer. nat.)

genehmigten Dissertation.

Vorsitzender		Prof. Dr. Tom Nilges
Prüfer der Dissertation	1.	Prof. Dr. Thomas Brück
	2.	Prof. Dr. Wolfgang Eisenreich
	3.	Prof. Dr. Uwe Bornscheuer (schriftliche Beurteilung)
		Prof. Dr. Thomas Fässler (mündliche Prüfung)

Die Dissertation wurde am 26.09.2019 bei der Technischen Universität München eingereicht und durch die Fakultät für Chemie am 19.11.2019 angenommen.

I Abstracts

Chapter I

In the first chapter, the optimization of the SCCO₂ extraction of microalgae derived biomass in an industrially relevant pilot plant that adheres to ATEX standards was reported for the first time. The SCCO₂ extraction procedure of the lipid containing biomass of the microalgae strains *Scenedesmus obliquus* and *Scenedesmus obtusiusculus* was optimized with batch sizes of up to 1,3 kg of dried biomass. Under optimal conditions lipid recovery up to 92% w/w of the total lipids fraction could be achieved. Moreover, we addressed the purification of crude microalgae lipid extracts obtained by the SCCO₂ extraction procedure. We could identify high amounts of hydrophobic contaminants (e.g. chlorophylls or carotenoids) in the crude lipid extract, which we could effectively remove by the application of the standard mineral adsorber bentonite. The obtained, clean microalgae oil can directly be further processed to lubricants, cosmetics or nutraceutical products.

This is the first time that a combined SCCO₂ extraction and purification process for algae lipids has been developed that could be integrated into existing industrial processes.

Chapter II

In the second chapter, we could identify a new oleate hydratase (OH) from the ubiquitous, soil bacterium *Rhodococcus erythropolis*, by targeted genome mining. The enzyme, stated and registered as OhyRe (PDB: 5ODO), was biochemically and biophysically characterized and exhibited hydration activity in a wide pH and temperature range. Surprisingly, the solvation of its crystal structure and multi angle light scattering (MALS) experiments revealed a monomeric structure for the active OhyRe enzyme. Further, structural analysis of the enzyme allowed an indexing of OhyRe into the Hfam3 family of OHs. Moreover, we constructed two mutants of *OhyRe* (M77E and V393T) to further investigate the reaction mechanism of the new OH. The chosen positions, for the two conservative amino acid substitutions, were based on the studies of Engleder et al., who showed that these particular amino acids are highly conserved within the OH family of enzymes. Unexpectedly, the replacement of the native amino acids by the conserved ones resulted in a strong decrease in hydration activity for the *OhyRe* mutants of 80 to 90 %.

The monomeric structure of OhyRe offers plenty of options for a further engineering of the enzyme, especially in case of enzyme immobilization for an enhanced industrial application of this catalyst. The new OH, OhyRe, is to our knowledge the first monomeric OH and the first member of the HFam3 family of OHs published so far.

II Zusammenfassungen

Kapitel I

Das erste Kapitel befasst sich mit der Optimierung der SCCO₂-Extraktion von Mikroalgenbiomasse, die erstmals in einer industriellen Pilotanlage, welche den ATEX Standards entspricht, durchgeführt wurde. Der Extraktionsprozess mit SCCO₂ wurde für lipidhaltige Biomasse der Mikroalgenstämme *Scenedesmus obliquus* und *Scenedesmus obtusiusculus*, mit Biomassemengen von bis zu 1,3 kg (pro Extraktion), optimiert und es konnten, unter optimalen Bedingungen, Ausbeuten von bis zu 92% (w/w) der enthaltenen Lipidfraktion erreicht werden. Des Weiteren wurde eine Aufarbeitung der erhaltenen Rohextrakte durchgeführt, um die in großer Menge vorhandenen, hydrophoben Kontaminanten (z.B. Chlorophylle oder Carotinoide) aus dem Öl zu entfernen. Durch die Behandlung der Rohextrakte mit dem mineralischen Adsorber Bentonit konnte eine saubere Mikroalgen-Öl-Fraktion gewonnen werden, welche sich zur direkten Weiterverarbeitung zu verschiedenen Produkten (Schmierstoffe, Kosmetika, Nahrungsergänzungsmittel) eignet.

Hiermit wurden erstmalig ein SCCO₂-Extraktionsprozess und eine Produktaufreinigung kombiniert, welche direkt in bestehende, industrielle Prozesse integriert werden kann.

Kapitel II

Im zweiten Kapitel wurde, mittels gezielter Genom Durchmusterung, eine neue Ölsäure-Hydratase (OH) aus dem ubiquitären, im Sediment lebenden Bakterium *Rhodococcus erythropolis* identifiziert. Das Enzym, beschrieben und registriert als OhyRe, wurde biochemisch und biophysisch charakterisiert und zeichnete sich durch Hydratase-Aktivität in einem weiten pH- und Temperaturbereich aus. Überraschenderweise enthüllte die Lösung der Kristallstruktur der OH, sowie „multi angle light scattering (MALS)“ Experimente, dass es sich bei dem aktiven Enzym um ein Monomer handelt. Weitere strukturelle Untersuchungen des Enzyms erlaubten eine Einordnung der OH in die Hfam3 Familie von OH.

Zur weiteren Untersuchung des Reaktionsmechanismus wurden zusätzlich zwei Mutanten von OhyRe (M77E und V393T) hergestellt, wobei die ausgewählten Positionen für die Mutationen auf den Untersuchungen von Engleder et al. basieren. Die Arbeitsgruppe konnte zeigen, dass diese Positionen in anderen OHs in höchstem Maße konserviert sind und vermutlich eine Rolle in der katalytischen Reaktion spielen. Unerwarteter Weise sorgte die Substitution der beiden Aminosäuren für einen drastischen Aktivitätsverlust von 80 bis 90 % in den beiden Mutanten.

Die monomere Struktur von OhyRe eröffnet viele Möglichkeiten für ein weiteres „engineering“ des Enzyms, besonders im Hinblick auf mögliche Immobilisierungsstrategien für eine

industrielle Anwendung. Unseres Wissens nach ist OhyRe die bislang erste beschriebene, monomere OH und das erste publizierte Mitglied der Hfam3 Familie von OHs.

III Acknowledgements

Ich möchte mich zu aller erst bei Prof. Dr. Thomas Brück für die Möglichkeit zur Promotion in seiner Arbeitsgruppe bedanken. Obwohl ich länger für meine Promotion gebraucht habe, als es eigentlich geplant war, und die Kommunikation zwischen Kiel und München zeitweise etwas mühsam war, hattest Du immer Zeit, ein offenes Ohr, oder auch mal eine ganze Etage Deines Hauses für mich. Neben der fachlichen Betreuung und den stets interessanten und (beidseitig) ergebnisoffen geführten, wissenschaftlichen Diskussionen, hat auch die ein oder andere abendliche Diskussionsrunde zu einer sehr schönen Promotionszeit beigetragen. Vielen Dank für alles!

Vielen Dank an Prof. Dr. Tom Nilges, Prof. Dr. Wolfgang Eisenreich, Prof. Dr. Uwe Bornscheuer und Prof. Dr. Thomas Fässler für die Bewertung und Prüfung meiner Dissertation.

Ich möchte weiterhin unseren Postdocs Dr. Farah Qoura, Dr. Daniel Garbe, Dr. Norbert Mehlmer und Dr. Monika Fuchs für die hervorragende fachliche Unterstützung während der gesamten Zeit danken, wobei besonders die beiden letztgenannten großen Anteile am Gelingen meiner Experimente und dem Lösen von wissenschaftlichen Problemen hatten.

Außerdem möchte ich mich speziell bei Martina Haack für die große Unterstützung in der Analytik, bei Tom Schuffenhauer für stets tatkräftige Unterstützung im Labor, sowie bei Dr. Dominik Maslak für die Betreuung im Technikum und bei Gülnaz Celik für die Organisation im Sekretariat bedanken.

Größter Dank gebührt natürlich auch meinen restlichen Kollegen Matthias, Elias, Max, Wolle, Johannes, Veronika, Kati, Sam, Dania, Dirk, Felix, Markus, Mahmoud, Wojtech, Tobias, Pariya, Christian und Patrick, die ebenfalls immer mit Rat und Tat zur Seite standen und auch abseits der Wissenschaft, bei unzähligen „soft-skill-Seminaren“ und anderen Veranstaltungen, immer vollen Einsatz gezeigt haben. Mit euch hat die Zeit in München wirklich viel Spaß gemacht.

Ebenfalls möchte ich mich bei Kai Rubin für die Unterstützung und meine Freiräume während meiner Zeit bei der Rubin Yachttechnik GmbH bedanken.

Zu guter Letzt möchte ich mich noch bei meiner Familie, meinen Freunden und ganz besonders bei Sophie für den ständigen Rückhalt und die große Unterstützung (trotz der Distanz) bedanken.

IV Contents

I Abstracts	I
Chapter I.....	I
Chapter II.....	I
II Zusammenfassungen	II
Kapitel I.....	II
Kapitel II.....	II
III Acknowledgements	V
IV Contents	VI
V List of Abbreviations.....	VIII
1. Introduction	1
1.1 The Advanced Biomass Value (ABV) Project.....	1
1.2 Introduction Chapter I: Extraction of Microalgae Derived Lipids with Supercritical Carbon Dioxide in an Industrial Relevant Pilot Plant	3
1.2.1 Microalgae as a Source of High Value Compounds	4
1.2.2 General Lipid Extraction Methods	4
1.2.3 Supercritical Carbon Dioxide (SCCO ₂) for the Extraction of Nonpolar Compounds	5
1.2.4 Bentonite Based Cleaning Procedure for Microalgae Extracts	6
1.3 Introduction Chapter II: <i>Rhodococcus erythropolis</i> Oleate Hydratase: A New Member in the Oleate Hydratase Family Tree – Biochemical and Structural Studies.....	6
1.3.1 <i>Rhodococcus erythropolis</i>	7
1.3.2 Oleate Hydratases	8
1.3.3 Oleate Hydratase Reaction Mechanism	8
1.3.4 Identification of Potential Targets for Site Directed Mutagenesis.....	9
1.3.5 Hydroxy Fatty Acids in Industrial Applications	11
2. Methods	12
<i>Microalgae Strains & Cultivation</i>	12
<i>Microalgae Preparation</i>	12
<i>Conventional Solvent Extraction</i>	12
<i>Supercritical Carbon Dioxide (SCCO₂) Extraction</i>	13
<i>Lipid Analysis</i>	14
<i>Purification of Crude Microalgae Extracts</i>	17
<i>Bacterial Strains</i>	18
<i>Cloning for Characterization Experiments</i>	18

<i>Mutant Construction</i>	19
<i>Protein Expression and Protein Purification for Characterization Experiments</i>	19
<i>Enzyme Characterization</i>	20
3. Publications.....	21
3.1 Summaries of Included Publications	21
Extraction of microalgae derived lipids with supercritical carbon dioxide in an industrial relevant pilot plant.....	21
<i>Rhodococcus erythropolis</i> Oleate Hydratase: a New Member in the Oleate Hydratase Family Tree – Biochemical and Structural Studies	23
3.2 Full Length Publications	25
Extraction of microalgae derived lipids with supercritical carbon dioxide in an industrial relevant pilot plant	25
<i>Rhodococcus erythropolis</i> Oleate Hydratase: a New Member in the Oleate Hydratase Family Tree – Biochemical and Structural Studies.....	34
4. Discussion & Outlook	57
5. List of Publications	65
6. Reprint Permission	66
1. Extraction of microalgae derived lipids with supercritical carbon dioxide in an industrial relevant pilot plant.....	66
2. <i>Rhodococcus erythropolis</i> Oleate Hydratase: a New Member in the Oleate Hydratase Family Tree – Biochemical and Structural Studies	66
7. Figures & Tables	72
8. Literature	73

V List of Abbreviations

°C	degree Celsius
10-HSA	10-hydroxystearic acid
12-HSA	12-hydroxystearic acid
Å	Ångström
AA	amino acid
ABV	Advanced Biomass Value
Al	aluminum
AMP-CHT	chitosan-coated macro particles
approx.	approximately
atm	atmosphere
BSTFA	N,O-Bis(trimethylsilyl) trifluoroacetamide
CMP	carboxylated magnetic particles
CO ₂	carbon dioxide
d	day
dcw	dry cell weight
ddH ₂ O	double distilled water
E	Glutamic acid
<i>E. coli</i>	<i>Escherichia coli</i>
EtOAc	ethyl acetate
FA	fatty acid
FAD	flavin adenine dinucleotide
FFA	free fatty acid
GC	gas chromatography
ha	hectare
HCl	hydrochloride
His	histidine
IPTG	isopropyl β-D-1-thiogalactopyranoside
K	Kalvin
k _{cat}	turnover number
kg	kilo gram
K _M	Michaelis constant
LB	lysogeny broth

M	Methionine
mg	milligram
MIBK	methyl isobutyl ketone
min	minute
mM	mill molar
MPa	mega pascal
MS	mass spectroscopy
N	nitrogen
nmol	nano Mol
OA	oleic acid
OH	oleate hydrates
OhyA	oleate hydratase from <i>Elizabethkingia meningoseptica</i>
OhyRe	oleate hydratase from <i>Rhodococcus erythropolis</i>
P	phosphate
PUFA	polyunsaturated fatty acid
SCCO ₂	supercritical carbon dioxide
Si	silicon
t	metric ton
T	Threonine
Tris	Tris(hydroxymethyl)-aminomethan
V	Valine
w/v	weight per volume
w/w	weight per weight
wt%	weight percent
y	year

1. Introduction

1.1 The Advanced Biomass Value (ABV) Project

The Advanced Biomass Value (ABV) Project was a joint research project, funded by the German Federal Ministry of Education and Research (Project: 03SF0446C), of industrial and medium size business partners (EADS, NATECO2, Fuchs Schmierstoffe, BBSI) and academic partners (EMAU, TUM, BHL). The ABV project has been targeting the future supply of the aviation industry with biofuels and bio based lubricants from renewable feedstock. The project followed a new concept of using microalgae biomass, as a renewable “3rd generation” feedstock, by a mass-efficient conversion/usage and by avoiding any kind of waste streams.

Starting point of the project was a screening for halophile microalgae possessing special properties. In order to reach an efficient application of the selected microalgae strain in the downstream process chain of the ABV project, the strain should be growing fast, accumulate high amounts of lipids, exhibit a high amount of carbon and low amounts of amino acids, as well as ash in the residual biomass. The screening included a wide range of microalgae strains originating not only from different habitats around the world (e.g. Bahamas, Mexico, Kazakhstan) but also from local habitats like the Baltic Sea. After selecting the most promising candidate, a cultivation optimization has been performed. During this optimization stage, the microalgae biomass was further analyzed and its composition has been optimized for the following downstream processing.

The biomass, resulting from this optimized cultivation, was subsequently applied for a lipid extraction with supercritical carbon dioxide (SCCO₂). The extraction with supercritical carbon dioxide allowed an efficient and environmentally friendly separation of the microalgae lipid fraction from the residual biomass, without contaminating the resulting fractions. These extractions were carried out in an industrial relevant pilot plant with batch sizes of up to 1.3 kg of microalgae biomass.

The obtained microalgae lipid fraction represented the raw material for a further enzymatic modification step. The lipid fraction, which was mainly composed of triacylglyceroles, was lipolytically hydrolyzed to obtain a fraction of free fatty acids (FFAs). By exposing these FFAs to different types of enzymes, specific modifications of the carbon chains, e.g. the addition of functional groups (hydroxy-, keto- or amino groups), could be achieved. These modified FFAs served as high value additives for the lubricant formulation and have been evaluated by an industrial partner.

The residual material from the SCCO_2 extraction, consisting mainly of cell wall fragments (carbon hydrates) and proteins, was used as raw material for the fermentation of oleaginous yeast. The biomass was enzymatically hydrolyzed to set free monomeric sugars, which are the main components of the microalgae cell wall. The hydrolysate, containing the free sugars and the microalgal protein fraction, could be completely metabolized by particular oleaginous yeast, which are able to accumulate high amounts of intracellular lipids, of up to 80 % of the dry cell weight.

At the end of the fermentation process, the oleaginous yeast were harvested and utilized for a thermo-catalytic conversion reaction. Products of this chemical conversion reaction are bio kerosene (main fraction) and tar (minor fraction), containing long chain hydrocarbons and inorganic components (P, Si, Al, N). The produced bio kerosene is an alternative for aviation fuel and represents a “drop-in” alternative for fossil fuels, used in the aviation industry.

The tar fraction, normally a “waste stream” from the thermo-catalytic conversion, was used as an additive for the production of CO_2 adsorbing building materials. The addition of the tar fraction in different quantities allows a precise variation of the binding properties and the pore size of the building materials. This allows a more efficient carbonization of the material and leads to a higher CO_2 uptake during the hardening period.

In addition to the experimental procedures a techno economically evaluation of the overall project has been carried out. This economical reflection identified expensive and/or inefficient steps inside the process chain and allowed a more efficient development of industrially compatible processes in an early stage of the project.

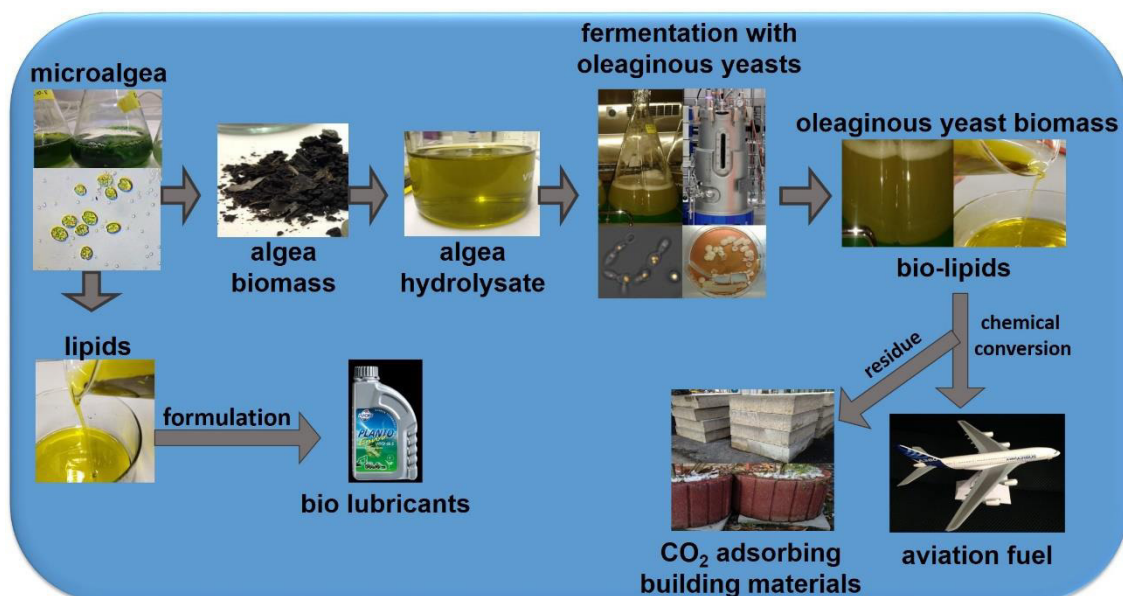


Figure 1: Schematic diagram of the ABV project, including the main steps of the process chain.

With this unique process chain the ABV project depicts an efficient and sustainable way for utilizing microalgae biomass as a new “3rd generation” feedstock in the future of aviation industries.

1.2 Introduction Chapter I: Extraction of Microalgae Derived Lipids with Supercritical Carbon Dioxide in an Industrial Relevant Pilot Plant

Driven by demands of the food, chemical- and pharmaceutical industry the production of plant and animal based lipids increased by approximately 65% in the last decade. While about 70% are still used for food purposes, the application of natural oils for biofuels, oleo chemicals and bioactive substances is expanding rapidly. In this respect, the application of plant oils for non-food use accelerates land use and climate change, which in turn negatively impacts biodiversity. Further, the majority of pharmaceutically active high value lipids, such as long chain polyunsaturated fatty acids (PUFAs), are still sourced from fish and crustaceans, thereby negatively impacting already strained marine ecosystems.

Microalgae derived oils have been designated as a sustainable alternative to (terrestrial) plant and animal based lipids. Microalgae are able to reach high intracellular lipid contents of up to 70% (w/w) of the dry cell weight and are rich in long chain PUFAs. They show a high biomass productivity (up to 10 times higher than terrestrial plants) at a low area consumptions and are not competing with agricultural utilized lands. Microalgae can be cultivated in salt or brackish water and preserve fresh water resources for human utilization. Furthermore, like terrestrial plants, microalgae utilize the greenhouse gas CO₂ for the de-novo production of lipids.

For the utilization of microalgae derived, high value compounds, like PUFAs, it is essential to have an efficient and scalable extraction method. More recently extraction of plant and algae biomass with supercritical carbon dioxide (SCCO₂) gained momentum in industrial process development. In contrast to conventional extraction methods, e.g. following the work of Bligh & Dyer, the SCCO₂ extraction works with CO₂ as a non-toxic solvent, which can be removed residue-free from the extracted compounds. This non-toxic and preserving extraction technique is of particular interest for the food and cosmetics industries.

Recently published data for SCCO₂ extractions of lipids from microalgae derived biomass are either conducted with polar co-solvents (e.g. ethanol), or performed the extractions with very small batch sizes (0,5 - 1g). The application of polar co-solvents, like ethanol, cannot be integrated in existing SCCO₂ extraction plants, due to implemented ATEX directives. Therefore, data including the use of co-solvents in small batch sizes are not transferrable to industrial application.

1.2.1 Microalgae as a Source of High Value Compounds

Microalgae are a group microscopic, photosynthetic autotrophs, which are the bases of the aquatic food chain. Microalgae are found in almost all aquatic habitats, from the cold arctic and Antarctic waters to the equatorial seas and from fresh-, over brackish-, to extremely salty waters. The wide distribution of these organisms led to a versatile evolution of metabolic pathways, offering a great toolbox of metabolites and enzymes for today's challenges in modern biotechnology. Although only a small part of the existing potential for biotechnological applications has been exploited in recent decades, many interesting and successful approaches have already been implemented commercially.

Mainly driven by the high biomass productivity (e.g. *Chlorella* 60 – 75 tons dry cell weight (dcw) ha⁻¹ y⁻¹)², microalgae already have been cultivated for the last decades for the supplementation of human diets and as animal feed. Particularly the high protein content, which is 4 – 10 times higher, compared to terrestrial plants per area³, is of high interest as an alternative to common protein feedstock, like soybeans. The production of pigments for the food, cosmetic and pharmaceutical industry, like β -carotenoids⁴ or astaxanthin⁵, especially from *Haematococcus* species, has already become a well-established branch in the biotechnological industry. The most promising approaches of applying microalgae for industrial processes is the use of microalgae biomass for the bioethanol production⁶, by fermenting the cellular sugars, and the use of intracellular lipids for the biodiesel production. Since microalgae show a very diverse composition of synthesized fatty acids, comprising high amounts of long-chain PUFAs⁷, they also gained increasing interest in the pharmaceutical sector.

1.2.2 General Lipid Extraction Methods

Many different methods for the extraction of lipids from biological materials are available today. Most of these methods are based on the two methods described in the following two paragraphs.

The Soxhlet extraction (after Franz Ritter von Soxhlet, 1879) is a continuous, solvent based extraction method and was invented for the extraction of milk fats. A thimble containing the sample to be processed is placed inside the Soxhlet extractor. The extractor is set on a still pot, which contains the extraction solvent. The solvent is heated and the arising steam rises through the distillation path (separated from the thimble) to a condenser. The condensed solvent drops continuously from the top on the sample to be extracted and when the solvent level reaches the siphon top, the solvent-extract-mixture flows back into the still pot. Thus a continuous extraction process is realized, that can be performed over a variable period of time, depending on the sample size and the solubility of the compound to be extracted.

The lipid extraction after Bligh & Dyer⁸ is a relatively rapid, solvent based extraction method, especially suitable for samples with a high water content. The sample to be extracted is homogenized with chloroform and methanol and the mixture is filtered. The filtrate is collected and after the complete separation of the biphasic system, the upper layer (methanol water mixture) is discarded. The remaining chloroform layer contains the extracted lipids, which can be purified by evaporating the solvent. When applying this method for lipid extraction, it is essential to set the right ratio between the two solvents (chloroform and methanol) and the water content of the extracted sample. The ratio should be adjusted to the following chloroform : methanol : water = 1 : 2 : 0.8.

These “basic” procedures for lipid extraction exist today with numerous different modifications for an increasing extraction performance. Most of these modifications are associated with the sample preparation, previous to the actual extraction and support the liberation of intracellular lipids. These modifications include for example enzymatic treatment, high pressure homogenization, ultra-sonication, osmotic shock treatment or microwave assisted techniques⁹⁻¹¹.

1.2.3 Supercritical Carbon Dioxide (SCCO₂) for the Extraction of Nonpolar Compounds

Beside the described, solvent based extraction methods, the extraction of nonpolar compounds from different kind of tissues using supercritical fluids became an effective tool within the last years. Especially the usage of carbon dioxide (CO₂) as a supercritical fluid attempted high attention during this time.

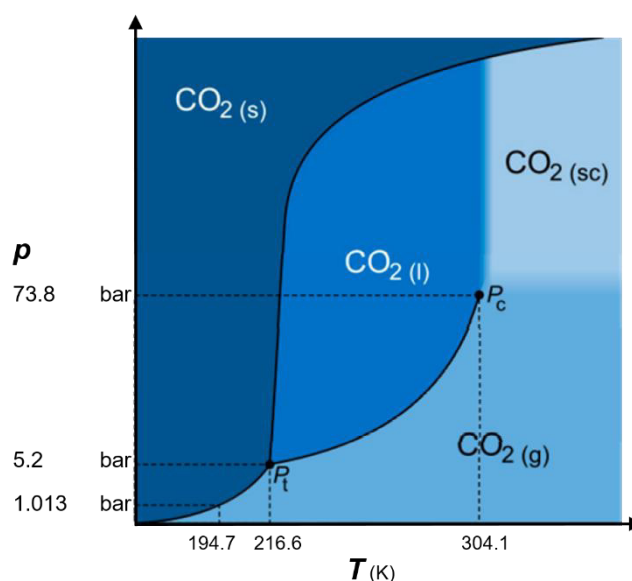


Figure 2: Pressure and temperature phase diagram of CO₂. K: Kelvin, p: pressure, T: temperature, sc: supercritical, l: liquid, g: gaseous, s: solid. After Nowak et al.¹

Under standard conditions (room temperature; 1 atm pressure) CO₂ behaves like “normal” gas. Depending on the applied temperature and pressure CO₂ can change from a gaseous to either a solid (dry ice), or a liquid state. When temperature and pressure are raised above the critical point of CO₂ (304.1 K; 7.38 MPa), it exhibits the properties of both a gas and a liquid. In this supercritical state CO₂ can be used for the extraction of nonpolar compounds from e.g. different kinds of biomass. The usage of SCCO₂ as a solvent for extraction shows several benefits. The extraction is carried out under mild conditions, preserving a denaturation of the compounds being extracted. The method is carried out in a closed system, environmental friendly and the extracted compounds can easily be separated from the CO₂ after the extraction.

1.2.4 Bentonite Based Cleaning Procedure for Microalgae Extracts

Although the extraction of microalgae lipids by SCCO₂ is an efficient process, the extracts appear as greenish, brownish, heterogenic liquids (see Table 5 in publication 1). These primary extracts are containing many impurities, like chlorophyll, carotenoids and proteins, which are co-extracted during the procedure. These contaminants prevent the extracts from a direct downstream use, as they might interfere with applied catalysts or influence the stability of potential lubricant formulations. To overcome this obstacle a simple and scalable cleaning procedure for the microalgae extracts is of high importance. Based on these requirements, the extracts were processed by a bentonite based cleaning procedure.

Bentonite is an aluminum phyllosilicate clay, which is mainly consisting of montmorillonite. The leaf structure of the montmorillonite, exposing a very large surface to the applied sample, and its ion exchange quality make the bentonite an efficient adsorbent and a suitable material for the cleaning of microalgae derived primary oils.

1.3 Introduction Chapter II: *Rhodococcus erythropolis* Oleate Hydratase: A New Member in the Oleate Hydratase Family Tree – Biochemical and Structural Studies

To this day approx. 95 % of all products in the lubricant industry are based on fossil oils, whereas only 5 % of the products are based on renewable feedstock, like vegetable oils. Current European specifications for the lubricant producing industries request a strong increase in the bio-based share of lubricants until the year 2020. In this respect, especially high value lubricant additives are a potential target for biochemically produced alternatives. Nevertheless, new biocatalysts are required for a mass efficient production of these biological

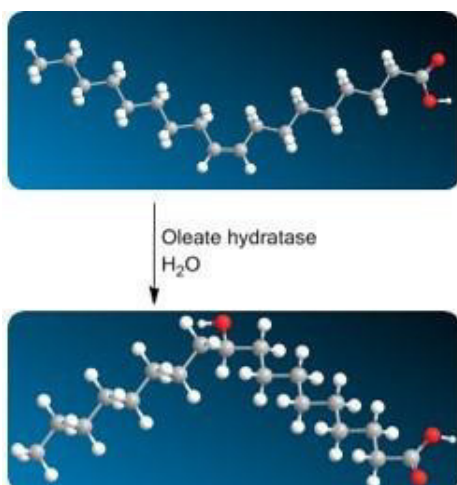


Figure 3: Oleate hydratase (OH) reaction scheme.

alternatives. Recently, oleate hydratases (OHs: EC 4.2.1.53), which catalyse the hydration of oleic acid to 10-hydroxystearic acid (10-HSA), have been intensively studied. This class of catalysts exhibits several beneficial properties, like high activity over a broad pH and temperature range and the lack of cofactor recycling. The reaction product 10-HSA can be used as an alternative for the commonly utilized lubricant additive 12-hydroxystearic acid (12-HSA), produced from castor oil.

To this day, only three crystal structures of OHs have been published, namely the structures of OhyA from *Elizabethkingia meningoseptica*, LAH from *Lactobacillus acidophilus* and OhySt from *Stenotrophomonas sp.* KCTC 12332. These enzymes belong to the Hfam2 and Hfam11 family of OHs, respectively. All three enzymes were shown to be homodimers in their active form, which are connected by the N- and C-terminal ends of their polypeptide chains.

1.3.1 *Rhodococcus erythropolis*

The genus *Rhodococcus* represents a group of non-motile, non-sporulating, Gram-positive, filamentous, rod-shaped bacteria of the family of nocardiaceae. *Rhodococcus erythropolis* in particular, is a very wide spread representative of this genus and is found from deep sea sediments¹² and coastal sediments¹³ over Arctic and Antarctic sediment samples¹⁴ to alpine sediments¹⁵. The genome of the *Rhodococcus erythropolis* strain CCM2595 has been deciphered in 2014 by Strnad et al.¹⁶ and consist of a circular chromosome with a length of 6.28 mbp and a circular plasmid with a length of 90 kbp.

The wide geographic distribution, the ability of adapting to many different habitats and the large bacterial genome with 5,830 predicted coding genes is also reflected in the impressive enzymatic “toolbox” exhibited by *R. erythropolis*. This enzymatic toolbox comprises in different strains the ability for oxidation (e.g. the oxidation of terpenoids by an FAD/NADH-dependent monooxygenase)¹⁷, dehydrogenation (e.g. the reduction of poorly water soluble ketones by a formate dehydrogenase)¹⁸, epoxidation (e.g. the epoxidation of limonene by the limonene-1,2-epoxide hydrolase)¹⁷, hydroxylation (e.g. the hydroxylation of steroids by a monooxygenase)¹⁹, hydrolysis (e.g. the ring opening of lactones by a monoterpene α -lactone hydrolase)²⁰, dehalogenation (e.g. the degradation of fluorphenols by a phenol hydroxylase) and desulfurization reactions (e.g. the desulfurization of dibenzothiophenes (DBT) by a desulfinase)²¹.

1.3.2 Oleate Hydratases

Oleate hydratases (OHs; EC 4.2.1.53) belong to the enzyme class of lyases (EC 4), representing catalysts that are able to split or link two molecules, without the consumption of ATP. More precisely OHs belong to the subclass of carbon-oxygen lyases (EC 4.2), acting only on carbon-oxygen bonds. Even more precisely OHs belong to the class of hydro-lyases (EC 4.2.1), catalysts that remove/add hydroxyl groups from/to a carbon bond under the formation/consumption of H₂O. OHs specifically act on the cis-9-10 double bond of oleic acid and incorporate a hydroxyl group at the C10-position of the carbon chain.

The ability of some bacteria to hydrate oleic acid to 10-HSA has been described for the first time in 1962 by Wallen et al.²². An isolated pseudomonade strain was shown to carry out the hydration reaction under the consumption of H₂O at the 9-10 double bond of the oleic acid with a high stereo selectivity. Four years later, G.J. Schroepfer further examined this reaction and demonstrated, by deuterium based experiments, that the hydration reaction is associated with cleavage of a H₂O molecule. Still, the enzyme responsible for the reaction had not been distinctly identified for more than 40 years. Although different publications dealt with the hydration of oleic acid or the dehydration of 10-HSA^{23,24} it lasted until 2009 when Bevers et al.²⁵ identified the responsible enzyme as an OH, originating from *Elizabethkingia meningoseptica*, namely OhyA. In 2013 Volkov et al. published the first crystal structure of an OH originating from *Lactobacillus acidophilus*²⁶. In 2015 Engleder et al. were able to crystallize OhyA and to identify catalytically relevant residues for the same²⁷.

1.3.3 Oleate Hydratase Reaction Mechanism

The first attempt to gain insights into the reaction mechanism of an OH was carried out by Volkov et al.²⁶ for the fatty acid double bond hydratase LAH from *Lactobacillus acidophilus*. LAH is, like all described OHs so far, a FAD binding hydratase, with C16 and C18 non-esterified, unsaturated fatty acids being its preferred substrates. The enzyme could be crystallized in two forms, the apo-state and bound to linoleic acid (C18:2). The structural analysis revealed that LAH is a homodimer in its active form, with each polypeptide chain being structured in four domains. Domains 1-3 were identified to be responsible for the FAD and substrate binding, whereas domain 4 represents a kind of lid structure, which covers the substrate channel. In the absence of substrate both protomers form a symmetric dimer without significant conformational differences. When one protomer (asymmetric protomer) binds to the substrate (linoleic acid), domain 4 of the second protomer (symmetric protomer) undergoes a conformational change and exposes parts of the surface area of its substrate-binding domain. It is therefore suggested that the activity of LAH is controlled by this specific substrate

recognition mechanism. Unfortunately, Volkov et al. could not identify specific residues that are responsible for the hydration reaction of LAH.

In 2015 Engleder et al. published the second crystal structure of an OH²⁷. Based on the work of Bevers et al.²⁵ they were able to crystallize OhyA from *Elizabethkingia meningoseptica* and carry out a detailed characterization of the enzyme. Moreover, they were able to identify residues being essential for the hydration activity of this catalyst.

OhyA is, like LAH, a homodimeric, FAD-binding hydratase in its active form. Each monomer has a molecular weight of approx. 73 kDa and is composed of 646 amino acids. It was suggested by docking experiments, that the residues Q265, T436, N438 and H442 build a hydrophilic region inside the active site cavity, which is closely associated to the carboxylate group of the FA substrate and therefore responsible for substrate binding. Furthermore, the amino acids E122, Y241 and Y456, as well as the isoalloxazine ring of the FAD, were shown to be in close proximity to the *cis* double bond of the FA and were presupposed to be responsible for the actual hydration of the FA double bond. The generation of mutants of these identified residues resulted in a strongly decreased (T436A, N438A, H442A) hydration activity of the enzyme or even in a loss of the same (E122A, Y241F). Based on these results it was postulated that Y241 protonates the FA double bond and E122 is accounted for the activation of a H₂O molecule for the *re*-side attack on the partially charged double bond.

The third crystal structure for an OH, excluding the structure of OhyRe, was published by Park et al. in 2018²⁸. The crystallization of the *Stenotrophomonas sp. KCTC 12332* OH, OhySt, revealed the homodimeric structure of another representative from the Hfam11 family of OHs, the same family like OhyA. It was shown that the enzyme, like OhyA, exhibits a flexible region close to the cofactor FAD, but the reaction mechanism could not further be clarified.

The exact reaction mechanism of OHs could not completely be decrypted to date, although many promising approaches were made.

1.3.4 Identification of Potential Targets for Site Directed Mutagenesis

As described above, Engleder et al.²⁷ identified amino acid residues being crucial for the reactivity of the OH from *E. meningoseptica*. The authors also compared the amino acid sequence of OhyA with the sequences of nine other OHs. The performed alignment revealed that five of the seven crucial amino acids are almost strictly conserved within all compared OHs. Since the OH from *R. erythropolis* only showed low identity in the amino acid sequence compared to other known OHs (maximum identity of 35.9 %), a sequence alignment with 13 other OHs was performed to take a closer look at the conserved amino acids (Fig. 4).

Introduction

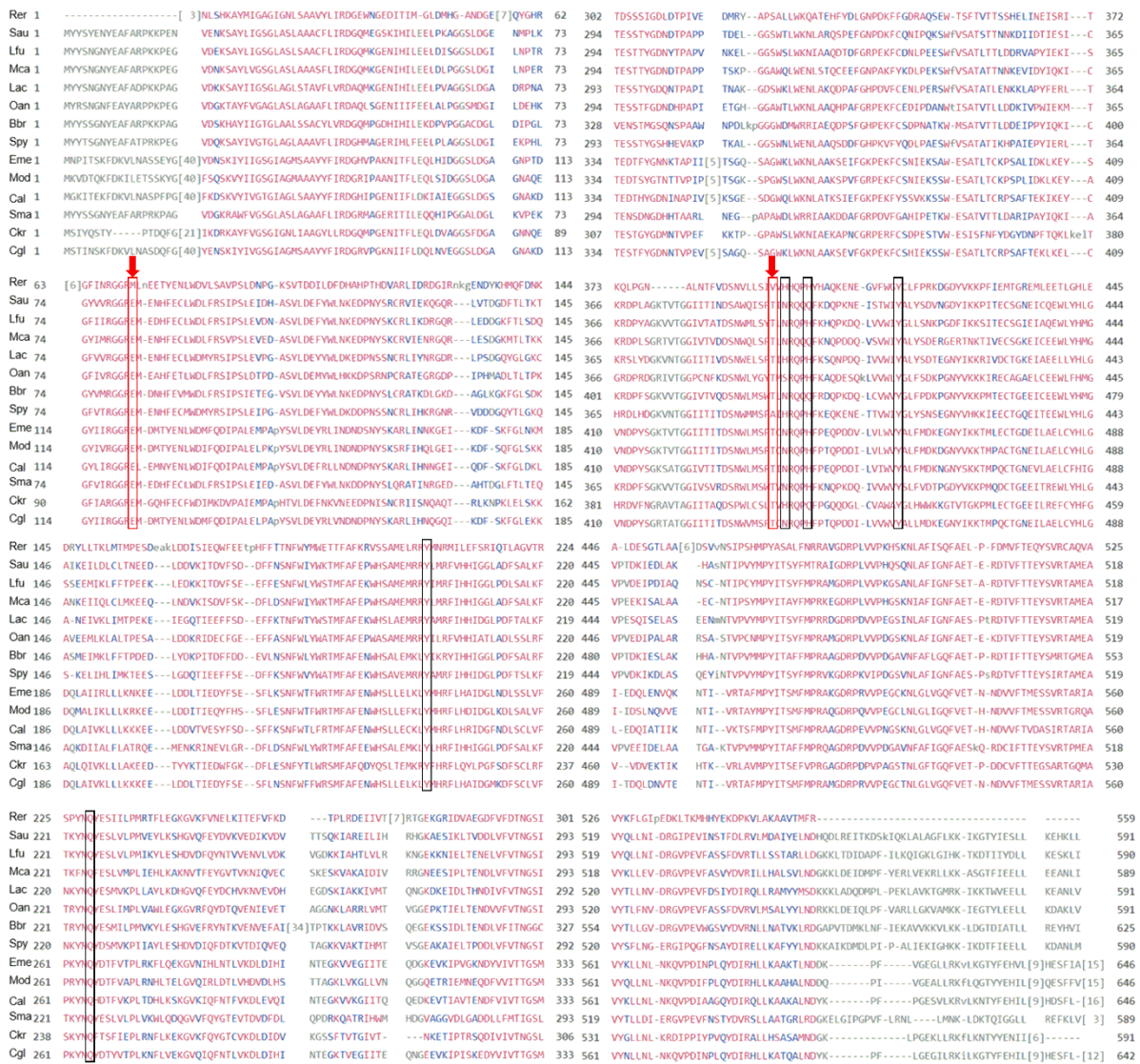


Figure 4: Sequence alignment of 14 different OHs from *Rhodococcus erythropolis* (Rre; HFam3), *Staphylococcus aureus* (Sau; HFam2), *Lysinibacillus fusiformis* (Lfu; HFam2), *Macrocococcus caseolyticus* (Mca; HFam2), *Lactobacillus acidophilus* (Lac; HFam2), *Ochrobactrum anthropi* (Oan; HFam2), *Bifidobacterium breve* (Bbr; HFam2), *Streptococcus pyogenes* (Spy; HFam2), *Elizabethkingia meningoseptica* (Eme; HFam11), *Myroides odoratus* (Moc; HFam11), *Cellulophaga algicola* (Cal; HFam11), *Stenotrophomonas maltophilia* (Sma; HFam2), *Corynebacterium kroppenstedtii* (Ckr; HFam10) and *Chryseobacterium gleum* (Cgl; HFam11). The seven crucial amino acids, identified by Engleder et al. are highlighted with boxes. The two differing positions are highlighted with red boxes

The multiple sequence alignment of 14 OHs confirmed the data from Engleder et al. but at the same time identified two positions which differed in OhyRe. The two residues in these positions, namely M77 and V393 (red boxes with arrows in Fig. 4), correspond to the residues E122 and T436 from OhyA and OhyB confirmed the position of the two residues inside

To clarify whether the two amino acids are in the same position of the three-dimensional protein, models were calculated, using the swiss-model server (expasy.org). As the three-dimensional alignment of OhyRe and OhyA confirmed the position of the two residues inside

the tertiary protein structure, these residues were finally chosen for site directed mutagenesis. As the residues E122 and T436 are highly conserved in all investigated OHs, conservative substitutions via overlap extension PCR were performed to produce the two mutants M77E and V393T.

1.3.5 Hydroxy Fatty Acids in Industrial Applications

Hydroxy fatty acids are already applied for decades for many different industrial products, mostly relying on their excellent thickening qualities in different formulation. In the food industry these modified fatty acids are for example used as thickeners for different edibles ²⁹ and as precursors for flavor molecules like γ -decalactones ³⁰. Approaches have also been made to use hydroxy fatty acid based organogels for food stability ^{31,32} and for pharmaceuticals ³³. Hydroxy fatty acids are further utilized to produce lacquer resins ³⁴, spray coatings ³⁵ and as plasticizers for biodegradable resins ³⁶. In the cosmetic industry, hydroxy fatty acids are for example applied in formulations for transfer resistant cosmetics ³⁷ and other make-up products ³⁸. The most common hydroxy fatty acid in industrial applications is 12-hydroxystearic acid (12-HSA). 12-HSA is gained from the catalytic hydration of castor oil, or more specifically from the hydration of ricinoleic acid (12-hydroxy-9-cis-octadecanoic acid) and is today the only commercially available hydroxy fatty acid which can be delivered in relevant amounts.

2. Methods

Microalgae Strains & Cultivation

Two different batches of algae biomass have been applied for SCCO₂ extraction. The first batch was provided by Hochschule Anhalt, a heterologous culture consisting of 85-90 % *Scenedesmus obliquus*, low percentages of *Chlorella vulgaris* and *Chlorella kesslerie* as well as traces of *Chlorella vacuolatus*. The algae were cultivated under non-limiting conditions with natural sunlight illumination in a tubular reactor system. The second batch analyzed was an unialgal culture of *Scenedesmus obtusiusculus*, cultivated in BG-11 medium under non-limiting conditions, using LED-assisted natural sunlight illumination in a flat panel photo bioreactor. Since the cultivation was carried out under non-limiting conditions, low lipid accumulating (approx. 15 – 20 % w/w) were expected. After the cultivation period, the cells were harvested from the cultivation broth and stored at -20 °C until use.

Microalgae Preparation

The stored microalgae samples were defrosted over two days at 4 °C. After defrosting, the samples were diluted with ddH₂O to approx. 20 % w/w (biomass / water), to reach an optimal density for the subsequent high pressure homogenization (HPH). The HPH was carried out with a NS3015H homogenizer from GEA Niro Soavi with the following program: the flowrate was adjusted to 100 L h⁻¹ at a pressure of 900 bar (single-stage homogenizing valve). The samples (approx. 40 L) were recirculated four times (four complete volume transfers through the homogenizer) in a cooled and stirred 200 L stainless steel tank. The maximum temperature of the samples was kept below 40 °C throughout the whole duration of the process.

After the homogenization, the microalgae samples were cooled down to 4 °C and sent for lyophilization to NaProFood GmbH & Co. KG (Bruckberg, Germany).

Conventional Solvent Extraction

The conventional solvent extraction of lipids from microalgae biomass was performed according to the work of Bligh & Dyer⁸. The homogenized and lyophilized samples were mixed with hexane as single solvent for 8 hours under constant stirring at room temperature. After the extraction time, the hexane phase was separated from the water phase and subsequently dried in a rotary evaporator to gain the extracted lipid fraction. The amount of the lipids was gravimetrically determined and the samples were analyzed as described in the section “Lipid analysis”.

Supercritical Carbon Dioxide (SCCO₂) Extraction

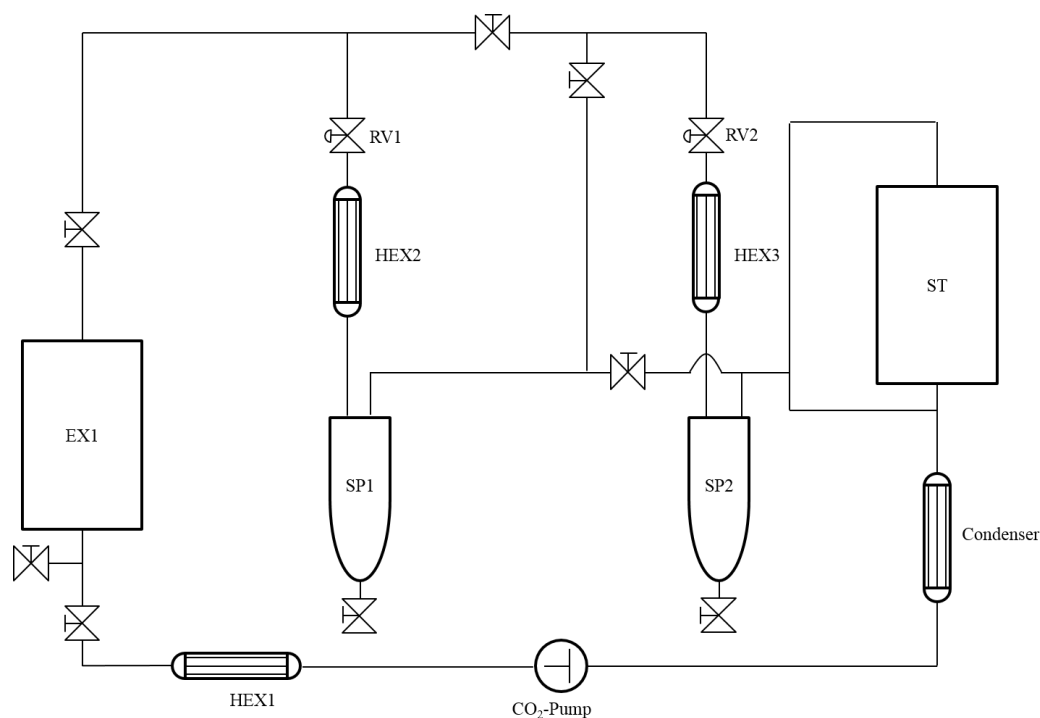


Figure 5: Schematic diagram of the employed extraction pilot plant.

The extraction of the microalgae derived lipids was performed in a small scale extraction pilot plant, with a maximum batch size of 5 kg dried biomass. This pilot plant equates to large scale extraction plants that are commonly used for the SCCO₂ extraction of different hydrophobic compounds, for example caffeine or astaxanthin.

The liquid CO₂ from the storage tank (ST) is pressurized by a CO₂-pump and heated to the extraction temperature by a heat exchanger (HEX 1). Subsequently the CO₂ flows into the extraction vessel (EX1) containing the biomass. The CO₂/extract mixture is separated, by controlled pressure reduction and simultaneous warming by heat exchangers (HEX2, HEX3), into a CO₂ vapor and an extract phase (separators SP1, SP2). The extracts are removed from the process while the gaseous CO₂ remains in the process. Afterwards the CO₂ is liquefied by a condenser and recirculated.

All extractions were performed with samples sizes from 650 – 1300 g of lyophilized microalgae biomass. In terms of the high amount of biomass required for the extraction in the pilot plant, not all experiments could be carried out in duplicates. For the bentonite bleaching, the adsorber was directly placed into the extraction chamber and the procedure was carried out as described above. The online bentonite bleaching was only tested on the biomass of the unialgal *Scenedesmus obtusiusculus* culture. The tests were focused on this strain, because it showed the most promising process parameters in terms of cultivation stability and biomass yields and therefore became the leading strain in the Advanced Biomass Value (ABV) project.

Lipid Analysis

For the analysis of the microalgae derived lipids via gas-chromatography (GC), the generation of fatty acid methyl esters (FAMES) is necessary. The direct transesterification of the lipid samples was performed according to a modified protocol from Griffiths et al. ³⁹ with the following modifications: the replacement of the C17-TAG by a C12-TAG, the replacement of BF3 methanol by a HCL-methanol solution and the C19-ME was omitted. Before the transesterification procedure the HCl-methanol solution, the sodium methoxide solution and the two utilized solvents, hexane and toluene, were placed on ice and kept there for the whole procedure, to minimize evaporation effects. Lipid samples to be analyzed were dissolved in ethyl acetate to a final concentration of 10 mg/ml and 200 μ l were taken for FAMES production. The samples were mixed with 450 μ l toluene, 50 μ l of the C12-tag stock solution (2 mg/ml), 100 μ l 2,2-dimethoxypropane and 1 ml of the sodium methoxide solution. The samples were vortexed and placed in a thermos shaker (DITABIS) for 20 min at 80°C and maximum mixing speed. After a subsequent cooling of the samples, for 5 min on ice, 1 ml of HCl-methanol solution was added. The samples were vortexed again and the heating and cooling procedure was repeated. After cooling down the samples, 400 μ l ddH₂O and 400 μ l hexane were added and the probes were again vortexed. To reach a complete phase separation, the samples were centrifuged for 1 min at 4000 rpm. 200 μ l of the upper phase, containing the FAMES, were taken for the following GC analysis.

The resulting FAMES were either analyzed by GC-FID or GC-MS with the following specifications.

For GC-MS analysis 1 μ l sample was injected into a Thermo Scientific™ TRACE™ Ultra Gas Chromatograph coupled to a Thermo DSQ™ II mass spectrometer and the Triplus™ Autosampler injector. Column: Stabilwax® fused silica capillary (30 m x 0.25 mm, film thickness 0.25 μ m, Restek). The GC-program was chosen as following: initial column temperature 150 °C, increasing (5°C min⁻¹) up to a final temperature of 250 °C. To gain a higher resolution additional, longer programs were chosen: initial column temperature 50 °C, increasing (4 °C min⁻¹) up to a final temperature of 250 °C. Hydrogen was taken as carrier gas at a flow rate of 3.5 ml min⁻¹.

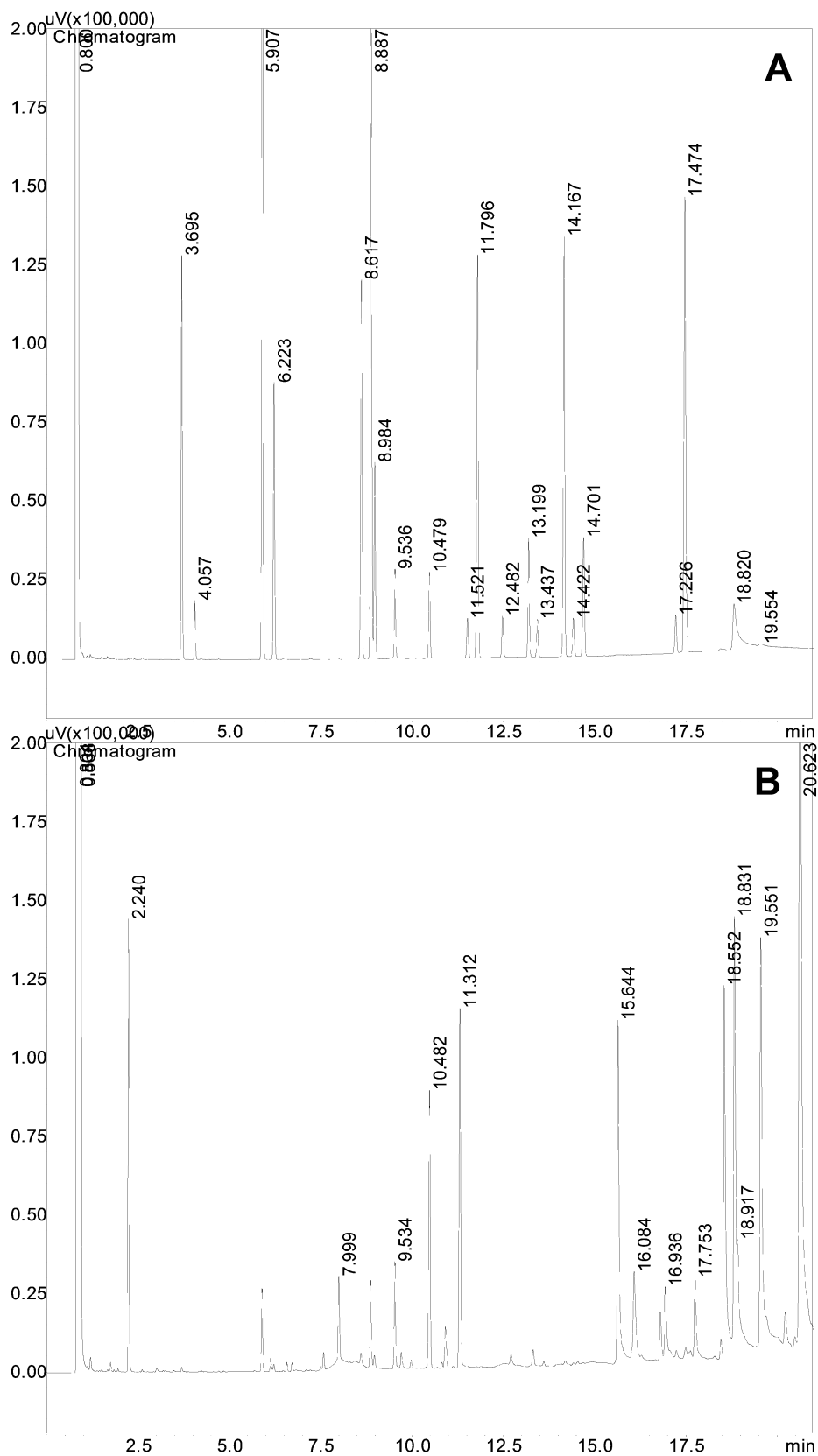


Figure 6: GC-chromatograms of the marine oil standard FAMES (A) and a microalgae extract from *S. obtusiusculus* (B), the corresponding retention times (RT) and fatty acids for the standard are found in Table 1.

RT	Fatty Acid
2.24	C12:0 Lauric acid
3.70	C14:0 Myristic acid
4.06	C14:1 Myristoleic acid
5.91	C16:0 Palmitic acid
6.22	C16:1 Palmitoleic acid
8.62	C18:0 Stearic acid
8.89	C18:1 Oleic acid
8.98	C18:1 Vaccenic acid
9.54	C18:2 Linoleic acid
10.48	C18:3 Linolenic acid
11.52	C20:0 Arachidic acid
11.80	C20:1 Eicosenoic acid
12.48	C20:2 Eicosadienoic acid
13.20	C20:4 Arachidonic acid
13.44	C20:3 Eicosatrienoic acid
14.17	C20:5 Eicosapentaenoic acid
14.42	C22:0 Behenic acid
14.70	C22:1 Erucic acid
17.23	C24:0 Lignoceric acid
17.47	C22:6 Docosaheptaenoic acid

Table 1: Fatty acids included in the marine oil mix with the corresponding retention times (RT), corresponding to Figure 6.

Figure 6 shows two chromatograms resulting from GC measurements (A: chromatogram of the marine oil standard FAMES; B: chromatogram of a microalgae extract from *S. obtusiusculus*) and Table 1 the list of FAs included in the marine oil standard FAMES mix, with the corresponding retention times. By comparing the retention times of the peaks from the unknown sample to the retention times of the peaks from the marine oil standard, the natural FAs, comprised inside the unknown sample, can be identified. Peaks that cannot be identified by this comparison are often not FAs, but fragments of co-extracted hydrophobic compounds from the microalgae cell. These appearing peaks are, if possible, further analyzed by comparison of their specific molecular masses to an appropriate library.

The procedure for the identification of the reaction products from the enzymatic conversion experiments with the OHs was similar to the method described above. The only difference in the sample preparation was the esterification method. The samples, gained from the OH reactions, were esterified by silylation, instead of methylation. The silylation procedure was performed according to Volkov et al.⁴⁰ and comprised the following steps. The sample, solved in EtOAc, was dried completely under a nitrogen stream and subsequently dissolved in 200 μ l of a 0.1 M solution of BSTFA [N,O-Bis (trimethylsilyl)trifluoroacetamide] in methanol. The mixture was incubated for 10 min at room temperature and subsequently applied for GC analysis.

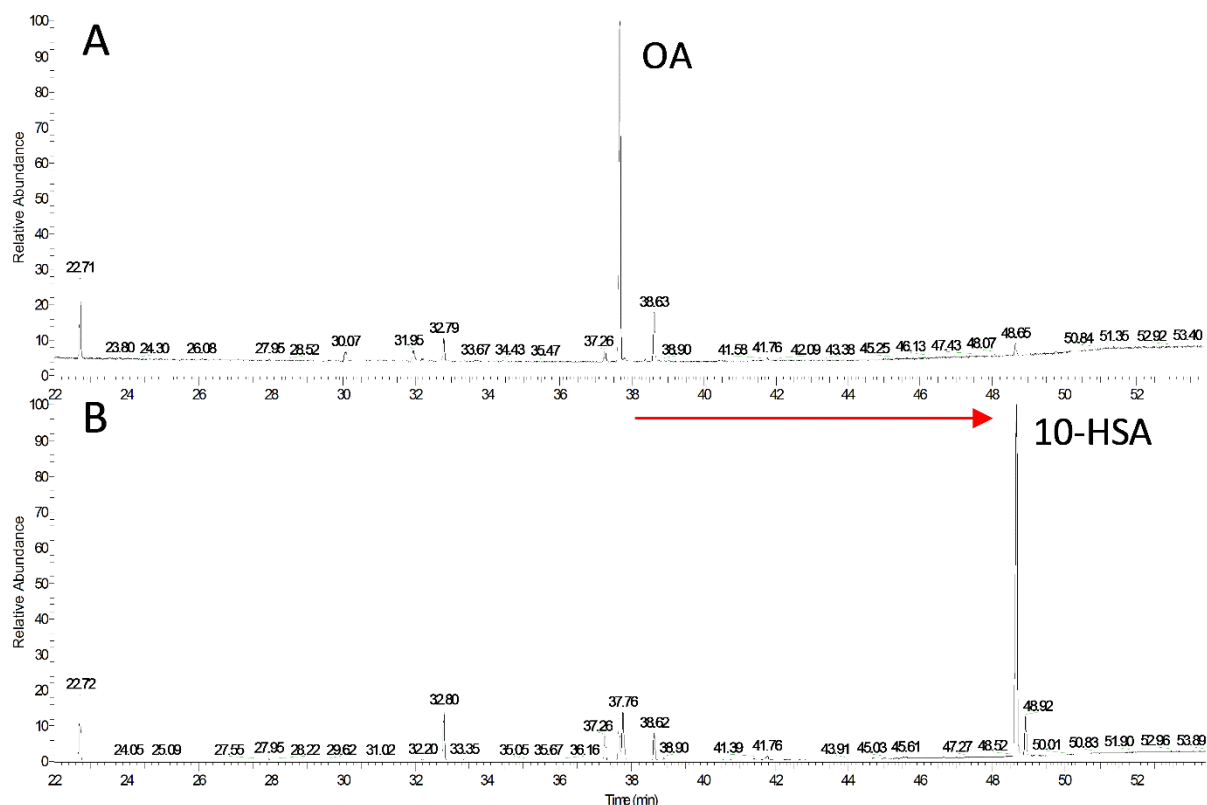


Figure 7: GC-MS chromatograms documenting the conversion of oleic acid (OA) to 10-hydroxystearic acid (10-HSA) after 90 min reaction time. A) negative control without oleate hydratase and B) sample after reaction with oleate hydratase.

To document the successful conversion of oleic acid to 10-HSA, samples were taken from the negative control (reaction mixture without OH) and the reactions containing OH. Figure 7 A) shows the GC chromatogram of the negative control, representing the spectrum of the utilized oleic acid with the dominant peak for oleic acid (RT: 37.75 min). The oleic acid applied for the experiments was not GC grade, but had a purity of 93 %. The smaller peaks, present in the spectrum, represent other fatty acids included in the utilized oleic acid. Figure 7 B) shows the GC chromatogram of a sample after 90 min reaction time with the OH from *Rhodococcus erythropolis*. The peak representing oleic acid is decreased by approx. 90 %, in contrast a new dominant peak appears at RT: 48.69 min. This peak represents the 10-HSA and the clear shift from the oleic acid peak to the 10-HSA peak demonstrates the efficiency of the applied catalyst.

Purification of Crude Microalgae Extracts

The lipid fractions resulting from the SCCO₂ extractions were purified with an adsorbent based on montmorillonite. 20 g Tonsil 510® from Clariant Produkte (Deutschland) GmbH were filled into a column with n-hexane and incubated for 10 minutes at room temperature to swell in the solvent. 2 – 3 g algae oil were applied to the column and given time to sink completely into the adsorbent. The elution was done with n-hexane until 150 ml eluate was collected. After

removing the solvent with a rotary evaporator and an extra drying step at 110 °C for 1 hour, the oil was analyzed via inductively coupled plasma optical emission spectroscopy (ICP-OES) with a Perkin Elmer Optima 3300 DV (analog to DIN EN ISO 11885). The analysis allows the detection of particular ions inside the samples and the adsorbance of the same by the applied bentonite.

Bacterial Strains

The *Escherichia coli* strains XL-1 Blue and DH5α were employed for cloning and subcloning of the OH and its mutants. Both strains carry the common mutations for a laboratory cloning strain. The mutations encompass a mutation in the *recA* gene (*recA1*), avoiding recombination of the plasmid and the bacterial genome, the mutation *endA1*, resulting in an endonuclease A deficiency, and the mutation *gyrA96* (in the *NalR* gene), leading to a nalidixic acid resistance. Furthermore, both strains are K strains that carry the mutation *hsdR17*(r_K^- , m_K^+). The mutation knocks out the EcoKI endonuclease, to prevent plasmid DNA digestion, but keeps the active DNA methylase. Thus, replicated plasmid DNA is still methylated and thereby not recognized as foreign DNA. In addition, both strains carry the *lacZΔ* mutation, making these cells suitable for blue/white selection.

The heterologous protein expression was carried out in *E. coli* BL21(DE3) cells or in Rosetta2 cells, strains explicitly designed for the (heterologous) expression of proteins. The strains carry mutations in the *ompT* and *lon* genes, resulting in a deficiency for the two corresponding proteases. Both strains express the T7 RNA polymerase, originating from the λDE3 prophage, and can therefore be employed for T7 expression, when transformed with an appropriate T7 expression plasmid.

strain	genotype
DH5α	$F^- \phi 80/lacZ\Delta M15 \Delta(lacZYA-argF)U169 recA1 endA1 hsdR17(r_K^-, m_K^+) phoA supE44 \lambda^- thi-1 gyrA96 relA1$ (ThermoFisher Scientific)
XL1-Blue	<i>recA1 endA1 gyrA96 thi-1 hsdR17 supE44 relA1 lac</i> [F' <i>proAB lac^g ZΔM15 Tn10</i> (Tet ^r)] (Stratagene)
BL21(DE3)	$F^- ompT hsdS_B (r_B^-, m_B^-) gal dcm$ (DE3) (ThermoFisher Scientific)
Rosetta 2	$F^- ompT gal dcm lon hsdS_B (r_B^- m_B^-) \lambda(DE3 [lacI lacUV5-T7p07 ind1 sam7 nin5]) [malB^+]_{K-12}(\lambda^S)$

Table 2: Utilized *E. coli* strains with respective genotypes.

Cloning for Characterization Experiments

The putative OH from *Rhodococcus erythropolis* CCM2595 was identified by targeted genome mining. Based on the amino acid sequence of the already studied OH ohyA from *Elizabethkingia meningoseptica*, a homology search was performed via the BLAST (Basic Logical Alignment Search Tool) service on the NCBI server. The identified nucleotide

sequence for the putative OH was taken as a template for a codon-optimized gene-synthesis (Life Technologies, Regensburg Germany) for an *E. coli* host strain.

The plasmid, including the codon-optimized gene for the *R. erythropolis* OH, was transformed into chemically competent *E. coli* DH5 α to increase the amount of DNA for further cloning steps. After plasmid preparation, the OH insert was cut from the plasmid using the flanking restriction enzymes NheI and XhoI. The utilized expression vector pET28a was also cut with these restriction enzymes and the OH insert was ligated into the vector's multiple cloning site, using T4-ligase. The plasmid, carrying the OH gene, was subsequently transformed into chemically competent *E. coli* BL21(DE3) cells for protein expression.

Mutant Construction

The comparison of the amino acid sequences of OhyRe and 13 other oleate hydratases (Fig. 4) revealed two interesting positions in the polypeptide chain that differ from the other OHs. These two positions, namely M77 and V393, correspond with two positions that have been identified by Engleder et al.²⁷ and are speculated to be crucial for the functionality of the OH. To evaluate the importance of these two residues for the biocatalytical activity of OhyRe, amino acid substitutions were carried out in the described positions. The two single mutants were constructed by overlap extension PCR and the resulting vectors were subsequently transformed into *E. coli* BL21DE3 cells for protein expression.

Protein Expression and Protein Purification for Characterization Experiments

The expression of the native OhyRe, or respective mutants thereof, was carried out in *E. coli* BL21DE3 cells, grown in lysogeny broth (LB) medium. Pre-cultures were inoculated from a cryo-stock and grown over night in 100 ml LB in a 500 ml baffled flask at 120 rpm and 37°C. Main cultures were grown up to an optical density, measured at 600 nm (OD_{600 nm}), of 0.6 – 0.8, before the expression was induced by the addition of isopropyl β -D-1-thiogalactopyranoside (IPTG) to a final concentration of 0.1 mM. The heterologous expression was carried out for 16 h at a reduced incubation temperature of 16°C. By reducing the incubation temperature the bacterial metabolism is decelerated, resulting in a decreasing risk for the formation of inclusion bodies or other aggregates. After the incubation time the cells were harvested by centrifugation and the resulting pellets were either stored at -20°C or resuspended in 20 mM Tris-HCl buffer, containing 25 mM imidazole (pH 7.2), for direct use. The resuspended cell pellets were disrupted by high pressure homogenization (EmulsiFlex-B15, AVESTIN). Each sample was disrupted by three passages through the device and the samples were cooled on ice between the passages. A subsequent centrifugation step at 20.000 g for 40 min at 4°C (Beckmann coulter J-20 XP) was applied for the separation of the

cell debris from the soluble protein fraction. The soluble protein fraction was utilized for affinity chromatography via a Ni²⁺-NTA His-trap column (HisTrap FF, GE Healthcare; flow rate 1 ml/min). The purified protein solution was desalted using HiPrep 26/10 desalting column (GE Healthcare). Protein amounts were quantified using 2-D quant kit (GE Healthcare) according to manufacturer's instructions.

Enzyme Characterization

After the successful expression of OhyRe, the enzymatic properties were determined. As the enzyme has not been characterized yet, the basic reaction parameters were experimentally identified, using stated cultivation conditions for *Rhodococcus erythropolis* (DMSZ) as an orientation. The tests were carried out in a reaction volume of 200 µl in 20 mM Tris-HCl buffer (pH 7.2), containing the purified enzyme (final conc. of 5 µM), FAD (final conc. 20 µM) and 720 µM OA as substrate at 28°C for 15 min (stated as standard conditions in the study). Thermostability was tested in a temperature range from 20 – 45°C. pH tolerance was monitored in a range from pH 5 – 8. To determine the substrate specificity of the myosin-cross-reactive antigen from *Rhodococcus erythropolis* CM2595, the purified enzyme was tested on myristic acid (C14:0), myristoleic acid (C14:1), palmitic acid (C16:0), palmitoleic acid (C16:1), stearic acid (C18:0), vaccenic acid (C18:1 *trans*-11) oleic acid (C18:1, *cis*-9), linoleic acid (C18:2), linolenic acid (C18:3), eicosatrienoic acid (C20:3), eicosatetraenoic acid (C20:4) and triolein as potential substrates. For the determination of the kinetic parameters of OhyRe towards oleic acid, different substrate concentrations (90 µM to 1.44 mM) and reaction times (1 to 15 min) were tested under standard conditions. The reactions were stopped by the addition of an equal volume of ethyl acetate (EtOAc) and instant, intensive vortexing. After a short centrifugation step, to support phase separation, the solvent phase, containing the extracted lipids, was applied for silylation and subsequent GC analysis.

3. Publications

3.1 Summaries of Included Publications

Extraction of microalgae derived lipids with supercritical carbon dioxide in an industrial relevant pilot plant

The article “Extraction of microalgae derived lipids with supercritical carbon dioxide in an industrial relevant pilot plant” has been published in the Journal of Bioprocess and Biosystems Engineering in February 2017 (<https://link.springer.com/article/10.1007%2Fs00449-017-1755-5>). The author of this thesis, Jan Lorenzen, developed the concept of the publication, evaluated the experimental data and wrote the manuscript.

The aim of the publication entitled “Extraction of microalgae derived lipids with supercritical carbon dioxide in an industrial relevant pilot plant” is based on the concept of the ABV project. In times of climate change and increasing environmental pollution, caused by the use of fossil fuels, the development of new and sustainable feedstock is absolutely essential. Microalgae biomass is one of the most promising future feedstock, exhibiting high potential for pharmaceutical and chemical industries.⁴¹ In this respect, especially the naturally occurring medium and long chain polyunsaturated fatty acids (PUFAs) are of high interest.⁴² The most complex challenge in making these PUFAs available for industrial applications, is the efficient and environmentally friendly extraction of the same from the microalgae biomass. To achieve this target, the extraction via supercritical CO₂ was applied. As this method only has been applied for microalgae biomass in a laboratory scale until today,⁴³ an industrial relevant scale up of this technique was of high interest.

The first priority was the experimental identification of the most efficient profile for temperature, pressure and CO₂ to biomass ratio for the extraction from *Scenedesmus* biomass (as a model substrate). The first profiles tested were based on previous astaxanthin extractions from microalgae biomass (pressure: 30 – 80 MPa; temperature: 50 – 80 °C; CO₂ to biomass ratio: 100 – 200; lipid yields: 5.8 – 7.6 % w/w), but the applied reaction conditions appeared to be too harsh, as they resulted in inhomogeneous dark brownish, almost black extracts. However, for a proper downstream processing, the extracts should be as clear and homogeneous as possible. Hence, the following extractions were carried out under milder conditions (pressure: 7 – 15 MPa; temperature: 20 °C; CO₂ to biomass ratio: 20 – 100; lipid yields: 6.5 – 8.3 % w/w), resulting in the expected clearer and homogeneous extracts. The best results were achieved with the extraction profile 4: pressure: 12 MPa; temperature: 20 °C; CO₂ to biomass ratio: 100; lipid yield: 8.3 % w/w. With these optimized conditions, batch sizes of up 1.3 kg of dried microalgae biomass were processed. Samples of all extracts were methylated and subsequently analyzed by GC-MS. The analysis of the fatty acid profiles of the different

extracts depicted no statistically relevant difference in their compositions. The main fatty acids identified were, linolenic acid (C18:3), hexadecatetraenoic acid (C16:4), linoleic acid (C18:2), oleic acid (C18:1) and palmitic acid (C16:0), in descending order.

Albeit the obtained extracts were relatively clear and homogeneous, a coloring, resulting from co-extracted compounds, like chlorophyll and carotenoids, was still present. A direct use of the extracted oil (e.g. for lubricant formulation) or a further downstream processing (e.g. enzymatic modification) requires a pure substrate, exhibiting a minimized content of contaminants. Hence, a subsequent cleaning step was added to the process. The bentonite based cleaning procedure applied, represents a cost efficient, effective and scalable way to eliminate existing contaminants from the microalgae extracts (see publication Table 5).

In summary, the lipid extraction from *Scenedesmus* biomass via SCCO₂ has been optimized in an industrial relevant pilot plant, with batch sizes of up to 1.3 kg. Furthermore, a scalable bentonite based cleaning procedure has been subsequently applied, resulting in clear, homogenous lipid extracts.

***Rhodococcus erythropolis* Oleate Hydratase: a New Member in the Oleate Hydratase Family Tree – Biochemical and Structural Studies**

The article “*Rhodococcus erythropolis* Oleate Hydratase: a New Member in the Oleate Hydratase Family Tree – Biochemical and Structural Studies” has been published in the journal CHEMCATCHEM at first online in October 2017 and appeared again as a cover feature in Issue 2, 2018 (<https://onlinelibrary.wiley.com/doi/abs/10.1002/cctc.201701350>). The author of this thesis, Jan Lorenzen, and Ronja Driller contribute equally to the work and writing of this publication. Jan Lorenzen identified the new enzyme, developed the concept of the publication and carried out the experimental procedure, except for the crystallography.

The aim of the publication entitled “*Rhodococcus erythropolis* Oleate Hydratase: a New Member in the Oleate Hydratase Family Tree – Biochemical and Structural Studies” was the identification and characterization of a new biocatalyst for the production of 10-HSA. The identification of the DNA sequence of interest was achieved by targeted genome mining. Based on the known DNA sequence of OhyA, ²⁷ an OH originating from *Elizabethkingia meningoseptica*, a 1.68 kB sequence with 34 % identity to OhyA could be found inside the genome of *Rhodococcus erythropolis* CCM2595 and was named OhyRe. The gene was synthesized for the heterologous protein expression in an *E. coli* host strain and cloned into the pET28a vector. After the successful protein expression in the selected host strain, the biophysical properties of the enzyme were examined. The enzyme was shown to be FAD-dependent and exhibited OH activity. Its maximum conversion activity was detected at a temperature of 28°C and a pH of 7.2. The determination of the enzyme’s substrate specificity resulted in the highest specific activity for oleic acid ($1266 \pm 30.3 \text{ nmol mg}_{\text{enzyme}}^{-1} \text{ min}^{-1}$), closely followed by palmitoleic acid ($1205 \pm 70.6 \text{ nmol mg}_{\text{enzyme}}^{-1} \text{ min}^{-1}$) and low activities for γ -linolenic acid, α -linolenic acid and linoleic acid. The K_M and k_{cat} values for the conversion of oleic acid to 10-HSA were 0.49 ± 0.1 and $34 \pm 5 \text{ min}^{-1}$, respectively.

A multiple sequence alignment of OhyRe and 14 other OH sequences allowed the classification of OhyRe to the HFam3 family of OHs and disclosed significant differences between OhyRe and these sequences. In comparison to other published OH sequences OhyRe differs in two almost strictly conserved amino acid (AAs) residues, M77 and V393, inside the hypothetical active center of the enzyme. To control the importance of these AAs for the activity of OhyRe, two mutants were constructed by conservatively substituting the AAs to the conserved ones. The hydration activity of the mutants M77E and V393T was reduced to 18.9 % and 9.5 % of the wild type OhyRe activity, respectively.

To get a deeper insight into the protein’s structure and the reaction mechanism, the enzyme was crystallized by X-ray crystallography. The structure of OhyRe could be solved to a resolution of 2.64 Å and was found to be assembled of four domains (I: residues 6–115, 223–

300, 322–344, and 478–540; II: residues 116–131, 301–321, and 345–477; III: residues 132–222; IV: 541–559), with domains I – III building the core domains. In contrast to LAH and OhyA, the only two OHs that have been crystallized to that date, the crystallization, as well as size exclusion experiments and MALS experiments revealed that OhyRe is a monomer in its active form. This monomeric appearance can most probably be explained by the truncated N- and C-terminal ends of OhyRe, which build the main part of the dimeric interface in LAH and OhyA. Unfortunately, OhyRe could not be crystallized together with a substrate molecule. Without a bound substrate molecule, a definite identification of the catalytically crucial residues of the enzyme's active site is not possible.

In summary, a new OH, OhyRe, from *Rhodococcus erythropolis* could be identified and characterized. The crystal structure of OhyRe is the first structure of a representative of the HFam3 family of OHs, as well as the first published structure of a monomeric OH.

3.2 Full Length Publications

Extraction of microalgae derived lipids with supercritical carbon dioxide in an industrial relevant pilot plant

Extraction of microalgae derived lipids with supercritical carbon dioxide in an industrial relevant pilot plant

Jan Lorenzen¹ · Nadine Igl² · Marlene Tippelt² · Andrea Stege³ · Farah Qoura¹ · Ulrich Sohling³ · Thomas Brück¹

Received: 2 December 2016 / Accepted: 21 February 2017

© The Author(s) 2017. This article is published with open access at Springerlink.com

Abstract Microalgae are capable of producing up to 70% w/w triglycerides with respect to their dry cell weight. Since microalgae utilize the greenhouse gas CO₂, they can be cultivated on marginal lands and grow up to ten times faster than terrestrial plants, the generation of algae oils is a promising option for the development of sustainable bioprocesses, that are of interest for the chemical lubricant, cosmetic and food industry. For the first time we have carried out the optimization of supercritical carbon dioxide (SCCO₂) mediated lipid extraction from biomass of the microalgae *Scenedesmus obliquus* and *Scenedesmus obtusiusculus* under industrially relevant conditions. All experiments were carried out in an industrial pilot plant setting, according to current ATEX directives, with batch sizes up to 1.3 kg. Different combinations of pressure (7–80 MPa), temperature (20–200 °C) and CO₂ to biomass ratio (20–200) have been tested on the dried biomass. The most efficient conditions were found to be 12 MPa pressure, a temperature of 20 °C and a CO₂ to biomass ratio of 100, resulting in a high extraction efficiency of up to 92%. Since the optimized CO₂ extraction still yields a crude triglyceride product that contains various algae derived contaminants, such as chlorophyll and carotenoids, a very effective and scalable purification procedure, based on cost efficient bentonite based adsorbers, was devised. In addition to the

sequential extraction and purification procedure, we present a consolidated online-bleaching procedure for algae derived oils that is realized within the supercritical CO₂ extraction plant.

Keywords Supercritical carbon dioxide extraction · Microalgae · *Scenedesmus* · Lipids · Bentonite

Abbreviations

SCCO ₂	Supercritical carbon dioxide
PUFA	Polyunsaturated fatty acid
FA	Fatty acid
MPa	Mega pascal
FAME	Fatty acid methyl ester

Introduction

Recently, governmental CO₂ emission regulations and an increased awareness of sustainability drive the development of renewable feedstocks based industrial processes. Hence, many different renewable feedstocks have been tested in the last decades, like organic waste, microbe-derived lipids or different types of plant seeds. With respect to sustainability and lipid productivity, microalgae are deemed to be one of the most relevant feedstocks for lipid type chemical products [1–3]. Conservative estimations postulate that about 72.000 algae species exist [4], most of them represented by microalgae. Compared to other renewable feedstocks for bio-lipid production, like rapeseed or soybeans, microalgae show several beneficial characteristics. In contrast to vascular plants, microalgae exhibit high growth rates at low area consumption. Lipid contents higher than 50% are reported for various species and can be controlled by the composition of the cultivation medium. A nitrogen starvation, for

✉ Jan Lorenzen
jan.lorenzen@tum.de

¹ Department of Chemistry, Technical University of Munich, Lichtenbergstrasse 4, 85748 Garching, Germany

² Hopfenveredlung St. Johann GmbH & Co. KG, Auenstr. 18-20, 85283 Wolnzach, Germany

³ Clariant Produkte (Deutschland) GmbH, Ostenrieder Str. 15, 85368 Moosburg, Germany

example, leads to a significant increase in lipid-storage in different microalgae [5–7]. In addition to these arguments, one of the most important advantage of microalgae is the lack of competition with agricultural activities. In this context, it is also important to mention that many lipid-producing microalgae can be cultivated in brackish or salt water, which secures valuable freshwater resources for human activity.

One of the main obstacles to overcome in the usage of microalgae derived lipids is to find a method for lipid extraction that is efficient, economically relevant and environmentally friendly. One of the most common lipid extraction methodologies is unspecific organic solvent extraction according to the work of Bligh and Dyer [8]. Other methods combine solvent and/ or enzyme assisted techniques that are either highly toxic (n-hexane, methanol) or energetically inefficient [9]. By contrast, lipid extraction with supercritical fluids, especially supercritical carbon dioxide, has recently risen as a powerful industrial tool for environmentally friendly lipid recovery from biomass. Recently, many reports have discussed the extraction of microalgae lipids with supercritical carbon dioxide in small pilot plants, in the majority of the cases with a polar co-solvent (e.g., ethanol or water [10, 11]), an approach that cannot be transformed to industrial scale due to legislative safety regulations.

In this study, we optimized the performance of an industrially relevant supercritical carbon dioxide extraction process for the recovery of lipids from dried microalgae biomass for the first time. The extraction of microalgae lipids with supercritical carbon dioxide was performed in a pilot plant according to European industrial standards for large

scale supercritical fluid extractions (ATEX directives). Furthermore, we present a subsequent purification procedure for the crude microalgae lipid extracts, to provide a lipid fraction that is applicable for bio-lubricant/bio-fuel and cosmetic applications.

Materials and methods

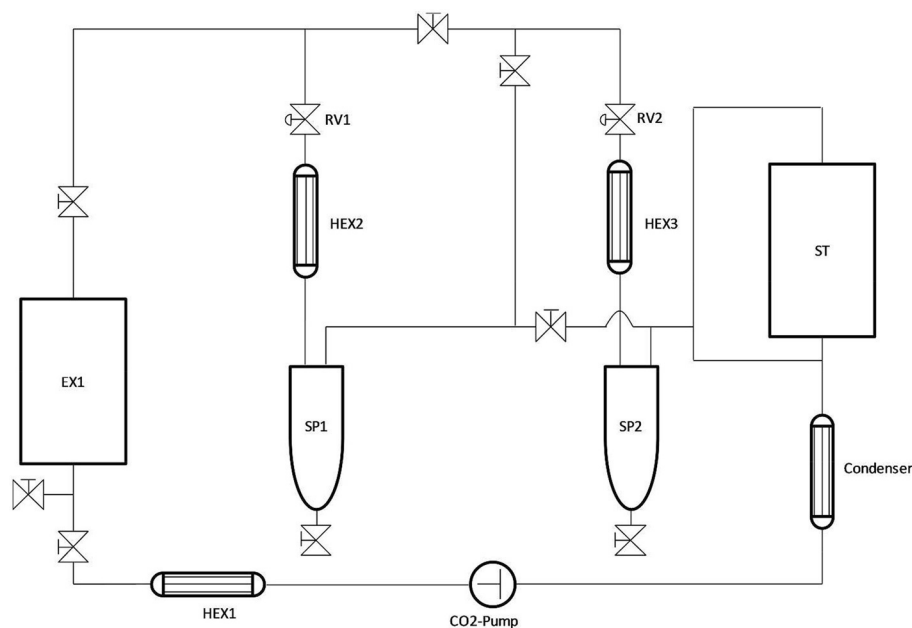
Strains and cultivation

Two different batches of algae biomass have been analyzed. The first batch was provided by Hochschule Anhalt, a heterologous culture consisting of 85–90% *Scenedesmus obliquus*, low percentages of *Chlorella vulgaris* and *Chlorella kessleri* as well as traces of *Chlorella vacuolatus*. The algae were cultivated under non-limiting conditions with natural sunlight illumination. The second batch analyzed was an unialgal culture of *Scenedesmus obtusiusculus*, cultivated in BG-11 medium under non-limiting conditions, using LED-assisted natural sunlight illumination. After the cultivation period, the cells were harvested from the cultivation broth, cracked by high pressure homogenization and lyophilized.

Conventional solvent extraction

The conventional extraction of lipids from microalgae biomass was performed according to Bligh and Dyer [8], with hexane as single solvent for 8 h.

Supercritical carbon dioxide (SCCO₂) extraction



Liquid CO₂ from the storage tank (ST) is pressurized by a CO₂-pump and heated to the extraction temperature by a heat exchanger (HEX 1). Subsequently, the CO₂ flows in the extraction vessel (EX1) containing the biomass. The CO₂/extract mixture is separated by controlled pressure reduction under simultaneous warming by heat exchangers (HEX2, HEX3) into a CO₂ vapour and an extract phase (separators SP1, SP2). The extracts are removed from the process while the gaseous CO₂ remains in the process. Afterwards, the CO₂ is liquefied by a condenser and recirculated.

All extractions were performed with sample sizes from 650 to 1300 g of lyophilized algae biomass. In terms of the high amount of biomass required for the extraction in the pilot plant, not all experiments could be carried out in duplicates. The online bentonite bleaching was only tested on the biomass of the unialgal *S. obtusiusculus* culture. The tests were focused on this strain, because it showed the most promising process parameters in terms of cultivation stability and biomass yields and therefore became the leading strain in the Advanced Biomass Value (ABV) project.

Purification and analysis of microalgae extracts

Lipid analysis

The direct transesterification of the algae derived lipids was performed according to a modified protocol of Griffiths et al. [12] with the following modifications: replacement of the C17-TAG by a C12-TAG, replacement of BF3 methanol by a HCL-methanol solution, and the C19-ME was omitted. Subsequently, the resulting fatty acid methyl ester (FAME) extract was injected into a Thermo Scientific™ TRACE™ Ultra Gas Chromatograph coupled to a Thermo DSQ™ II mass spectrometer and the Triplus™ Autosampler injector. Column: Stabilwax® fused silica capillary (30 m × 0,25 mm, film thickness 0.25 µm). (Program: initial column temperature 50 °C, increasing (4 °C/min) up to a final temperature of 250 °C. Carrier gas: hydrogen, flow rate 3.5 mL/min.) Peaks were identified by comparison to a marine oil standard (Restek) or by specific molecular masses detected.

Purification of crude micro algae extracts

The lipids were purified with an adsorbent based on montmorillonite. In a column with n-hexane 20 g Tonsil 510® from Clariant Produkte (Deutschland) GmbH were filled and given 10 min to swell in the solvent. 2–3 g algae oil were applied to the column and given time to sink completely into the adsorbent. The elution was done with n-hexane until 150 ml eluate was collected. After removing the solvent with a rotary evaporator and drying the oil at

Table 1 Adapted temperature and pressure profiles of astaxanthin extractions, applied to mixed, lyophilized *Scenedesmus* biomass and the corresponding extraction yields after SCCO₂ extraction and soxhlet extraction of the spent material

Extraction pressure (MPa)	Extraction temp. (°C)	CO ₂ : biomass ratio	Extraction yield (% w/w)	Soxhlet yields of spent material (% w/w)
30	50	100	6.9	1.2
50	60	100	6.7	0.5
60	60	200	5.8	0.9
80	80	100	7.6	0.2

Extraction time 540 min

110 °C for 1 h, the oil was analyzed via inductively coupled plasma optical emission spectroscopy (ICP-OES) with a Perkin Elmer Optima 3300 DV, analog to DIN EN ISO 11885. The samples were dissolved in kerosene.

Results

Effect of pressure and temperature on extraction yield

The major points of regulation during the process of SCCO₂ extraction are changes in extraction temperature and the applied pressure. For the first experiments, temperature and pressure profiles established in the pilot plant from astaxanthin extraction were tested on the lyophilized biomass of the mixed *Scenedesmus* culture (Table 1).

The different temperature and pressure profiles resulted in comparable quantities of extracted lipids, but showed large differences in the quality of the extracts. The extracts obtained from the profiles with lower temperature and pressure were unclear, greenish-brownish, viscous liquids, whereas the extracts gained from the profiles with high temperature and pressure appeared as very dark brownish, almost black and extremely viscous substance. For most of the downstream applications of the extracted algae lipid fractions, a clear and homogeneous extract is required. In terms of developing an economically and ecologically balanced extraction process and to obtain a more clear and homogeneous extract, the following experiments were carried out under milder conditions (Table 2).

The milder extraction conditions applied to the biomass samples resulted in lipid yields between 6.5 and 8.3% (w/w), suggesting that there is no statistically relevant distinction in the extraction efficiency compared to the extraction profiles applied before (Table 1). Although equal quantities were obtained, the quality of the extracts strongly improved. The obtained extracts are clear, homogenous liquids with slightly different colors. The extracts from the profiles 1 and 3 had a greenish color, while the extracts

Table 2 Different extraction profiles applied to mixed, lyophilized *Scenedesmus* biomass and the corresponding extraction yields after SCCO₂ extraction and soxhlet extraction of the spent material

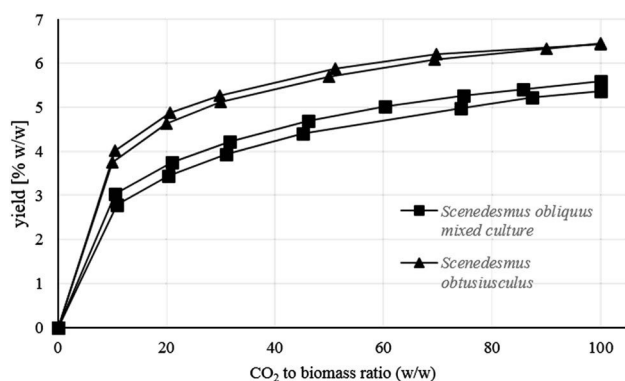
Profile	Extraction pressure (MPa)	Extraction temp. (°C)	CO ₂ : biomass ratio	Extraction yield (% w/w)	Soxhlet yields of spent material (% w/w)
1	7	20	20	6.5	1.0
2	7	20	100	6.6	2.0
3	12	20	20	6.6	1.8
4	12	20	100	8.3	2.1
5	12	20	100	7	2.8
	15	20	100	6.6	3.0
	15	20	100	6.5	2.8

Extraction time 540 min

Table 3 Extraction parameters applied to *Scenedesmus obtusiusculus* biomass (unialgal culture) and the corresponding extraction yields after SCCO₂ extraction and soxhlet extraction of the spent material (in duplicate)

Extraction pressure (MPa)	Extraction temp. (°C)	CO ₂ : biomass ratio	Extraction yield (% w/w)	Soxhlet yields of spent material (% w/w)
12	20	100	6.4	0.5
12	20	100	6.4	0.9

Extraction time 540 min

**Fig. 1** Algae lipid extraction yields from two samples of a mixed *Scenedesmus obliquus* culture (square markers) and from two samples of an unialgal *Scenedesmus obtusiusculus* culture (triangle markers), expressed as a function of increasing CO₂ to biomass ratio. Extraction time 840 min

from the other three profiles showed a more brownish to orange color.

The extraction profile 4 showed the best results in this experimental set-up, with respect to the extraction efficiency and sustainability, and was employed for subsequent extractions.

As a proof of concept the extraction profile was applied to an unialgal *S. obtusiusculus* culture (Table 3) and was used to monitor the extraction efficiency (Fig. 1).

The transferability of the extraction profile to other microalgae species within the *Scenedesmus* family is depicted in Table 3. Both quantity and quality of the extracts were comparable to those of the mixed *S. obliquus* culture extracted previously.

The extraction curves in Fig. 1 depict the extraction yields (in % w/w) of four different samples, two samples of a mixed *S. obliquus* culture (square markers) and two samples of an unialgal *S. obtusiusculus* culture (triangle markers), as a function of the CO₂ to biomass ratio. The four extraction curves follow a sigmoidal function and are almost reaching a plateau of maximum lipid yield at a ratio of 100 (CO₂/biomass), matching the results shown in Table 1. In addition, the technical duplicates of the extraction curves demonstrate that the extraction method is reproducible.

Microalgae extract analysis

Fatty acid composition of extracts obtained from different extraction profiles

The analysis of the fatty acid (FA) composition of the microalgae extracts (Table 4) showed no significant difference for the extraction profiles tested. The major compounds in these extracts are linolenic acid (C18:3), hexadecatetraenoic acid (C16:4), linoleic acid (C18:2), oleic acid (C18:1) and palmitic acid (C16:0). The FA profile of the unialgal culture of *S. obtusiusculus* was similar to the one from the mixed *S. obliquus* culture in its major components, but the percentage of FAs identified from the total lipid extract is reduced by 20–30%. The obtained FA profiles accord with previously published profiles.


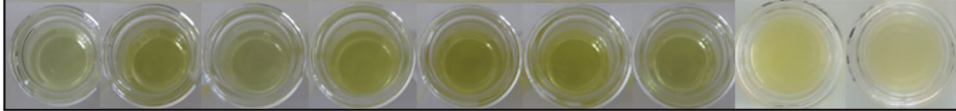
Table 4 Major fatty acid (FA) components in microalgae extracts from different extraction profiles, expressed as percentage of the total lipid extract (mean ± standard deviation)

Profile	<i>S. obliquus</i>					<i>S. obtusiusculus</i>			
	1	2	3	4	5	4		4	
Pressure (MPa)	7	7	12	12	12	15	15	12	
CO ₂ : biomass ratio	20	100	20	100	100	100	100	100	
C14	0.29±0.01	0.27±0.02	0.27±0.01	0.29±0.01	0.30±0.01	0.29±0.02	0.29±0.02	0.16±0.00	
C16	6.30±0.19	6.38±0.09	6.46±0.22	6.01±0.05	5.68±0.03	6.56±0.09	6.07±0.02	3.25±0.05	
C16:1 cis ω7	0.72±0.02	0.72±0.01	0.74±0.03	0.74±0.03	0.78±0.02	0.77±0.01	0.77±0.01	0.45±0.01	
C16:1 ω9	1.40±0.06	1.83±0.02	1.53±0.05	2.16±0.03	2.03±0.02	2.01±0.00	1.89±0.01	0.41±0.03	
C16:2 ω6	1.24±0.04	1.31±0.02	1.27±0.04	1.43±0.02	1.48±0.07	1.44±0.02	1.41±0.01	0.71±0.01	
C16:3 ω3	2.31±0.09	2.54±0.02	2.28±0.04	2.77±0.03	2.77±0.03	2.72±0.02	2.70±0.01	1.13±0.02	
C16:4 ω3	9.81±0.33	11.93±0.02	9.56±0.55	13.25±0.09	13.28±0.44	12.66±0.23	12.53±0.16	3.91±0.07	
C18	0.13±0.00	0.15±0.00	0.14±0.00	0.16±0.00	0.15±0.01	0.15±0.00	0.14±0.00	0.17±0.01	
C18:1 ω9	6.59±0.14	7.02±0.08	6.93±0.23	7.43±0.08	7.45±0.07	7.24±0.09	7.25±0.07	4.09±0.03	
C18:1 ω7	1.20±0.02	1.28±0.01	1.25±0.04	1.38±0.04	1.38±0.01	1.34±0.02	1.34±0.03	0.79±0.00	
C18:2 ω6	9.04±0.18	9.75±0.11	9.18±0.05	10.20±0.07	10.21±0.08	9.94±0.15	9.94±0.10	6.93±0.07	
C18:3 ω3	24.78±0.44	27.44±0.24	24.75±0.59	28.12±0.16	28.44±0.28	27.69±0.35	27.75±0.07	20.62±0.29	
C18:4 ω3	2.26±0.09	2.81±0.02	2.25±0.12	3.02±0.03	3.07±0.01	2.96±0.05	2.95±0.01	0.88v ±0.02	
C20	ND	ND	ND	0.03±0.04	0.02±0.00	0.02±0.00	ND	ND	
C20:1 ω9	0.05±0.04	0.10±0.01	0.05±0.04	0.08±0.00	0.08±0.01	0.08±0.01	0.10±0.01	ND	
FA yield	65.72±1.58	73.53±0.37	66.66±0.83	77.07±0.48	77.09±0.87	75.87±0.59	75.11±0.09	43.52±0.52	

All extractions were carried out at 20 °C

FA yield percentage of FAs from total lipids, ND not detectable

Table 5 Microalgae oils obtained from different extraction profiles before (crude) and after (purified) the processing with a bentonite

profile	<i>S. obliquus</i>					<i>S. obtusiusculus</i>			
	1	2	3	4	5	4		4+ bentonite	
pressure [MPa]	7	7	12	12	12	15	15	12	12
CO ₂ : biomass ratio	20	100	20	100	100	100	100	100	100
crude microalgae oil									
purified microalgae oil									

Processing of microalgae oils with bentonites

The microalgae lipid fractions obtained from the mild extraction profiles show a higher quality than the ones obtained under harsh extraction conditions. Anyway the coloring of the extracts implements a relatively high amount of substances like chlorophylls and carotenoids. As

these substances could be problematic for any downstream usage of the microalgae oils, e.g., in technical applications, the lipid fractions were processed with the bentonite Tonsil 510®.

The results of a single treatment of microalgae oils with the bentonite are shown in Table 5. After the processing the lipid fractions appear as a clear, liquid oil, suggesting that

Table 6 Ion analysis of microalgae lipid fractions obtained from different extraction profiles, before (crude) and after (cleaned) a bentonite processing (in mg/kg)

Profile	<i>S. obliquus</i>												<i>S. obtusiusculus</i>											
	1		2		3		4		5		12		15		4		12		100					
Pressure (MPa)	7	7	12	12	12	12	100	100	100	100	100	100	100	100	100	100	100	100	100	100				
CO ₂ : biomass ratio	20	100	20	20	20	20	100	100	100	100	100	100	100	100	100	100	100	100	100	100				
Al	Crude	Cleaned	Crude	Cleaned	Crude	Cleaned	Crude	Cleaned	Crude	Cleaned	Crude	Cleaned	Crude	Cleaned	Crude	Cleaned	Crude	Cleaned	Crude	Cleaned				
	0.9	<0.5	1.9	<0.5	5	<0.5	5.5	<0.5	5.4	<0.5	3.8	<0.5	3.8	<0.5	3.3	<0.5	3.3	<0.5	0.8	<0.5				
Ca	6.9	1.3	22	0.9	19	0.9	31	0.5	33	1.2	19	1.2	19	15	0.8	1.4	1.9	1.9	1.4	1.9				
Cu	<0.5	2	<0.5	0.9	<0.5	<0.5	<0.5	1	<0.5	<0.5	<0.5	<0.5	<0.5	<0.5	<0.5	<0.5	<0.5	<0.5	0.7	<0.5				
Fe	<0.5	<0.5	<0.5	<0.5	<0.5	<0.5	<0.5	<0.5	<0.5	<0.5	<0.5	<0.5	<0.5	<0.5	<0.5	<0.5	<0.5	<0.5	0.9	<0.5				
K	<0.5	1.9	<0.5	2.8	<0.5	0.8	<0.5	0.8	<0.5	0.7	<0.5	<0.5	<0.5	1	<0.5	0.7	<0.5	<0.5	0.7	<0.5				
Mg	1	<0.5	<0.5	0.7	<0.5	<0.5	<0.5	<0.5	<0.5	<0.5	<0.5	<0.5	<0.5	<0.5	<0.5	<0.5	<0.5	<0.5	<0.5	<0.5				
Nia	<5	10	<5	9	<5	5	<5	6	<5	6	<5	<5	<5	<5	<5	<5	<5	<5	10	<5				
P	21	<4	18	<4	35	<4	34	<4	30	<4	31	<4	31	30	<4	<4	30	<4	<4	<4				

the coloring substances like chlorophyll and carotenoids have been completely removed from the extracts.

Ion analysis of microalgae lipid extracts

For a further comparison of the microalgae extracts before and after the processing with a bentonite, the amounts of selected ions were analyzed (Table 6).

The results in Table 6 show no significant differences between the applied extraction profiles. All analyzed elements occur in very low amounts (e.g., maximum 33 mg/kg for calcium or 35 mg/kg for phosphor). After treating the samples with the bentonite, the amounts of calcium and phosphor strongly decrease whereas the amount of potassium, sodium and copper slightly increase.

SCCO₂ with online bentonite processing

Based on the results shown above an online processing of microalgae biomass with bentonite was tested. The bentonite was implemented directly into the extraction vessel and the resulting extracts were compared with extracts obtained from standard extractions. The total lipid yield of the extraction with implemented bentonite was with 6.7% (w/w) in the range of the standard extractions. The color and viscosity was also similar to the extracts obtained with the extraction profile 4 obtained before the subsequent bentonite bleaching.

The comparison of the microalgae extracts gained from standard extraction and online bentonite processing shows minor differences in the FA composition. The amount of polyunsaturated fatty acids (PUFA) is slightly increased, but the accuracy of the measurements is lower (Table 7).

The comparison of the ion analysis between microalgae oils gained from standard extraction and online bentonite processing is shown in Table 8. The results show similar amounts of the analyzed elements in both samples, before and after the subsequent cleaning procedure. The ion concentration does not significantly differ between the analyzed oils from standard extraction and online bentonite processing.

Discussion

Effect of pressure and temperature on extraction yield

The different extraction yields shown in the Tables 1 and 2 all result from the same biomass processed, but small differences, especially in the soxhlet-yields after the extraction, are detectable. These differences are a result of a marginal loss of lipids on the inner surfaces of the processing equipment. The combination of this low loss and slightly

Table 7 Major fatty acid (FA) components in microalgae extracts from standard extractions (standard) compared to extractions with online bentonite processing (bentonite), expressed as percentage of the total lipid extract (mean \pm standard deviation)

Profile	<i>S. obtusiusculus</i>	
	Standard	Bentonite
C14	0.16 \pm 0.00	0.21 \pm 0.04
C16	3.25 \pm 0.05	4.69 \pm 1.00
C16:1 cis ω 7	0.45 \pm 0.01	0.55 \pm 0.07
C16:1 ω 9	0.41 \pm 0.03	1.07 \pm 0.44
C16:2 ω 6	0.71 \pm 0.01	1.09 \pm 0.29
C16:3 ω 3	1.13 \pm 0.02	1.66 \pm 0.42
C16:4 ω 3	3.91 \pm 0.07	7.07 \pm 2.58
C18	0.17 \pm 0.01	0.18 \pm 0.01
C18:1 ω 9	4.09 \pm 0.03	4.98 \pm 0.69
C18:1 ω 7	0.79 \pm 0.00	0.96 \pm 0.16
C18:2 ω 6	6.93 \pm 0.07	8.51 \pm 1.24
C18:3 ω 3	20.62 \pm 0.29	24.3 \pm 3.11
C18:4 ω 3	0.88 \pm 0.02	1.67 \pm 0.68
C20	ND	ND
C20:1 ω 9	ND	ND
FA yield	43.52 \pm 0.52	56.94 \pm 10.66

All extractions were carried out at 20 °C

FA yield percentage of FAs from total lipids, ND not detectable

Table 8 Ion analysis of microalgae lipid fractions obtained from standard extraction and online bentonite processing of *S. obtusiusculus*, before (crude) and after (cleaned) a final bentonite processing (in mg/kg)

Profile	<i>S. obtusiusculus</i>			
	4		4	
	Crude	Cleaned	Crude	Cleaned
Al	0.8	<0.5	1.2	<0.5
Ca	1.4	1.9	1.7	0.7
Cu	0.7	<0.5	0.6	<0.5
Fe	0.9	<0.5	1.2	<0.5
K	0.7	<0.5	0.6	<0.5
Mg	<0.5	<0.5	0.6	<0.5
Na	10	<5	<5	<5
P	<4	<4	<4	8.5

differing batch sizes leads to differences in the lipid yields in a low percentage range. This effect can be reduced by increasing batch sizes and continuous extractions in the same plant.

The dark extracts obtained from the first extractions under harsh conditions suggest that the combination of high temperature and pressure lead to a denaturation of some algae cell components. The different coloring of the

extracts after extractions under milder conditions can be explained by the varying concentrations of chlorophyll (green) and carotenoids (reddish-brown) inside the samples. This hypothesizes an increasing extraction efficiency of carotenoids by an increased CO₂ to biomass ratio.

The maximum lipid yields obtained with the applied extraction protocol (Tables 1, 2, 3) are relatively low, compared to other published data for *S. obliquus* [11]. This can be explained by the single use of carbon dioxide as solvent for the extraction. The technique of using polar co-solvents to increase the extraction yields is commonly found in the literature [13]. An implementation of this technique into existing industrial extraction facilities is, with respect to the current ATEX directives (2014/34/EU), extremely complicated and expensive. In addition, it is important to mention that the processed microalgae have not been cultivated under optimal conditions for lipid production. Under nitrogen starving conditions, an increase of intracellular lipids of 200% is reported for *S. obtusiusculus* [14]. Furthermore, there is a big difference between the sample sizes processed in this work (650–1300 g dried biomass) and the data published so far. Since most of the data published result from sample sizes of 0.5–1 g of dried biomass in laboratory-scale plants, it is unclear if these results are reproducible at a technically relevant scale.

Processing of microalgae oils with bentonites

For any downstream application of microalgae oils a high quality and purity is essential. High concentrations of trace elements, for example, are not only problematic for chemical catalysts [15], but can also influence the activity of biological catalysts. Therefore, a concentration of trace elements higher than 5 ppm should not be exceeded. The scalable cleaning procedure applied to the microalgae lipid fractions, using bentonites, showed excellent results (Table 5). Besides the visible removal of the coloring compounds inside the microalgae extracts, the processing with bentonite also reduces the concentration of trace elements (Table 6) under the level of 5 ppm.

SCCO₂ with online bentonite processing

The online bleaching of the microalgae extracts by implementing the bentonite directly into the extraction vessel had only a minor visual effect on the extracts (Table 5), although the bentonite showed a strong green coloring after the extraction. However, the online processing had an effect on the subsequent cleaning step. The extracts obtained from the online bleaching showed a lower viscosity and enhanced flow behaviour on the cleaning column. The analysis of the corresponding FA profiles (Table 7) showed that the major components were similar to standard

extractions. Nevertheless, further optimization steps for the online bleaching, e.g., differing amounts of bentonite inside the extraction vessel, need to be tested to reach higher purities for microalgae extracts.

Conclusion

In this study, we optimized the process for SCCO₂ extraction of algae biomass under industrially relevant conditions for the first time. All reactions were carried out in an industrial pilot plant (operated under ATEX directives) to maximize the lipid extraction performance from dried microalgae biomass and to obtain a high quality product with minimized concentrations of organic and inorganic contaminants. The mild extraction conditions (12 MPa pressure, a temperature of 20 °C and a CO₂ to biomass ratio of 100) applied in the optimized process resulted in a high lipid recovery of up to 92% w/w of total lipids (containing up to 59% w/w of PUFAs) from the microalgae biomass. To utilize the crude microalgae lipid fractions for following downstream applications, a scalable purification procedure, using the bentonite type industrial adsorber Tonsil 510®, was successfully integrated into the process. The microalgae lipid fractions generated by this procedure comply with all qualifications as a feedstock stream to in end-product formulations particularly for biolubricant and nutraceutical applications.

Acknowledgements We gratefully acknowledge the financial support by the German Federal Ministry of Education and Research (Project: Advanced Biomass Value, 03SF0446C). We also want to thank Martina Haak for her excellent technical support in the analytics.

Open Access This article is distributed under the terms of the Creative Commons Attribution 4.0 International License (<http://creativecommons.org/licenses/by/4.0/>), which permits unrestricted use, distribution, and reproduction in any medium, provided you give appropriate credit to the original author(s) and the source, provide a link to the Creative Commons license, and indicate if changes were made.

References

1. Yen HW, Yang SC, Chen CH, Jesisca, Chang JS (2015) Supercritical fluid extraction of valuable compounds from microalgal biomass. *Bioresour Technol* 184:291–296. doi:[10.1016/j.biortech.2014.10.030](https://doi.org/10.1016/j.biortech.2014.10.030)
2. Santos-Sanchez NF, Valadez-Blanco R, Hernandez-Carlos B, Torres-Arino A, Guadarrama-Mendoza PC, Salas-Coronado R (2016) Lipids rich in omega-3 polyunsaturated fatty acids from microalgae. *Appl Microbiol Biotechnol* 100(20):8667–8684. doi:[10.1007/s00253-016-7818-8](https://doi.org/10.1007/s00253-016-7818-8)
3. Bellou S, Baeshen MN, Elazzazy AM, Aggeli D, Sayegh F, Aggelis G (2014) Microalgal lipids biochemistry and biotechnological perspectives. *Biotechnol Adv* 32(8):1476–1493. doi:[10.1016/j.biotechadv.2014.10.003](https://doi.org/10.1016/j.biotechadv.2014.10.003)
4. Guiry MD (2012) How many species of algae are there?. *J Phycol* 48(5):1057–1063. doi:[10.1111/j.1529-8817.2012.01222.x](https://doi.org/10.1111/j.1529-8817.2012.01222.x)
5. Rodolfi L, Chini Zittelli G, Bassi N, Padovani G, Biondi N, Bonini G, Tredici MR (2009) Microalgae for oil: strain selection, induction of lipid synthesis and outdoor mass cultivation in a low-cost photobioreactor. *Biotechnol Bioeng* 102(1):100–112. doi:[10.1002/bit.22033](https://doi.org/10.1002/bit.22033)
6. Griffiths MJ, van Hille RP, Harrison ST (2014) The effect of nitrogen limitation on lipid productivity and cell composition in *Chlorella vulgaris*. *Appl Microbiol Biotechnol* 98(5):2345–2356. doi:[10.1007/s00253-013-5442-4](https://doi.org/10.1007/s00253-013-5442-4)
7. Griffiths MJ, van Hille RP, Harrison STL (2011) Lipid productivity, settling potential and fatty acid profile of 11 microalgal species grown under nitrogen replete and limited conditions. *J Appl Phycol* 24(5):989–1001. doi:[10.1007/s10811-011-9723-y](https://doi.org/10.1007/s10811-011-9723-y)
8. Bligh EG, Dyer WJ (1959) A rapid method of total lipid extraction and purification. *Can J Biochem Physiol* 37(8):911–917
9. Li Y, Naghdi FG, Garg S, Adarme -Vega TC, Thuracht KJ, Ghafor WA, Tannock S, Schenk PM (2014) A comparative study: the impact of different lipid extraction methods on current microalgal lipid research. *Microb Cell Fact*. doi:[10.1186/1475-2859-13-14](https://doi.org/10.1186/1475-2859-13-14)
10. Mendes RL, Nobre BP, Cardoso MT, Pereira AP, Palavra AF (2003) Supercritical carbon dioxide extraction of compounds with pharmaceutical importance from microalgae. *Inorg Chim Acta* 356:328–334. doi:[10.1016/s0020-1693\(03\)00363-3](https://doi.org/10.1016/s0020-1693(03)00363-3)
11. Solana M, Rizza CS, Bertuccio A (2014) Exploiting microalgae as a source of essential fatty acids by supercritical fluid extraction of lipids: comparison between *Scenedesmus obliquus*, *Chlorella protothecoides* and *Nannochloropsis salina*. *J Supercrit Fluids* 92:311–318. doi:[10.1016/j.supflu.2014.06.013](https://doi.org/10.1016/j.supflu.2014.06.013)
12. Griffiths MJ, van Hille RP, Harrison ST (2010) Selection of direct transesterification as the preferred method for assay of fatty acid content of microalgae. *Lipids* 45(11):1053–1060. doi:[10.1007/s11745-010-3468-2](https://doi.org/10.1007/s11745-010-3468-2)
13. Cheng CH, Du TB, Pi HC, Jang SM, Lin YH, Lee HT (2011) Comparative study of lipid extraction from microalgae by organic solvent and supercritical CO₂. *Bioresour Technol* 102(21):10151–10153. doi:[10.1016/j.biortech.2011.08.064](https://doi.org/10.1016/j.biortech.2011.08.064)
14. Schulze C, Reinhardt J, Wurster M, Ortiz-Tena JG, Sieber V, Mundt S (2016) A one-stage cultivation process for lipid- and carbohydrate-rich biomass of *Scenedesmus obtusiusculus* based on artificial and natural water sources. *Bioresour Technol* 218:498–504. doi:[10.1016/j.biortech.2016.06.109](https://doi.org/10.1016/j.biortech.2016.06.109)
15. Bartholomew C (2001) Mechanisms of catalyst deactivation. *Appl Catal A* 212(1–2):17–60

Rhodococcus erythropolis Oleate Hydratase: a New Member in the Oleate Hydratase Family Tree – Biochemical and Structural Studies

Heterogeneous & Homogeneous & Bio- & Nano-

CHEM **CAT** CHEM

CATALYSIS



2/2018

Cover Feature:

J. Lorenzen, R. Driller et al.

Rhodococcus erythropolis Oleate Hydratase: a New Member in the Oleate Hydratase Family Tree – Biochemical and Structural Studies

A Journal of



WILEY-VCH

www.chemcatchem.org

Rhodococcus erythropolis Oleate Hydratase: a New Member in the Oleate Hydratase Family Tree—Biochemical and Structural Studies

Jan Lorenzen^{+, [a]} Ronja Driller^{+, [b]} Ayk Waldow,^[b] Farah Qoura,^[a] Bernhard Loll,^{*[b, c]} and Thomas Brück^{*[a]}

Recently, the enzyme family of oleate hydratases (OHs: EC 4.2.1.53) has gained increasing scientific and economic interest, as these FAD-binding bacterial enzymes do not require cofactor recycling and possess high thermal and pH stability. Their products, hydroxy fatty acids, are used in specialty chemical applications including surfactant and lubricant formulations. The “oleate hydratase engineering database”, established by Schmid et al. (2017), divides all OHs into 11 families (HFam1 to

11). To date, only two crystal structures of homodimeric OHs from the families HFam2 and HFam11 have been reported. In this study, we biophysically characterized an OH belonging to the HFam3 family, originating from the marine bacterium *Rhodococcus erythropolis*, for the first time. The crystal structure revealed that this new OH (OhyRe) surprisingly is a monomer in its active form. This particular feature provides new avenues for enzyme engineering and recycling through immobilization.

Introduction

Unsaturated fatty acids are toxic to several bacteria owing to their surfactant properties, the destabilization of membranes, and the inhibitory effect that unsaturated fatty acids have on fatty acid biosynthesis.^[1] Hence, mechanisms have evolved to counteract these effects. On exposure of organisms to unsaturated fatty acids, such as linoleic acid or oleic acid, they are hydrogenated and become saturated fatty acids. An intermediate step in this hydration process is catalyzed by fatty acid hydratases.^[2] Hydration of unsaturated fatty acids has so far only been identified in Gram-negative and Gram-positive bacteria^[1a] and is mediated by hydratases.

Hydratases are a group of lyases that catalyze hydration and dehydration of a substrate.^[3] Even though many hydratases are known, only few oleate hydratases (OHs) have been described.^[2] OHs belong to the group of fatty acid hydratases (EC 4.2.1.53) and convert oleic acid into (*R*)-10-hydroxystearic acid

(10-HSA) (Scheme 1).^[4] To date all characterized OHs bind an FAD cofactor,^[2] albeit the role of FAD remains an enigma.

Two structures of OHs have been reported. One OH from *Lactobacillus acidophilus* (LAH), crystallized in both the apo-state as well as bound to the preferred substrate linoleic acid.^[5] The second structure of an OH (OhyA) has been determined from *Elizabethkingia meningoseptica*, bound to its cofactor FAD (flavin adenine dinucleotide).^[6] Even though LAH and OhyA convert different substrates, both utilize FAD as a cofactor. The bound FAD was oxidized in both hydratases, but reduced FAD led to significantly higher activity in OhyA.^[6]

Most recently, Schmid et al. assembled a “hydratase engineering database” including a total of 2046 protein sequences.^[7] Sequence comparison revealed 11 distinct families (HFam1 to 11) with a sequence identity of 62% within the respective family. The only two structurally characterized OHs, LAH and OhyA fall into two different families, HFam2 and HFam11. For all other families structural information has remained elusive. Remarkably, in regions attributed to the active site, amino acid sequences are not strictly conserved within these families.

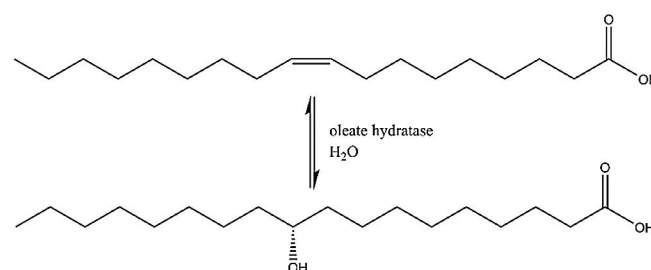
[a] J. Lorenzen,⁺ F. Qoura, Prof. Dr. T. Brück
Professorship for Industrial Biocatalysis
Technical University Munich
Lichtenberg Str. 4, 85748 Garching (Germany)
E-mail: brueck@tum.de

[b] R. Driller,⁺ A. Waldow, Dr. B. Loll
Institute of Chemistry and Biochemistry
Structural Biochemistry
Freie Universität Berlin
Takustr. 6, 14195 Berlin (Germany)
E-mail: loll@chemie.fu-berlin.de

[c] Dr. B. Loll
moloX GmbH
Takustr. 6, 14195 Berlin (Germany)

[*] These authors contributed equally to this work

Supporting information and the ORCID identification number(s) for the author(s) of this article can be found under:
<https://doi.org/10.1002/cctc.201701350>.



Scheme 1. Oleate hydratase (OH) reaction scheme.

Hydratases are particularly interesting for commercial applications since their products, hydroxyl fatty acids, have a wide range of industrial and pharmaceutical applications. They can be utilized in applications for the food industry as precursors of lactones,^[8] as well as an emollient for cosmetics. Further applications include employment as a surfactant or as additives in lubricant formulation and as a green material in polymer science.^[9]

In this study, we aimed at obtaining novel insights into the reaction mechanism of the OhyRe enzyme of *R. erythropolis*, using a combined structural, biophysical and biochemical approach. The OhyRe enzyme was biochemically characterized in terms of optimums for pH and temperature as well as substrate specificity. The kinetic constants were determined for the conversion reaction of oleic acid to 10-HSA. Furthermore, we were able to solve the crystal structure of OhyRe at 2.64 Å resolution. The structure of OhyRe provides structural information for the OH HFam3 family of OHs for the first time. We have compared the overall architecture as well as structural features of the OhyRe active site to a set of reported OHs. As we identified two key residues, which differed in OhyRe structure, these were replaced by site directed mutagenesis to residues conserved in the other family members. Most interestingly, these conservative amino acid replacements resulted in a strong decrease of hydration activity, indicating that OhyRe may follow a distinct reaction mechanism.

Results & Discussion

Isolation & characterization of OhyRe derived from *R. erythropolis*

R. erythropolis is a Gram-positive, non-motile representative of the nocardiaceae family.^[10] *R. erythropolis* is a wide spread soil bacterium which is mainly found in marine habitats, from coastal to deep sea sediments,^[11] and exhibits a broad range of biochemically interesting enzymes.^[12] As the genome of *R. erythropolis* has recently been deciphered,^[13] we have performed sequence specific genome mining, targeting alternative OH activities in this extremophile organism.

To this end we have identified the 1.68 kB sequence related to known OHs albeit at a very low sequence identity level of a maximum 38%. The gene for the putative OH was termed OhyRe, according to the nomenclature used by Bevers et al.^[4a] for the *Elizabethkingia meningoseptica* OH ohyA. The corresponding OhyRe protein is composed of 559 amino acids with a calculated molecular weight of 66.3 kDa. The N-terminally His₆-tagged protein was successfully expressed in *Escherichia coli* BL21(DE3) cells. Initial activity tests with the crude extract resulted in high conversion rates (approximately 85%) from oleic acid to 10-HSA, confirming that OhyRe indeed displayed OH activity. To further characterize the enzyme, we have devised a Ni²⁺-affinity purification protocol. After final His-Trap HP affinity chromatography, the purified enzyme was colorless and lost its hydration activity (Figure S1). This observation suggested a loss of the FAD cofactor, which has been uniformly reported to be essential for the hydration activity in all known

OHs. Moreover, the only reported loss of FAD during purification was also associated with a strong decrease in hydration activity.^[5] Therefore, the addition of various FAD concentrations (5 μM to 100 μM) to the purified enzyme preparation has been evaluated to reconstitute the activity of purified OhyRe. The addition of FAD to a final concentration of 20 μM led to the recovery of the enzymatic activity of OhyRe and was applied for all following experiments. After establishing an efficient purification protocol, OhyRe was biochemically characterized.

Initial tests demonstrated that purified OhyRe has a temperature optimum for hydration activity at 28 °C (Figure 1). Interestingly, OhyRe exhibits a relatively wide temperature tolerance with high activity in the low temperature region (72% of maximum at 20 °C) and still moderate activity in the high temperature area (21% of maximum at 45 °C). This wide temperature tolerance might reflect the diversity of the occurrence of *R. erythropolis* from coastal to deep sea habitats.

The determination of the pH optimum (Figure 2) showed a high pH tolerance in a range from pH 5.0 to 8.0 for OhyRe, the highest activity was reached at pH 7.2.

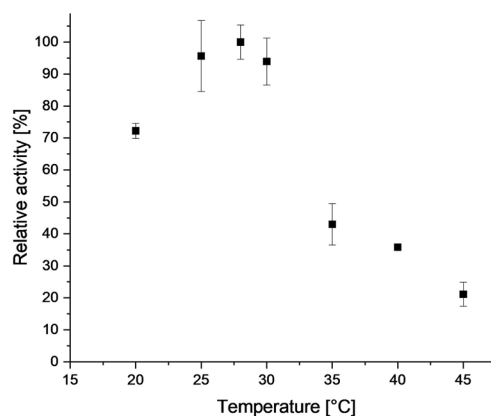


Figure 1. Determination of the temperature optimum for the oleate hydratase (OH) OhyRe from *R. erythropolis* in 20 mM Tris-HCl buffer at pH 7.2. Relative activity is given to the temperature optimum at 28 °C (100%). All experiments were performed in biological duplicates and technical triplicates.

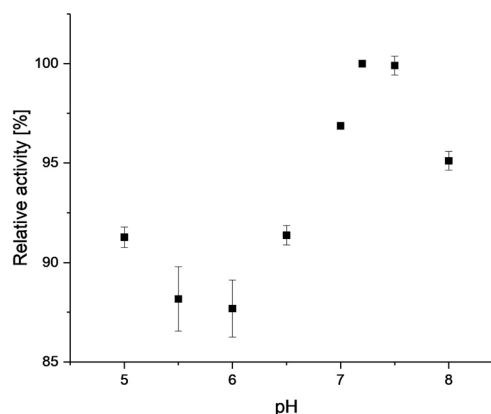


Figure 2. Determination of the pH optimum for the oleate hydratase (OH) OhyRe from *R. erythropolis* at 28 °C. Relative activity is given to the optimum at pH 7.2 (100%). All experiments were performed in biological duplicates and technical triplicates.

Table 1. Tested substrates, identified products and corresponding specific activity of conversion reaction with OhyRe. All experiments were performed in biological duplicates and technical triplicates.

Substrate	Product	Specific activity [nmol mg _{enzyme} ⁻¹ min ⁻¹]	
C16:1 ω7	palmitoleic acid	10-hydroxypalmitic acid	1205 ± 70.6
C18:1 ω9	oleic acid	10-hydroxystearic acid	1266 ± 30.3
C18:2 ω6	linoleic acid	10-hydroxy-12(Z)-octadecenoic acid	156 ± 3.3
C18:3 ω3	α-linolenic acid	10-hydroxy-12,15(Z,Z)-octadecadienoic acid	150 ± 1.7
C18:3 ω6	γ-linolenic acid	10-hydroxy-6,12(Z,Z)-octadecadienoic acid	615 ± 36.0

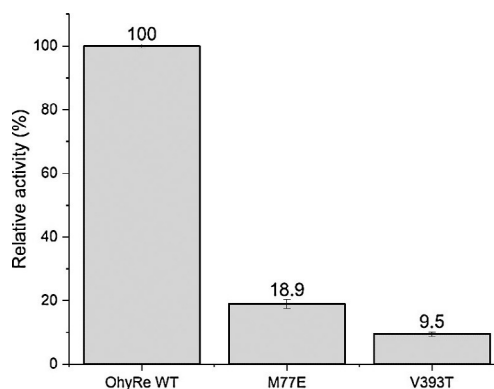
These results correlate with the recommended cultivation conditions for *R. erythropolis* published by the German Collection of Microorganisms and Cell Culture (Leibniz Institute DMSZ).

The substrate spectrum of OhyRe was experimentally determined in reactions with the purified enzyme and different free fatty acids (FFAs) (Table 1). All experiments were performed in biological duplicates and technical triplicates. The enzyme showed neither detectable activity for any saturated fatty acid tested (C14:0 to C18:0), nor for myristoleic acid, vaccenic acid, eicosatrienoic acid and eicosatetraenoic acid, respectively. Low conversion rates could be observed for linoleic acid, α- and γ-linolenic acid. The highest affinity, under the given conditions, was detected for oleic acid, followed by palmitoleic acid. Complex lipids, such as the tested triolein or microalgae derived oils were not converted by the enzyme. These results correspond to published data for other known OHs^[5] and confirm the preference of OHs for the 9-Z double bond in the fatty acid carbon chain. The kinetic parameters were experimentally defined for OhyRe, with oleic acid as the preferred substrate, and resulted in a K_M value of 0.49 ± 0.1 mM and a k_{cat} value of 34 ± 5 min⁻¹.

OhyRe mutants

Engleder et al.^[6] demonstrated, by multiple sequence alignment of 10 OHs, that the catalytically crucial residues are highly conserved within the OH family. The alignment of OhyRe with 14 different OHs (Figure S2) predominantly confirmed this hypothesis, but also depicted two exceptions. Interestingly, two amino acid residues that are highly conserved in all other OHs differ in the sequence of OhyRe, namely the residues M77 and V393. Further structural comparison of OhyRe and OhyA (Figure S3) showed that these residues correlate with the residues E122 and T436 from OhyA, which are responsible for the activation of the water molecule or the binding of the carboxylate,^[6] respectively. A conservative substitution of the two identified residues to the familial conserved residues (M77E, V393T) was executed by site directed mutagenesis and resulted in the effect depicted in Figure 3.

Figure 3 shows the relative hydration activity of the OhyRe wild type enzyme compared to the two constructed mutants M77E and V393T with oleic acid as substrate. The conservative substitution of both residues resulted in a strong decrease in the conversion efficiency from oleic acid to 10-HSA of 81 %

**Figure 3.** Relative conversion activity from oleic acid to 10-HSA from OhyRe wild type enzyme (OhyRe WT), set as 100%, and its respective mutants (M77E, V393T). All experiments were performed in biological duplicates and technical triplicates.

and 90%, respectively. This strong decrease in hydration activity supports the hypothesis that OHs from the HFam3 family might follow a distinct catalytic mechanism.

In comparison to the two other structurally characterized OHs LAH^[5] and OhyA,^[6] OhyRe shows a sequence identity of 35% and 34%, respectively. Beside the low sequence identity, both the LAH and OhyA have large N- and C-terminal amino acid sequence extensions (Figure S4 and 6A,B), which are absent in OhyRe. To understand whether those extensions are common for all other OHs, we performed a sequence alignment (Figure S2). Interestingly, OH sequences can be roughly divided in sequences with amino acid extensions at the N- and the C-termini present or absent. Consequently, this raised the question, whether OhyRe might be structurally different compared to the members of the HFam2 and HFam11 families. Hence we tried to crystallize the protein for structure determination by X-ray crystallography.

Overall structure

We obtained crystals of OhyRe that belong to space group $P6_322$. The diffraction of the OhyRe crystals was anisotropic, resulting in complete data set to a resolution of 2.64 Å. The structure of OhyRe was determined by molecular replacement with two protein chains in the asymmetric unit corresponding to a very high solvent content of about 75%. The structure was refined with good stereochemistry to good R factors

(Table S1, Supporting Information). Both polypeptide chains are practically identical with a root mean square deviation (rmsd) of 0.1 Å for 522 pairs of C α -atoms. The structure is complete, except for the 5 N-terminal residues and a loop region ranging from residue 42 to 67 owing to missing electron density caused by its high flexibility (Figure 4A). No redox cofactor could be identified in the electron density maps. Hence our structure represents the apo-state of OhyRe from *R. erythropolis*.

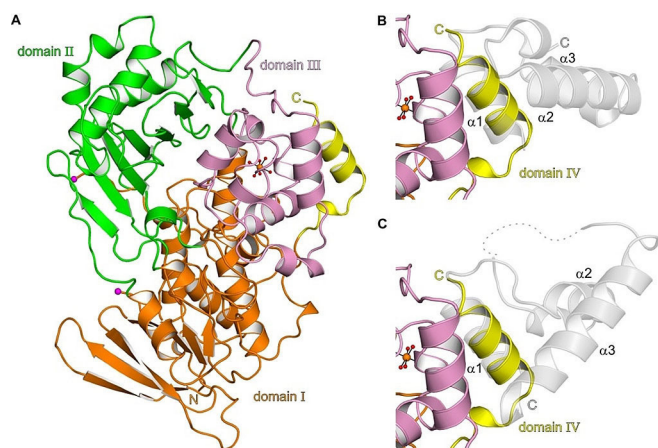


Figure 4. Overall structure of OhyRe in cartoon representation. (A) Domain organization of OhyRe: Domain I in orange, domain II in green, domain III in pink and domain IV in yellow. The bound Mg²⁺ and coordinating waters are shown as orange and red spheres, respectively. Magenta spheres indicate the borders of a flexible linker, ranging from residue 61 to 86, which could not be modelled owing to its flexibility. (B) Zoom onto domain IV of OhyRe with a superposition of OhyRe and LAH, domain IV of LAH is shown in gray. (C) Superposition of OhyRe and OhyA, domain IV of OhyA is shown in gray. Dashed line indicates an un-modelled loop region.

The closest related structures, as analyzed by the DALI software,^[14] are the OHs LAH (PDB-id 4ia6) and OhyA (PDB-id 4uir). OhyRe superimposes with a rmsd of 1.8 Å for 500 pairs of C α -atoms and 1.6 Å for 501 pairs of C α -atoms, respectively. In analogy to the structures of LAH and OhyA, OhyRe is composed of three core domains (residues 1–540; Figure 4A and 5) that are related to other FAD-dependent enzymes. Domain I (residues 6–115, 223–300, 322–344, and 478–540) is a mixed α /

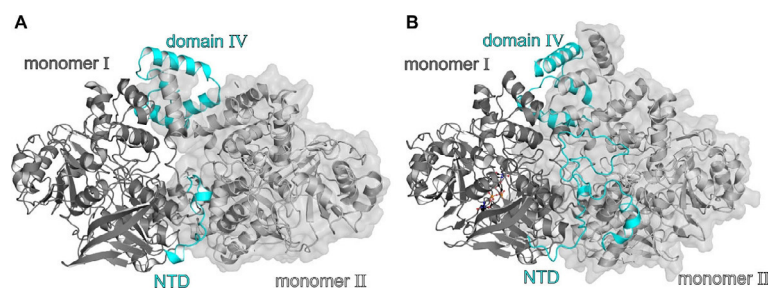


Figure 5. Oligomeric state of oleate hydratases (OHs). (A) LAH monomer I is shown in dark gray. Monomer II in surface and cartoon representation (light gray). The N-terminal domain (NTD) and domain IV in cyan. (B) The NTD OhyA of each monomer meanders into the other monomer.

β domain composed of a parallel five-stranded β -sheet packed between two α -helices on one side and a three-stranded antiparallel β -sheet on the other side (Figure 4A), resembling a variant of the Rossmann fold. Domain II (residues 116–131, 301–321, and 345–477) consists of an antiparallel β -sheet (Figure 4A) flanked by three α -helices defining the cofactor- and substrate-binding site in conjunction with domain I. Domain III (residues 132–222) is exclusively α -helical (Figure 4A) and its fold is structurally related to monoamine oxidases.^[15] Domain IV (residues 541–559) of OhyRe is composed of merely one single α -helix. In contrast to the structures of LAH and OhyA the C-terminal domain is truncated by 32 or 48 residues, respectively. As a consequence two α -helices are absent in domain IV of OhyRe (Figure 4B,C). The structure of LAH has been determined in apo- and product-bound state. Upon substrate recognition and binding the two C-terminal α -helices of domain IV undergo a large conformational change and thereby allow the substrate to enter a cavity that ends at a cleft between domain I and III.^[15]

For both the LAH and OhyA a homodimeric quaternary structure in solution as well as in crystallo has been reported.^[5,6] For other OHs, such as the one from *L. fusiformis*,^[16] *S. maltophilia*^[17] and *M. caseolyticus*,^[18] dimers in solution were reported as well. As analyzed by the PISA server,^[19] OhyRe is a monomer in crystallo. To analyze the situation in solution and to confirm our structural analysis, we performed multi-angle light scattering (MALS) experiments. Our experiments clearly revealed that OhyRe is monomeric in solution (Figure S5). The latter finding is in agreement with our observations for OhyRe assembly in the crystal and strengthens our hypothesis that OHs, lacking N- and C-terminal extensions, are monomers. Additionally we examined whether the extensions might have functional implications. As discussed above, in the structure of LAH, domain IV reflects the C-terminal extension, suggested to be involved in substrate gating. Since the two reported, and our crystal structures cover nearly the complete amino acid sequence of the respective protein, we superimposed the structures and inspected the monomer-monomer interfaces of dimeric LAH and OhyA. Most of the dimer interface is established by residues that reside within the N- or C-terminal extension, including domain IV of LAH (Figure 5A) and OhyA (Figure 5B). In summary, we propose that the presence or absence of N- and C-terminal extensions within the amino acid sequence directly influences the oligomeric state of OHs. In case of OhyRe the extensions are absent and hence the protein is monomeric in solution.

Notably, the crystal structure revealed a coordinated Mg²⁺ ion close to the putative active site of OhyRe (section S1). However, experimental data showed that the Mg²⁺ ion has no influence on the hydration activity of OhyRe.

FAD binding

All characterized OHs utilize FAD as cofactor.^[2] Different roles of the FAD cofactor have been proposed;

direct involvement in catalysis or indirect involvement, having merely a structural role to stabilize the enzyme. In the crystal structure of LAH, no FAD could be located in its binding site.^[5] In contrast, in the crystal structure of OhyA, FAD is bound, but only to one of the two polypeptide chains.^[6] Furthermore a K_d of 1.8×10^{-6} M was determined by isothermal calorimetry.^[6] All indicate a rather low binding affinity of FAD to studied OHs. For our structural studies, we attempted to add FAD prior to the final purification step or to incubate OhyRe with FAD prior to the crystallization experiments. Moreover, we tried to soak FAD in our apo OhyRe crystals. All our attempts to gain structural information of OhyRe bound to FAD remained unsuccessful. A primary sequence analysis reveals the presence of a characteristic recognition sequence GXGXXGX₂E/D for nucleotide binding, also reflected by the Rossmann fold of the protein. A superposition of the structures of OhyA and OhyRe (Figure 6A,B) clearly reveals that the cofactor binding site is large

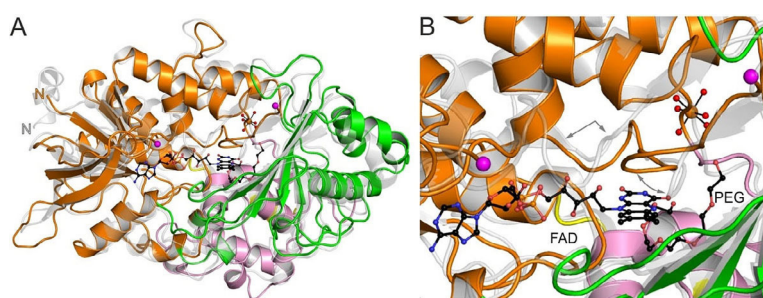


Figure 6. Superposition of OhyRe and OhyA. Same color coding as in Figure 3 A. (A) OhyRe is colored as in Scheme 1 and OhyA in gray. View on the active site of OhyA. Magenta spheres indicate the borders of a flexible linker in OhyRe, ranging from residue 42 to 67, which could not be modelled owing its flexibility. In contrast upon FAD binding in OhyA this loop region is getting structured, indicated by two gray arrows. Moreover a short loop fragment rearranges upon cofactor/substrate binding (gray arrow-headed arc). In general, there would be enough space in OhyRe to accommodate the cofactor as well as the substrate. Solvent exposed on the back of the active site, the Mg^{2+} binding site located. (B) Same view in (A) zoomed on the FAD cofactor binding site of OhyA.

enough to accommodate a FAD molecule. Furthermore in the crystal structure of OhyA a PEG molecule was identified that might mimic a bound oleate molecule. For latter substrate enough space would be in the active site of our OhyRe structure (Figure 6A,B).

Putative active site with catalytically important residues

As mentioned above OHs can be, based on their amino acid sequences, sub-divided in 11 families.^[7] Based on the structure of OhyA, that belongs to the family HFam1,^[7] E122 was proposed to be important for cofactor binding and involvement in catalysis by activating a water molecule for the attack on the partially charged double bond of the substrate.^[6] Latter residue resides within a conserved loop region ¹¹⁸RGGREM¹²³, almost strictly conserved within all OHs. In the sequence of the OhyRe, that falls into the family HFam3, the ultimate and penultimate amino acids are different, but characteristic for members of the largest HFam1 as well HFam3 family.^[7] In the re-

spective loop region, OhyRe has the sequence ⁷³RGGRML⁷⁸. The exchange of OhyA E122 to OhyRe M77, will drastically alter the chemistry and can certainly not activate a water molecule. To investigate the influence of the amino acid at position 77 in OhyRe, we generated a point mutation M77E. This single mutation led to a drastic decrease in hydration activity of OhyRe. OhyA Y241 was also proposed to be important for catalysis, by protonation of the double bond^[6] and is conserved with OhyRe Y205. Hence, it is tempting to propose that OhyRe might have a different catalytic mechanism as proposed for OhyA.

Interestingly, the fatty acid double-bond hydratase from *Lactobacillus plantarum*, LPH,^[20] also exhibits the HFam3 family specific motive RGGREM. In contrast to LPH, which solely converts linoleic acid, OhyRe exhibits hydration activity for both, C16 and C18 unsaturated fatty acids. In addition, LPH was shown to be a homotrimer in its active form, whereas OhyRe is a monomer.

The exact binding site of the substrates of OHs could not yet be resolved. In the crystal structure of LAH, a cavity was observed running from the surface of the protein towards the interface formed by domain I and III. This site is known to be a substrate binding site in other related enzyme families. Volkov et al.^[5] identified a linoleic acid (LA) molecule bound in this cavity with its carboxylate oriented towards the protein surface and the hydrophobic tail pointing to the protein interior (Figure 7). In contrast, a PEG molecule has been identified close to the FAD cofactor in the structure of OhyA, possibly mimicking a bound substrate molecule (Figure 7). Strictly this binding site is fundamental different to the "interdomain"-binding site as described for LAH (Figure 6B and Figure 7). To date, there is no structural information on an OH with a real substrate bound

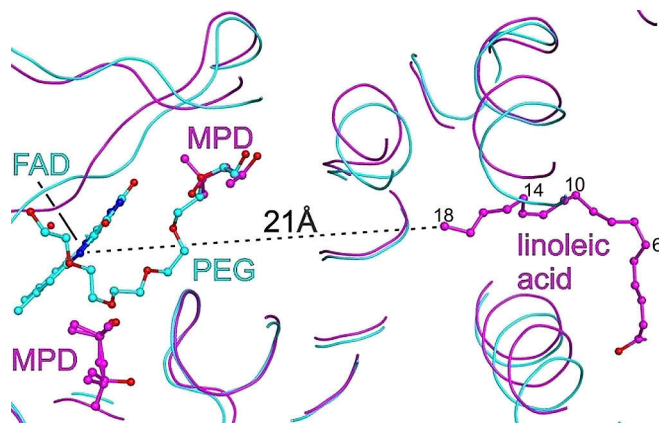


Figure 7. View on the potential nucleotide and substrate binding site. Superposition of LAH (magenta) and OhyA (cyan) as ribbon. FAD and PEG bound to LAH are shown in stick representation. The linoleic acid substrate of LAH and 2-methyl-2,4-pentanediol (MPD) molecules bound to LAH are shown in stick representation. Notably a 2-methyl-2,4-pentanediol (MPD) molecule in the LAH structure superimposed partially with the bound PEG molecule in the OhyA structure. The terminal carbon atom of linoleic acid is in distance of 21 Å to FAD, indicated by a dashed black line.

to the enzyme. Therefore it is very speculative which amino acid residues are crucial for catalysis. A definitive answer could only be provided by a structure with a bound substrate. This would allow the identification of key amino acids, important for catalysis. These residues could then be targeted by structure-based mutagenesis. Moreover, the given resolution of 2.64 Å of our OhyRe structure, does not allow the identification of water molecules within the active site. The location of the water molecules represents the second bottle neck for the identification of catalytically relevant residues, as the precise position of the water molecules might be as well crucial for catalysis. Based on the structure of OhyA, the T436A mutant had been generated, showing a dramatic decrease in activity. The latter observation was interpreted as the hydroxyl of T436 playing an important role in recognition and binding of the carboxylate function of the substrate. Taken together, both structures not only display distinct substrate binding sites, but also differ in the orientation of the carboxylate. To increase the enzymatic activity of OhyRe, we speculated that a mutation V393T (equivalent to T436 in OhyA) could potentially improve recognition and binding of the substrate. But unexpectedly, the activity was drastically reduced (Figure 3).

Conclusions

The enzyme family of oleate hydratases offers the sustainable conversion and valorization of biogenic fatty acids into high value lubricant additives. In contrast to heme dependent P450 hydroxylases, the conversion of oleic acid to 10-hydroxysteric acid by OHs can be accomplished without the need for co-factors. In this study a new OH from *R. erythropolis* could be identified by targeted genome mining. The biochemical characterization showed that the enzyme, OhyRe, exhibits a high pH-tolerance as well as high hydration activity over a wide temperature range. The crystal structure of OhyRe was solved to a resolution of 2.64 Å, surprisingly revealing a monomeric structure for the enzyme, which contrasts all other reported members of the OH family. These results were ultimately confirmed by MALS experiments of the protein in solution. To our knowledge, OhyRe is the first strictly monomeric OH and the first member of the HFam3 family of OHs that was characterized and crystallized so far. The HFam3 family of OHs has high potential for further biocatalytical applications, as the monomeric enzyme provides a variety of options for immobilization strategies. The free N- and C-terminal ends are not involved in dimer association and could, for example, be feasible targets for the fusion of anchor-proteins. Furthermore, two mutants of OhyRe, M77E and V393T, were generated to clarify the importance of these two residues in the catalytic mechanism of OhyRe. These conservative substitutions, to residues which are highly conserved within in the OH family, resulted in a drastic decrease of hydration activity of 80 to 90%. This suggests that OhyRe might follow a distinct reaction mechanism, which has to be clarified in future experiments.

Materials and Methods

Chemicals

All chemicals utilized in this work were purchased from Sigma-Aldrich (Munich, Germany) and Carl Roth (Karlsruhe, Germany), at the highest purity grade available.

Bacterial strains & plasmids

The *Escherichia coli* strains XL-1 Blue and DH5 α were used for cloning whereas the strains BL21 (DE3) and Rosetta2 were employed for protein expression. All plasmids and *E. coli* strains were obtained from Novagene/Merck Millipore.

Cloning for characterization experiments

The myosin-cross-reactive antigen coding gene O5Y 00450 from *Rhodococcus erythropolis* CCM2595, was taken as a template for a codon-optimized gene-synthesis (Life Technologies, Regensburg), for an *E. coli* host strain. The obtained synthetic gene was sub-cloned in a pET28a expression plasmid and transformed into chemically competent F cells.

Cloning for crystallization experiments

For protein production in *E. coli*, the OhyRe ORF was amplified with the forward primer 5'-TATACCATGGGAATGAGCAGCAATCTGAGCC-3' and reverse primer 5'-TATAAAGCTTTTAACGAAACATGGTAACTGCTGC-3' containing *HindIII* and *NcoI* recognition sites, respectively) and cloned into the pETM11 vector, resulting in a construct with N-terminal hexa-histidine-tag that could be cleaved off by TEV protease.

OhyRe mutant construction

The mutants OhyRe-M77E and OhyRe-V393T were constructed by overlap-extension-PCR using primer sets listed in Table S2 (Supporting Information).

Protein expression and protein purification for characterization experiments

The expression of the native OhyRe or respective mutants thereof was performed in *E. coli* BL21DE3 cells, grown in Laure Broth (LB) medium. Pre-cultures were inoculated from a cryo-stock and grown over night in 100 mL LB in a 500 mL baffled flask at 120 rpm at 37 °C. Main cultures were grown up to an optical density, measured at 600 nm (OD_{600}), of 0.6–0.8, before the expression was induced by the addition of isopropyl β -D-1-thiogalactopyranoside (IPTG) to a final concentration of 0.1 mM. After 16 h of incubation at 16 °C the cells were harvested and the resuspended (20 mM Tris-HCl buffer and 25 mM imidazole pH 7.2) cell pellets were disrupted by high pressure homogenization (EmulsiFlex-B15, AVESTIN). A subsequent centrifugation step at 20000 g for 40 min at 4 °C (Beckmann coulter J-20 XP) was applied for the separation of the

cell debris from the soluble protein fraction. The soluble protein fraction was utilized for affinity chromatography through a Ni²⁺-NTA His-trap column (HisTrap FF, GE Healthcare; flow rate 1 mL min⁻¹). The purified protein solution was desalted using HiPrep 26/10 desalting column (GE Healthcare). Protein amounts were quantified using 2D quant kit (GE Healthcare) according to manufacturer's instructions.

Protein expression and protein purification for crystallization experiments

OhyRe fused to an N-terminal hexa-histidine-tag in pET-M11 vector was transformed in *E. coli* Rosetta2. Protein was expressed in auto-induction media at 37 °C until an OD₆₀₀ of approximately 0.8 was reached and subsequently cooled down to 20 °C.^[21] Cells grew over night and were harvested by centrifugation (6 min, 6000 rpm at 4 °C). For resuspension of the cell pellet, buffer A was used (50 mM Tris/HCl pH 7.5, 500 mM NaCl, 30 mM imidazole and 1 mM DTT). Cells were lysed by homogenization at 4 °C and the lysate was cleared by centrifugation (1 h, 21 000 rpm at 4 °C). Ni²⁺-NTA beads (column volume (cv) 1 mL; GE Healthcare) were equilibrated with buffer A. OhyRe was loaded on the column and washed with 10 cv of buffer A. OhyRe was eluted in a linear gradient to buffer A supplemented to 500 mM imidazole. Pooled fractions were dialyzed over night against buffer B (20 mM Tris/HCl pH 7.5, 150 mM NaCl and 1 mM DTT) supplemented with TEV protease to cleave off the N-terminal His-tag. Uncleaved protein was separated from cleaved protein through an additional Ni²⁺-NTA affinity chromatography. Size exclusion chromatography was performed with a HighLoad Superdex S200 16/60 column (GE Healthcare), equilibrated with buffer B. Pooled protein fractions were concentrated with Amicon-Ultra 30 000 to 19.2 mg mL⁻¹ as measured by the absorbance at 280 nm.

Enzyme characterization

The determination of the enzymatic properties of the OH from *Rhodococcus erythropolis* CM2595 was (unless otherwise stated) executed under the following standard reaction conditions. The tests were performed in a reaction volume of 200 µl in 20 mM Tris-HCl buffer (pH 7.2), containing the purified enzyme (final conc. of 5 µM), FAD (final conc. 20 µM) and 720 µM OA as substrate at 28 °C for 15 min. Thermo-stability was tested in a temperature range from 20–45 °C. pH tolerance was monitored in a range from pH 5–8. To determine the substrate specificity of the myosin-cross-reactive antigen from *Rhodococcus erythropolis* CM2595, the purified enzyme was tested on myristic acid (C14:0), myristoleic acid (C14:1), palmitic acid (C16:0), palmitoleic acid (C16:1), stearic acid (C18:0), vaccenic acid (C18:1 *trans*-11) oleic acid (C18:1, *cis*-9), linoleic acid (C18:2), linolenic acid (C18:3), eicosatrienoic acid (C20:3), eicosatetraenoic acid (C20:4) and triolein as potential substrates. For the determination of the kinetic parameters of OhyRe towards oleic acid, different substrate concentrations (90 µM to 1.44 mM) and reaction times (1 to 15 min) were tested under standard conditions. The reactions were stopped by the addition of an equal

volume of ethyl acetate (EtOAc) and instant, intensive vortexing. The resulting solvent phase was separated from the water phase and applied for silylation and subsequent analysis.

Lipid analysis

The preparation of the extracted lipid fractions for GC measurements was performed according to Volkov et al.^[22] Hydroxylated fatty acids were identified by GC-MS by injecting 1 µL into a Thermo Scientific TRACE Ultra Gas Chromatograph coupled to a Thermo DSQ II mass spectrometer and the Triplus Autosampler injector. Column: Stabilwax fused silica capillary (30 m × 0.25 mm, film thickness 0.25 µm) Restek. (Program: initial column temperature 150 °C, increasing (4 °C min⁻¹) up to a final temperature of 250 °C. Carrier gas: hydrogen (flow rate 3.5 mL min⁻¹). Peaks were identified by comparison to fatty acid standards or by specific molecular masses detected. Extracts resulting from kinetic experiments were analyzed with the Shimadzu GC-2025 system equipped with a flame ionization detector. Column: Zebron ZB-WAX (30 m × 0.32 mm, film thickness 0.25 µm) Phenomenex. Carrier gas: hydrogen (3.00 mL min⁻¹). Program: initial column temperature 150 °C for 1 min; increasing 5 °C min⁻¹ to 240 °C, hold for 6 min. Peaks were identified by comparison to the respective standards.

Crystallization

Crystals were obtained by the sitting-drop vapor-diffusion method at 18 °C with a reservoir solution composed of 100 mM Bis-Tris/HCl pH 5.5 to pH 6.0, 255 mM to 300 mM magnesium formate and 5% (v/v) glycerol. Crystals were cryo-protected with 25% (v/v) MPD supplemented to the reservoir resolution and subsequently flash-cooled in liquid nitrogen.

Diffraction data collection, structure determination and refinement

Synchrotron diffraction data were collected at the beamline 14.1 of the MX Joint Berlin laboratory at BESSY (Berlin, Germany) or beamline P14 of Petra III (Deutsches Elektronen Synchrotron, Hamburg, Germany). X-ray data collection was performed at 100 K. Diffraction data were processed with X-ray detector software (XDS)^[23] (Table S1). The structure was solved through molecular replacement in PHASER^[24] by using the structure of the hydratase from *Lactobacillus acidophilus* (PDB 4ia5)^[5] as a search model. Crystals of OhyRe belong to the space group *P*6₅22, with two molecules in the asymmetric unit. For the refinement 2.8% of the reflections were set aside for the calculation of the R_{free}. Model building and water picking was performed with COOT.^[25] The structure was initially refined by applying a simulated annealing protocol and in later refinement cycles by maximum-likelihood restrained refinement using PHENIX.refine.^[26] Model quality was evaluated with MolProbity^[27] and the JCSG validation server.^[28] Secondary structure elements were assigned with DSSP^[29] and ALSCRIPT^[30] was used for secondary structure based sequence alignments. Figures were prepared using PyMOL.^[31]

Multi-angle light scattering (MALS)

MALS experiment was performed at 18 °C. OhyRe was loaded onto a Superdex 200 increase 10/300 column (GE Healthcare) that was coupled to a miniDAWN TREOS three-angle light scattering detector (Wyatt Technology) in combination with a RefractoMax520 refractive index detector. For calculation of the molecular mass, protein concentrations were determined from the differential refractive index with a specific refractive index increment (dn/dc) of 0.185 mL g⁻¹. Data were analyzed with the ASTRA 6.1.4.25 software (Wyatt Technology).

Accession numbers

The atomic coordinates and structure factor amplitudes have been deposited in the Protein Data Bank under the accession code 5ODO.

Acknowledgements

We gratefully acknowledge the financial support by the German Federal Ministry of Education and Research (Project: Advanced Biomass Value, 03SF0446C). We also want to thank Martina Haack for her excellent technical support in the analytics and Tom Schuffenhauer for his excellent experimental support. We are grateful to C. Alings for excellent technical support. We are grateful to M. Wahl for continuous encouragement and support. R. Driller is supported by the Elsa-Neumann stipend of the state of Berlin and the Nüsslein-Volhard foundation. We acknowledge beamtime and support at beamline P14 of PETRA III (Deutsches Elektronen Synchrotron, Hamburg, Germany). We accessed beamlines of the BESSY II (Berliner Elektronenspeicherung-Gesellschaft für Synchrotronstrahlung II) storage ring (Berlin, Germany) through the Joint Berlin MX-Laboratory sponsored by the Helmholtz Zentrum Berlin für Materialien und Energie, the Freie Universität Berlin, the Humboldt-Universität zu Berlin, the Max-Delbrück Centrum, and the Leibniz-Institut für Molekulare Pharmakologie.

Conflict of interest

The authors declare no conflict of interest.

Keywords: oleate hydratase · fatty acids · hydration · lyases · protein structure

- [1] a) D. L. Greenway, K. G. Dyke, *J. Gen. Microbiol.* **1979**, *115*, 233–245; b) C. J. Zheng, J. S. Yoo, T. G. Lee, H. Y. Cho, Y. H. Kim, W. G. Kim, *FEBS Lett.* **2005**, *579*, 5157–5162.
- [2] A. Hiseni, I. W. C. E. Arends, L. G. Otten, *ChemCatChem* **2015**, *7*, 29–37.
- [3] J. Jin, U. Hanefeld, *Chem. Commun.* **2011**, *47*, 2502–2510.
- [4] a) L. E. Bevers, M. W. Pinkse, P. D. Verhaert, W. R. Hagen, *J. Bacteriol.* **2009**, *191*, 5010–5012; b) E.-Y. Jeon, J.-H. Lee, K.-M. Yang, Y.-C. Joo, D.-K. Oh, J.-B. Park, *Process Biochem.* **2012**, *47*, 941–947.

- [5] A. Volkov, S. Khoshnevis, P. Neumann, C. Herrfurth, D. Wohlwend, R. Ficner, I. Feussner, *Acta Crystallogr. Sect. D* **2013**, *69*, 648–657.
- [6] M. Engleder, T. Pavkov-Keller, A. Emmerstorfer, A. Hromic, S. Schrempf, G. Steinkellner, T. Wriessnegger, E. Leitner, G. A. Strohmaier, I. Kaluzna, D. Mink, M. Schurmann, S. Wallner, P. Macheroux, K. Gruber, H. Pichler, *ChemBioChem* **2015**, *16*, 1730–1734.
- [7] J. Schmid, L. Steiner, S. Fademrecht, J. Pleiss, K. B. Otte, B. Hauer, *J. Mol. Catal. B* **2017**, *133*, S243–S249.
- [8] Y. Wache, M. Aguedo, A. Choquet, I. L. Gatfield, J. M. Nicaud, J. M. Belin, *Appl. Environ. Microbiol.* **2001**, *67*, 5700–5704.
- [9] a) C. T. Hou, *New Biotechnol.* **2009**, *26*, 2–10; b) J. W. Song, E. Y. Jeon, D. H. Song, H. Y. Jang, U. T. Bornscheuer, D. K. Oh, J. B. Park, *Angew. Chem. Int. Ed.* **2013**, *52*, 2534–2537; *Angew. Chem.* **2013**, *125*, 2594–2597.
- [10] M. Goodfellow, G. Alderson, *J. Gen. Microbiol.* **1977**, *100*, 99.
- [11] a) B. R. Langdahl, P. Bisp, K. Ingvorsen, *Microbiology* **1996**, *142*, 145–154; b) S. C. Heald, P. F. B. Brandao, R. Hardicre, A. T. Bull, *Antonie van Leeuwenhoek* **2001**, *80*, 169–183.
- [12] C. C. de Carvalho, M. M. da Fonseca, *Appl Microbiol Biotechnol* **2005**, *67*, 715–726.
- [13] H. Strnad, M. Patek, J. Fousek, J. Szokol, P. Ulbrich, J. Nesvera, V. Paces, C. Vlcek, *Genome Announc* **2014**, *2*, e00208-14.
- [14] L. Holm, P. Rosenstrom, *Nucleic Acids Res.* **2010**, *38*, W545–W549.
- [15] L. De Colibus, M. Li, C. Binda, A. Lustig, D. E. Edmondson, A. Mattevi, *Proc. Natl. Acad. Sci. USA* **2005**, *102*, 12684–12689.
- [16] B. N. Kim, Y. C. Joo, Y. S. Kim, K. R. Kim, D. K. Oh, *Appl. Microbiol. Biotechnol.* **2012**, *95*, 929–937.
- [17] Y. C. Joo, E. S. Seo, Y. S. Kim, K. R. Kim, J. B. Park, D. K. Oh, *J. Biotechnol.* **2012**, *158*, 17–23.
- [18] Y. C. Joo, K. W. Jeong, S. J. Yeom, Y. S. Kim, Y. Kim, D. K. Oh, *Biochimie* **2012**, *94*, 907–915.
- [19] E. Krissinel, K. Henrick, *J. Mol. Biol.* **2007**, *372*, 774–797.
- [20] J. Ortega-Anaya, A. Hernandez-Santoyo, *Biochim. Biophys. Acta Biomembr.* **2015**, *1848*, 3166–3174.
- [21] F. W. Studier, *Protein Expression Purif.* **2005**, *41*, 207–234.
- [22] A. Volkov, A. Liavonchanka, O. Kamneva, T. Fiedler, C. Goebel, B. Kreikemeyer, I. Feussner, *J. Biol. Chem.* **2010**, *285*, 10353–10361.
- [23] W. Kabsch, *Acta Crystallogr. Sect. D* **2010**, *66*, 125–132.
- [24] A. J. McCoy, R. W. Grosse-Kunstleve, P. D. Adams, M. D. Winn, L. C. Storoni, R. J. Read, *J. Appl. Crystallogr.* **2007**, *40*, 658–674.
- [25] P. Emsley, B. Lohkamp, W. G. Scott, K. Cowtan, *Acta Crystallogr. Sect. D* **2010**, *66*, 486–501.
- [26] a) P. D. Adams, P. V. Afonine, G. Bunkoczi, V. B. Chen, I. W. Davis, N. Echols, J. J. Headd, L. W. Hung, G. J. Kapral, R. W. Grosse-Kunstleve, A. J. McCoy, N. W. Moriarty, R. Oeffner, R. J. Read, D. C. Richardson, J. S. Richardson, T. C. Terwilliger, P. H. Zwart, *Acta Crystallogr. Sect. D* **2010**, *66*, 213–221; b) P. V. Afonine, R. W. Grosse-Kunstleve, N. Echols, J. J. Headd, N. W. Moriarty, M. Mustyakimov, T. C. Terwilliger, A. Urzhumtsev, P. H. Zwart, P. D. Adams, *Acta Crystallogr. Sect. D* **2012**, *68*, 352–367.
- [27] V. B. Chen, W. B. Arendall III, J. J. Headd, D. A. Keedy, R. M. Immormino, G. J. Kapral, L. W. Murray, J. S. Richardson, D. C. Richardson, *Acta Crystallogr. Sect. D* **2010**, *66*, 12–21.
- [28] H. Yang, V. Guranovic, S. Dutta, Z. Feng, H. M. Berman, J. D. Westbrook, *Acta Crystallogr. Sect. D* **2004**, *60*, 1833–1839.
- [29] W. Kabsch, C. Sander, *Biopolymers* **1983**, *22*, 2577–2637.
- [30] G. J. Barton, *Protein Eng.* **1993**, *6*, 37–40.
- [31] W. DeLano, The PyMOL Molecular Graphics System <http://www.pymol.org>. **2002**.

Manuscript received: August 17, 2017

Revised manuscript received: September 25, 2017

Accepted manuscript online: October 3, 2017

Version of record online: ■■■ 0000

Heterogeneous & Homogeneous & Bio- & Nano-

CHEM **CAT** CHEM

CATALYSIS

Supporting Information

***Rhodococcus erythropolis* Oleate Hydratase: a New Member in the Oleate Hydratase Family Tree—Biochemical and Structural Studies**

Jan Lorenzen^{+, [a]} Ronja Driller^{+, [b]} Ayk Waldow,^[b] Farah Qoura,^[a] Bernhard Loll,^{*[b, c]} and Thomas Brück^{*[a]}

cctc_201701350_sm_miscellaneous_information.pdf

Supporting Information

***Rhodococcus erythropolis* Oleate Hydratase, a New Member in the Oleate Hydratase Family Tree - Biochemical and Structural Studies**

Jan Lorenzen^[a,d], Ronja Janke^[b,d], Ayk Waldow^[b], Farah Qoura^[a], Bernhard Loll^[b,c,e] and Thomas Brück^[a,e]

Table of content:

1 Supplementary Figures and Sections

Figure S1: Adsorption spectra of final gel filtration chromatography of OhyRe at wave lengths of 260 nm, 280 nm and 450 nm.	3
Figure S2: Sequence alignment of 14 different OHs from <i>Rhodococcus erythropulus</i> (Rre; HFam3), <i>Staphylococcus aureus</i> (Sau; HFam2), <i>Lysinibacillus fusiformis</i> (Lfu; HFam2), <i>Macrococcus caseolyticus</i> (Mca; HFam2), <i>Lactobacillus acidophilus</i> (Lac; HFam2), <i>Ochrobactrum anthropi</i> (Oan; HFam2), <i>Bifidobacterium breve</i> (Bbr; HFam2), <i>Streptococcus pyogenes</i> (Spy; HFam2), <i>Elizabethkingia meningoseptica</i> (Eme; HFam11), <i>Myroides odoratus</i> (Mod; HFam11), <i>Cellulophaga algicola</i> (Cal; HFam11), <i>Stenotrophomonas maltophilia</i> (Sma; HFam2), <i>Corynebacterium kroppenstedtii</i> (Ckr; HFam10) and <i>Chryseobacterium gleum</i> (Cgl; HFam11).....	4
Figure S3: Superposition of putative active sites of OhyRe and OhyA. Highlighted in magenta are the residues M77 and V393 subjected to mutagenesis. (A) Residues of OhyRe residing in domain I are shown as orange sticks and residues of OhyA in gray (B) Residues of OhyRe residing in domain II are shown as green sticks and residues of OhyA in gray.	5
Figure S4: Structure-based sequence alignment of OhyRe and OhyA. Secondary structure assignment was performed with DSSP based on the respective crystal structure. Secondary structure elements of OhyRe are depicted above the primary sequence and below for OhyA. The sequence of OhyRe is colored according to the domain architecture. Slanted lines indicated sections of OhyRe and OhyA that are not included in the crystal structures. Gray triangles indicate residues of OhyRe that are involved in hydrogen bonding contact to Mg ²⁺ coordinating water molecules. Black triangle shows F548 in π -stacking interaction with the flavine moiety of FAD. Other residues in hydrogen bonding distance to FAD are labeled with a black circle. Golden circles show OhyA E122 and Y241 that were proposed to be of catalytic importance.	6
.....	7
Figure S5: SEC/MALS analysis of OhyRe. Refractive index signal is shown as green curve. Solid, green curve represents the refractive index trace and the red curve the molecular mass at the corresponding elution volumes.....	8
Figure S6: Octahedral Mg ²⁺ coordination. Same color coding as in Figure 5A. The bound Mg ²⁺ and coordinating waters are shown as orange and red spheres, respectively. Hydrogen bonding interactions, with a distance cut-off < 3.1 Å, to amino acid residues are shown as red dashed lines.	8
Figure S7: Octahedral Mg ²⁺ coordination to water molecules is indicated by black lines. Hydrogen bonding (< 3.1 Å) interactions to amino acid residues are shown as red dashed lines. 2Fo-Fc electron density contoured at 1.0 σ depicted as green mesh.....	8
Table S1: Crystallographic data collection and model refinement statistics.	9
Table S2: Primers used for OhyRe mutant construction.....	11

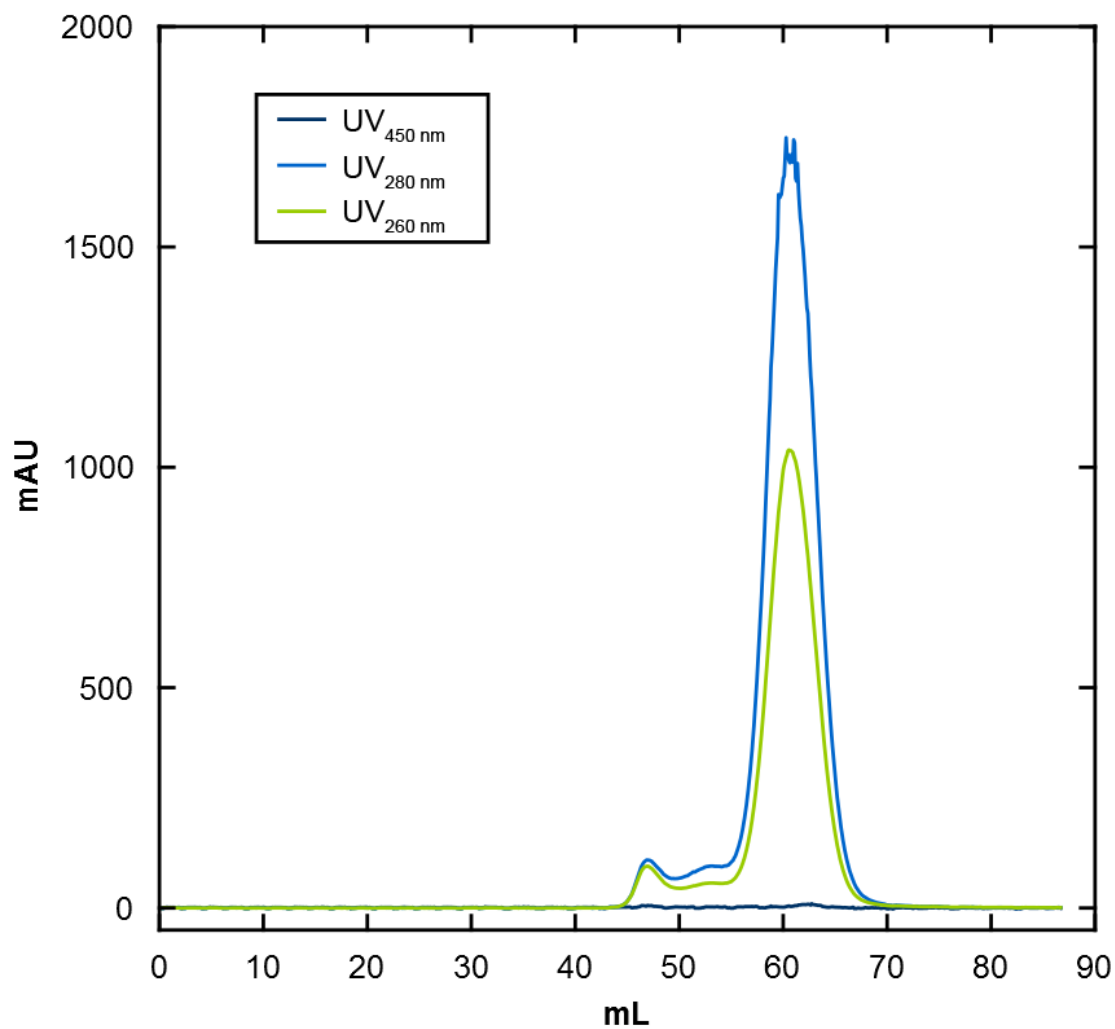


Figure S1: Adsorption spectra of final gel filtration chromatography of OhyRe at wave lengths of 260 nm, 280 nm and 450 nm.

The adsorption spectra of the gel filtration chromatography of OhyRe depicted in Fig. S1 show a clear peak for the enzyme at 260 nm and 280 nm. At 450 nm, the characteristic wave length for the detection of FAD, no corresponding peak could be detected. These data clearly show the loss of the FAD cofactor during the protein purification.

Rer 1	-----[3]NL	SHKAYHIGAGIGNLSAAVYLIRDGEMNGEDITIM-GLDPIHG-ANDGE[7]QYGRH	62	302	TDSSSDIGLDPTIPE	DMRY	--APSALLWRQATEHFYDLGNPKDFGDRQSEH-TSFTVTTSSHELLNEISRI	---T	372	
Sau 1	MYYSNGYEAFAARPKPEG	VENKSAYLIGSGLASLAACFLIRDDQMGESKCHIEELPKAGSGLDGE	NMPLK	73	294	TESSTYGGNDTPAPP	TDEL	--GGSATLWKNLARQSPFEGNPKFCQNIQPKSHFVSATITNNKDIIDIETSI	---C	365
Lfu 1	MYYSNGYEAFAARPKPEG	VDEKSAYLIGSGLASLAACFLIRDDQMGESKCHIEELPKAGSGLDGI	LNPR	73	294	TESSTYGGNDTPAPP	NKEL	--GGSATLWKNLARQSPFEGNPKFCQNIQPKSHFVSATITNNKDIIDIETSI	---C	365
Mca 1	MYYSNGYEAFAARPKPEG	VONKSAYLIGSGLASLAACFLIRDDQMGESKCHIEELPKAGSGLDGI	LNPR	73	294	TESSTYGGNDTPAPP	TSKP	--GGAQWLNENLSTQCEFGNPKFCQNIQPKSHFVSATITNNKDIIDIETSI	---C	365
Lac 1	MYYSNGYEAFAARPKPEG	VDEKSAYLIGSGLASLAACFLIRDDQMGESKCHIEELPKAGSGLDGI	DRPNA	73	293	TESSTYGGNDTPAPP	TNAK	--GDSNKLWENLAKQDFAGHPDVECEILNERSHFVSATITNNKDIIDIETSI	---C	364
Oan 1	MYYSNGYEAFAARPKPEG	VGTAYFYAGGLASLAGAFLIRDAQLSGENIIFEEALPGSSHMDI	LDHKK	73	294	TESSTYGGNDTPAPP	ETGH	--GGAATLWKNLARQSPFEGNPKFCQNIQPKSHFVSATITNNKDIIDIETSI	---C	365
Bbr 1	MYYSNGYEAFAARPKPEG	VDSKAYITIGTGLAALSACVLRDQMGPDHIELEKDPVGGACDGL	DIPGL	73	328	VENSTYGGNDTPAPP	NPDL	kpGGGDMWRRIAEQDPSFGHPKFCSDPNATK--HSATVITLDEIPYIQKI	---C	400
Spy 1	MYYSNGYEAFAARPKPEG	VDEKSAYLIGSGLASLAACFLIRDDQMGESKCHIEELPKAGSGLDGI	EKPHL	73	293	TESSTYGGNDTPAPP	TKAL	--GGSATLWKNLARQSPFEGNPKFCQNIQPKSHFVSATITNNKDIIDIETSI	---C	364
Eme1	MNPITSKFVKLVNASSEY[40]	VNSKAYITIGSGLASLAACVLRDQMGPDHIELEKDPVGGACDGL	GNPTD	113	334	TEDTYGGNDTPAPP	TSQK	--SAGNKLWKNLARQSPFEGNPKFCQNIQPKSHFVSATITNNKDIIDIETSI	---C	409
Mod1	MKVDITQKFDKILETSXYG[40]	FSQSKVYITIGSGLASLAACVLRDQMGPDHIELEKDPVGGACDGL	GNVAK	113	334	TEDTYGGNDTPAPP	TSQK	--SPGSLWKNLARQSPFEGNPKFCQNIQPKSHFVSATITNNKDIIDIETSI	---C	409
Cal 1	MKGITKFKVKNLNASPEP[40]	FKDSKAYITIGTGLAALSACVLRDQMGPDHIELEKDPVGGACDGL	GNVAK	113	334	TEDTYGGNDTPAPP	TSQK	--SDGWLWKNLARQSPFEGNPKFCQNIQPKSHFVSATITNNKDIIDIETSI	---C	409
Sma1	MYYSNGYEAFAARPKPEG	VDEKSAYLIGSGLASLAACFLIRDDQMGESKCHIEELPKAGSGLDGI	KVPEK	73	294	TENSDNGDHTAARL	NEG	--pAPAWLHRRRIAAKDDAGRPDVFAGHPKFCQNIQPKSHFVSATITNNKDIIDIETSI	---C	364
Ckr 1	MSIYQSTY-----PDTQGF[21]	DKRKYAVYSGSGLNLAAGVLRDQMGPDHIELEKDPVGGACDGL	GNVAK	89	307	TESTYGGNDTPAPP	KKTP	--GPAWSLWKNLARQSPFEGNPKFCQNIQPKSHFVSATITNNKDIIDIETSI	---C	409
Cgl 1	MSTINSKFVKLVNASSEY[40]	VNSKAYITIGSGLASLAACVLRDQMGPDHIELEKDPVGGACDGL	GNVAK	113	334	TESTYGGNDTPAPP	SAGQ	--SAGNKLWKNLARQSPFEGNPKFCQNIQPKSHFVSATITNNKDIIDIETSI	---C	409
Rer 63	[6]GFINRGRMLNEEYENLMDVLSAVPSLNDPQ-KSVTDDIDFDHHPHTEVARLIRDRGIRnkENDYHQ#QDNK		144	373	KQLPQN-----ALNTFVDSNLLSIVWHPHYHAKENE-GVFGYCLFRKGDVYKPPFEMTGREMLEETLGHLE				445	
Sau 74	GVYVIRGGRM-ENHFEELNDLFRSIPSLIEDH-ASVLDLRYLNKEDPNYSKRCVIEKQGRQ--- <td></td> <td>145</td> <td>366</td> <td>KRDPDLAKVTGGIITINDSAWQISFTINRQQDFKQPKNE-ISTWYALYSDVNDGVIKPKITFESGNEIQCEWLVHGL</td> <td></td> <td></td> <td></td> <td>444</td>		145	366	KRDPDLAKVTGGIITINDSAWQISFTINRQQDFKQPKNE-ISTWYALYSDVNDGVIKPKITFESGNEIQCEWLVHGL				444	
Lfu 74	GVYVIRGGRM-ENHFEELNDLFRSIPSLIEDH-ASVLDLRYLNKEDPNYSKRCVIEKQGRQ--- <td></td> <td>145</td> <td>366</td> <td>KRDPDLAKVTGGIITINDSAWQISFTINRQQDFKQPKNE-ISTWYALYSDVNDGVIKPKITFESGNEIQCEWLVHGL</td> <td></td> <td></td> <td></td> <td>444</td>		145	366	KRDPDLAKVTGGIITINDSAWQISFTINRQQDFKQPKNE-ISTWYALYSDVNDGVIKPKITFESGNEIQCEWLVHGL				444	
Mca 74	GVYVIRGGRM-ENHFEELNDLFRSIPSLIEDH-ASVLDLRYLNKEDPNYSKRCVIEKQGRQ--- <td></td> <td>145</td> <td>366</td> <td>KRDPDLAKVTGGIITINDSAWQISFTINRQQDFKQPKNE-ISTWYALYSDVNDGVIKPKITFESGNEIQCEWLVHGL</td> <td></td> <td></td> <td></td> <td>444</td>		145	366	KRDPDLAKVTGGIITINDSAWQISFTINRQQDFKQPKNE-ISTWYALYSDVNDGVIKPKITFESGNEIQCEWLVHGL				444	
Lac 74	GVYVIRGGRM-ENHFEELNDLFRSIPSLIEDH-ASVLDLRYLNKEDPNYSKRCVIEKQGRQ--- <td></td> <td>145</td> <td>366</td> <td>KRDPDLAKVTGGIITINDSAWQISFTINRQQDFKQPKNE-ISTWYALYSDVNDGVIKPKITFESGNEIQCEWLVHGL</td> <td></td> <td></td> <td></td> <td>444</td>		145	366	KRDPDLAKVTGGIITINDSAWQISFTINRQQDFKQPKNE-ISTWYALYSDVNDGVIKPKITFESGNEIQCEWLVHGL				444	
Oan 74	GVYVIRGGRM-ENHFEELNDLFRSIPSLIEDH-ASVLDLRYLNKEDPNYSKRCVIEKQGRQ--- <td></td> <td>145</td> <td>366</td> <td>KRDPDLAKVTGGIITINDSAWQISFTINRQQDFKQPKNE-ISTWYALYSDVNDGVIKPKITFESGNEIQCEWLVHGL</td> <td></td> <td></td> <td></td> <td>443</td>		145	366	KRDPDLAKVTGGIITINDSAWQISFTINRQQDFKQPKNE-ISTWYALYSDVNDGVIKPKITFESGNEIQCEWLVHGL				443	
Bbr 74	GVYVIRGGRM-ENHFEELNDLFRSIPSLIEDH-ASVLDLRYLNKEDPNYSKRCVIEKQGRQ--- <td></td> <td>145</td> <td>401</td> <td>KRDPDLAKVTGGIITINDSAWQISFTINRQQDFKQPKNE-ISTWYALYSDVNDGVIKPKITFESGNEIQCEWLVHGL</td> <td></td> <td></td> <td></td> <td>479</td>		145	401	KRDPDLAKVTGGIITINDSAWQISFTINRQQDFKQPKNE-ISTWYALYSDVNDGVIKPKITFESGNEIQCEWLVHGL				479	
Spy 74	GVYVIRGGRM-ENHFEELNDLFRSIPSLIEDH-ASVLDLRYLNKEDPNYSKRCVIEKQGRQ--- <td></td> <td>145</td> <td>365</td> <td>HRLDHDGKVTGGIITINDSAWQISFTINRQQDFKQPKNE-ISTWYALYSDVNDGVIKPKITFESGNEIQCEWLVHGL</td> <td></td> <td></td> <td></td> <td>443</td>		145	365	HRLDHDGKVTGGIITINDSAWQISFTINRQQDFKQPKNE-ISTWYALYSDVNDGVIKPKITFESGNEIQCEWLVHGL				443	
Eme114	GVYVIRGGRM-DMYENLMDVLSAVPSLNDPQ-KSVTDDIDFDHHPHTEVARLIRDRGIRnkENDYHQ#QDNK		185	410	VNDPYSKVTGGIITINDSAWQISFTINRQQDFKQPKNE-ISTWYALYSDVNDGVIKPKITFESGNEIQCEWLVHGL				488	
Mod114	GVYVIRGGRM-DMYENLMDVLSAVPSLNDPQ-KSVTDDIDFDHHPHTEVARLIRDRGIRnkENDYHQ#QDNK		185	410	VNDPYSKVTGGIITINDSAWQISFTINRQQDFKQPKNE-ISTWYALYSDVNDGVIKPKITFESGNEIQCEWLVHGL				488	
Cal 114	GVYVIRGGRM-DMYENLMDVLSAVPSLNDPQ-KSVTDDIDFDHHPHTEVARLIRDRGIRnkENDYHQ#QDNK		185	410	VNDPYSKVTGGIITINDSAWQISFTINRQQDFKQPKNE-ISTWYALYSDVNDGVIKPKITFESGNEIQCEWLVHGL				488	
Sma74	GVYVIRGGRM-DMYENLMDVLSAVPSLNDPQ-KSVTDDIDFDHHPHTEVARLIRDRGIRnkENDYHQ#QDNK		145	365	KRDPDLAKVTGGIITINDSAWQISFTINRQQDFKQPKNE-ISTWYALYSDVNDGVIKPKITFESGNEIQCEWLVHGL				443	
Ckr 90	GFIAIRGGRM-GQHFECFNDLMDVLSAVPSLNDPQ-KSVTDDIDFDHHPHTEVARLIRDRGIRnkENDYHQ#QDNK		162	381	HDPVYKVTGGIITINDSAWQISFTINRQQDFKQPKNE-ISTWYALYSDVNDGVIKPKITFESGNEIQCEWLVHGL				459	
Cgl 114	GVYVIRGGRM-DMYENLMDVLSAVPSLNDPQ-KSVTDDIDFDHHPHTEVARLIRDRGIRnkENDYHQ#QDNK		185	410	VNDPYSKVTGGIITINDSAWQISFTINRQQDFKQPKNE-ISTWYALYSDVNDGVIKPKITFESGNEIQCEWLVHGL				488	
Rer 145	DRYLTKLMTPESEaekLDDISTIEQNEEtpHFFTFNFWYMETTFaFRKSSAMELRRYNNRHLIEFSRIQTLAGVTR		224	446	A-LDESGLTAA[6]DSVNSIPSHMPYASALFNRRAGDRPLVPHKSLAFISQFAEL-P-FDMVFTEQYSRCAQVA				525	
Sau 146	ATKEILDLCLTNEED---LDDVKITDFVSD--DEFNSFNWYMTAFEFKQHSAMERRRYLRFVHHTIADLADLSLRF		220	445	VPTDKIEDLAK	-HASNTIPVYMPYITSYFHTRIAGDRPLVPHKSLAFISQFAEL-P-FDMVFTEQYSRCAQVA			518	
Lfu 146	SSEEMIKLFTFPEEK---LEDKKITDFVSD--DEFNSFNWYMTAFEFKQHSAMERRRYLRFVHHTIADLADLSLRF		220	445	VPTDKIEDLAK	-HASNTIPVYMPYITSYFHTRIAGDRPLVPHKSLAFISQFAEL-P-FDMVFTEQYSRCAQVA			518	
Mca 146	ANKEIILCLMKEEQ---LDDVKITDFVSD--DEFNSFNWYMTAFEFKQHSAMERRRYLRFVHHTIADLADLSLRF		220	445	VPEKISALAA	-EC-NTIPVYMPYITSYFHTRIAGDRPLVPHKSLAFISQFAEL-P-FDMVFTEQYSRCAQVA			517	
Lac 146	A-NEIVKILMTEPKE---IEGQITIEEFDSD--EFFKTNFWYMTAFEFKQHSAMERRRYLRFVHHTIADLADLSLRF		219	444	VPEKISALAA	-EC-NTIPVYMPYITSYFHTRIAGDRPLVPHKSLAFISQFAEL-P-FDMVFTEQYSRCAQVA			519	
Oan 146	AVEEMKLALTPESA---LDDVKITDFVSD--DEFNSFNWYMTAFEFKQHSAMERRRYLRFVHHTIADLADLSLRF		220	446	VPEKISALAA	-EC-NTIPVYMPYITSYFHTRIAGDRPLVPHKSLAFISQFAEL-P-FDMVFTEQYSRCAQVA			519	
Bbr 146	ASMEIMKLFPTPEED---LYDKKITDFVSD--DEFNSFNWYMTAFEFKQHSAMERRRYLRFVHHTIADLADLSLRF		220	480	VPTDKIEDLAK	-HASNTIPVYMPYITSYFHTRIAGDRPLVPHKSLAFISQFAEL-P-FDMVFTEQYSRCAQVA			553	
Spy 146	S-LEKQITIEEFDSD--DEFNSFNWYMTAFEFKQHSAMERRRYLRFVHHTIADLADLSLRF		219	444	VPEKISALAA	-EC-NTIPVYMPYITSYFHTRIAGDRPLVPHKSLAFISQFAEL-P-FDMVFTEQYSRCAQVA			519	
Eme186	DQLAIRLLLNKKEE---LDDITIEEFDSD--DEFNSFNWYMTAFEFKQHSAMERRRYLRFVHHTIADLADLSLRF		260	489	I-EDQLENQK	NTI--VRTAFMPYITSMFPRRAGDRPLVPHKSLAFISQFAEL-P-FDMVFTEQYSRCAQVA			560	
Mod186	DQMLIKLLLNKKEE---LDDITIEEFDSD--DEFNSFNWYMTAFEFKQHSAMERRRYLRFVHHTIADLADLSLRF		260	489	I-EDQLENQK	NTI--VRTAFMPYITSMFPRRAGDRPLVPHKSLAFISQFAEL-P-FDMVFTEQYSRCAQVA			560	
Cal 186	DQLAIRLLLNKKEE---LDDITIEEFDSD--DEFNSFNWYMTAFEFKQHSAMERRRYLRFVHHTIADLADLSLRF		260	489	I-EDQLENQK	NTI--VRTAFMPYITSMFPRRAGDRPLVPHKSLAFISQFAEL-P-FDMVFTEQYSRCAQVA			560	
Sma146	AQDKIALLFLATREQ---MENKRIENVLGR--DFLNSFNWYMTAFEFKQHSAMERRRYLRFVHHTIADLADLSLRF		220	444	VPEKISALAA	-EC-NTIPVYMPYITSYFHTRIAGDRPLVPHKSLAFISQFAEL-P-FDMVFTEQYSRCAQVA			518	
Ckr 163	AQLIVKLLLNKKEE---LDDITIEEFDSD--DEFNSFNWYMTAFEFKQHSAMERRRYLRFVHHTIADLADLSLRF		237	460	V--VDVETIK	HTK--VRLAVMPYITSEFVPRRAGDRPLVPHKSLAFISQFAEL-P-FDMVFTEQYSRCAQVA			530	
Cgl 186	DQLAIRLLLNKKEE---LDDITIEEFDSD--DEFNSFNWYMTAFEFKQHSAMERRRYLRFVHHTIADLADLSLRF		260	489	I-EDQLENQK	NTI--VRTAFMPYITSMFPRRAGDRPLVPHKSLAFISQFAEL-P-FDMVFTEQYSRCAQVA			560	
Rer 225	SPYNYQESIILMPTLLEGGKGVFVNLKITEFVKD	---TPLRDEIIVT[7]RTGKGRIDVAEGDFVDTNGST	301	526	VYKFLGTPEKLTQ#HYEKDQKVLAKAAVTFR-----				559	
Sau 221	TKYNYQESLVLMVYKLSHGQVFEYDQVVEDIKVQV	TTSQIARELTH	293	519	VYQLNI--DRGVEVFASSVDVRLLSSTARLDGKLLTDIADP--ILKQIGKGIH--TKDITIVYDL				591	
Lfu 221	TKYNYQESLVLMVYKLSHGQVFEYDQVVEDIKVQV	VGDKIAHTLVLR	293	519	VYQLNI--DRGVEVFASSVDVRLLSSTARLDGKLLTDIADP--ILKQIGKGIH--TKDITIVYDL				590	
Mca 221	TKFNQESLVLMVYKLSHGQVFEYDQVVEDIKVQV	SKEKVAKADIV	293	518	VYKLLV--DRGVEVFASSVDVRLLSSTARLDGKLLTDIADP--ILKQIGKGIH--TKDITIVYDL				589	
Lac 220	NKYNYQESLVLMVYKLSHGQVFEYDQVVEDIKVQV	EGOSKIAKLVMT	292	520	VYTLNV--DRGVEVFASSVDVRLLSSTARLDGKLLTDIADP--ILKQIGKGIH--TKDITIVYDL				591	
Oan 221	TKYNYQESLVLMVYKLSHGQVFEYDQVVEDIKVQV	AGGNKLARLVMT	293	520	VYTLNV--DRGVEVFASSVDVRLLSSTARLDGKLLTDIADP--ILKQIGKGIH--TKDITIVYDL				591	
Bbr 221	TKYNYQESLVLMVYKLSHGQVFEYDQVVEDIKVQV	QEGEKSSIDL	327	554	VYTLNV--DRGVEVFASSVDVRLLSSTARLDGKLLTDIADP--ILKQIGKGIH--TKDITIVYDL				625	
Spy 220	NKYNYQESLVLMVYKLSHGQVFEYDQVVEDIKVQV	TAGKIVAKT	292	520	VYFLNG--ERGIPQGSAYDIRELKAIFYLNDKKAIDKMDLPI--P-ALIEIKGHK--IKDITIEELL				590	
Eme261	PKYNYQDFTVPLRKLQEKGVNHLNLTNKKVDLQI	NTEGKVEEITE	333	561	VYKLLN--NKQVDPINLQYDIRHLKAAKTNDK-----PF-----VGEGLRKLKGTGYFHEHL[9]HESFIA[15]				646	
Mod261	PKYNYQDFTVPLRKLQEKGVNHLNLTNKKVDLQI	TTAGKLVKGLVW	333	561	VYKLLN--NKQVDPINLQYDIRHLKAAKTNDK-----PF-----VGEGLRKLKGTGYFHEHL[9]HESFIA[15]				646	
Cal 261	PKYNYQDFTVPLRKLQEKGVNHLNLTNKKVDLQI	NTEGKVEEITE	333	561	VYKLLN--NKQVDPINLQYDIRHLKAAKTNDK-----PF-----VGEGLRKLKGTGYFHEHL[9]HESFIA[15]				646	
Sma221	TKYNYQESLVLMVYKLSHGQVFEYDQVVEDIKVQV	QPDQKQATRHMM	293	519	VYTLNLI--DRGVEVFASSVDVRLLSSTARLDGKLLTDIADP--ILKQIGKGIH--TKDITIVYDL				589	
Ckr 238	SKYNYQSFTEPLRKLQEKGVNHLNLTNKKVDLQI	KGSSFTVTGLV	306	531	VYKLLN--NKQVDPINLQYDIRHLKAAKTNDK-----PF-----VGEGLRKLKGTGYFHEHL[9]HESFIA[15]				591	
Cgl 261	PKYNYQDFTVPLRKLQEKGVNHLNLTNKKVDLQI	NTEGKVEEITE	333	561	VYKLLN--NKQVDPINLQYDIRHLKAAKTNDK-----PF-----VGEGLRKLKGTGYFHEHL[9]HESFIA[15]				642	

Figure S2: Sequence alignment of 14 different Ots from *Rhodococcus erythropolis* (Rre; HFam3), *Staphylococcus aureus* (Sau; HFam2), *Lysinibacillus fusiformis* (Lfu; HFam2), *Macrococcus caseolyticus* (Mca; HFam2), *Lactobacillus acidophilus* (Lac; HFam2), *Ochrobactrum anthropi* (Oan; HFam2), *Bifidobacterium breve* (Bbr; HFam2), *Streptococcus pyogenes* (Spy; HFam2), *Elizabethkingia meningoseptica* (Eme; HFam11), *Myroides odoratus* (Mod; HFam11), *Cellulophaga algicola* (Cal; HFam11), *Stenotrophomonas maltophilia* (Sma; HFam2), *Corynebacterium kroppenstedtii* (Ckr; HFam10) and *Chryseobacterium gleum* (Cgl; HFam11).

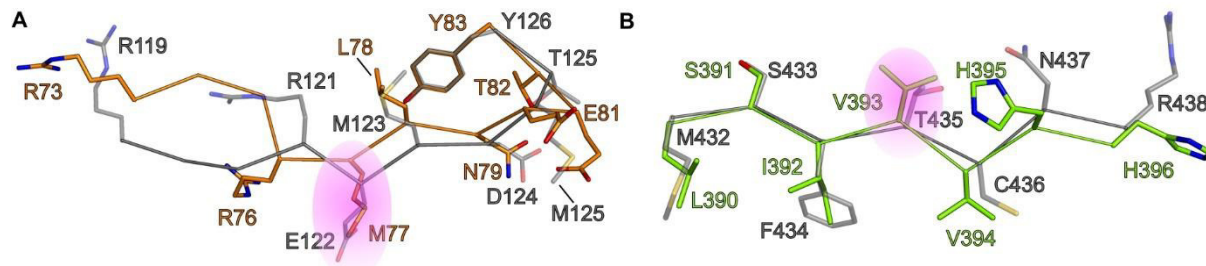


Figure S3: Superposition of putative active sites of OhyRe and OhyA. Highlighted in magenta are the residues M77 and V393 subjected to mutagenesis. (A) Residues of OhyRe residing in domain I are shown as orange sticks and residues of OhyA in gray (B) Residues of OhyRe residing in domain II are shown as green sticks and residues of OhyA in gray.

The superposition of the putative active sites of OhyRe (colored) and OhyA (gray), showed that the residues M77 and V393 from OhyRe are located in the exact same position in the three dimensional structure, like the residues E122 and T435 from OhyA.

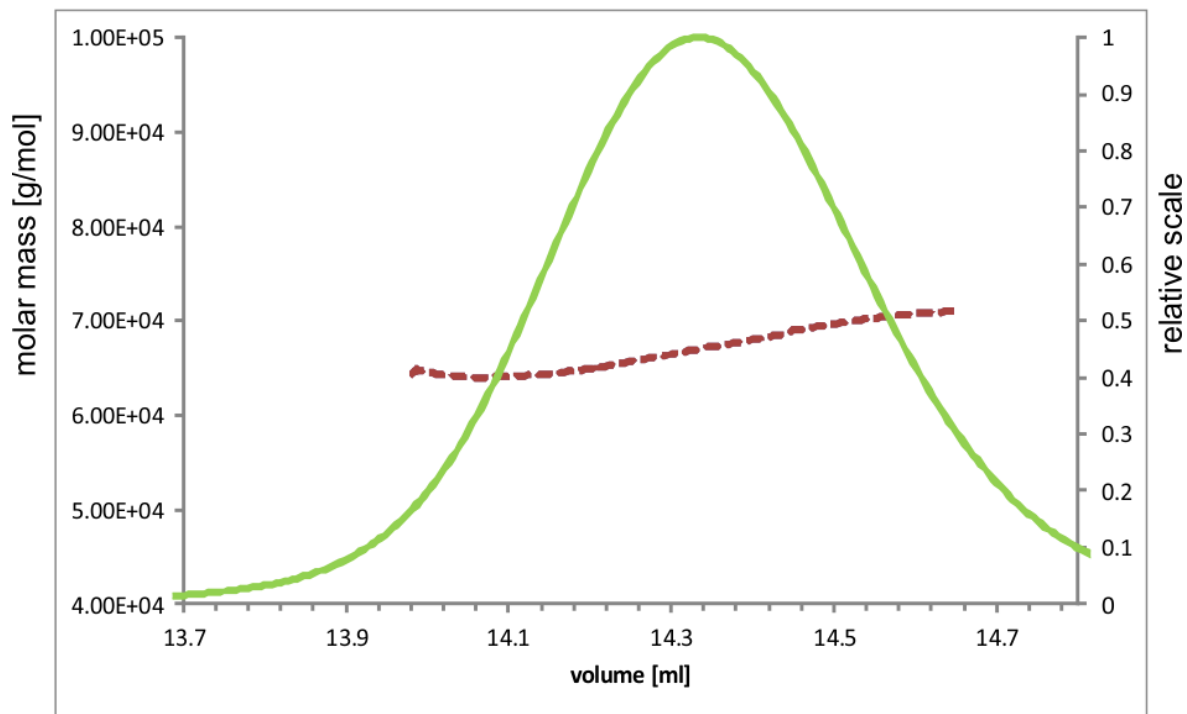


Figure S3: SEC/MALS analysis of OhyRe. Refractive index signal is shown as green curve. Solid, green curve represents the refractive index trace and the red curve the molecular mass at the corresponding elution volumes.

Section S1: Mg²⁺ binding site

In each monomer, we detected one Mg²⁺ binding site, being solvent exposed on the backside of the putative active site of OhyRe (Fig. 5A and S6). The binding site is located at the intersection of domain I, domain II and domain III. The Mg²⁺-ion is octahedral coordinated by six water molecules (Fig. S6 and S7) that are bound to the carboxylates of Glu80, Glu81, Asp111 and the hydroxyl of Thr223 as well as to the backbone carbonyls of Ala220, Gly221, and Val222. Notably amino acid residues in the second coordination sphere of Mg²⁺ are not conserved within other OHs. For the OhyA of *E. meningoseptica* a bound Ca²⁺-ion has been detected by plasma optical emission spectroscopy analysis, but no influence on the activity could be associated (Beveris et al. 2009). Furthermore, in its crystal structure no Ca²⁺ could be identified (Engleder et al. 2015). Given the close proximity to the putative active site, we questioned whether the Mg²⁺ could have an influence on the catalytic activity of the OhyRe enzyme. Hence we tested the enzymatic activity under standard conditions and added EDTA to a final concentration of 5 mM to the reaction mixture. The addition of EDTA had no detectable effect on the conversion activity of OhyRe, suggesting that the Mg²⁺ doesn't play a crucial role in the hydration reaction, but might have an effect on the protein stability.

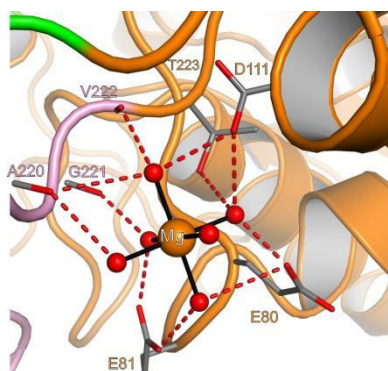


Figure S4: Octahedral Mg²⁺ coordination. Same color coding as in Figure 5A. The bound Mg²⁺ and coordinating waters are shown as orange and red spheres, respectively. Hydrogen bonding interactions, with a distance cut-off < 3.1 Å, to amino acid residues are shown as red dashed lines.

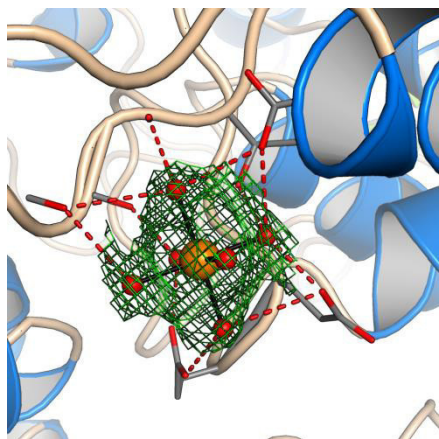


Figure S5: Octahedral Mg²⁺ coordination to water molecules is indicated by black lines. Hydrogen bonding (< 3.1 Å) interactions to amino acid residues are shown as red dashed lines. 2Fo-Fc electron density contoured at 1.0 σ depicted as green mesh.

Table S1: Crystallographic data collection and model refinement statistics.

Data Collection	
Wavelength [Å]	0.98141
Temperature [K]	100
Space group	<i>P6₅22</i>
Unit Cell Parameters	
a=b, c [Å]	261.75, 127.30
Resolution range [Å] ^a	50.00 - 2.64 (2.80 - 2.64)
Reflections ^a	
Unique	75230 (11910)
Completeness [%]	99.8 (99.4)
Multiplicity	22.2 (22.3)
Data quality ^a	
Intensity [I/σ(I)]	13.66 (1.80)
R _{meas} [%]	31.0 (217.4)
CC _{1/2} ^b	99.6 (78.8)
Wilson B value [Å ²]	46.2
Refinement	
Resolution range [Å] ^a	49.47 - 2.64 (2.73 - 2.64)
Reflections ^a	
Number	75186 (7348)
Test Set (2.8 %)	2097 (204)
R _{work}	0.190 (0.306)
R _{free}	0.221 (0.343)
Contents of the Asymmetric Unit	
Protein, Molecules, Residues, Atoms	1, 2, 1057, 8603

Ligands (Molecules)	Formate (14), glycerin (2), Magnesium (2)
Water, Molecules	417
Mean Temperature factors [\AA^2] ^b	
All Atoms	36.5
Macromolecules	36.6
Ligands	44.2
Water Oxygens	34.0
RMSD from Target Geometry	
Bond Lengths [\AA]	0.011
Bond Angles [$^\circ$]	0.84
Validation Statistics ^c	
Ramachandran Plot	
Residues in Allowed Regions [%]	3.0
Residues in Favored Regions [%]	97.0
MOLPROBITY Clashscore ^d	4.81

^a data for the highest resolution shell in parenthesis

^b calculated with PHENIX (Adams et al, 2010)

^c calculated with MOLPROBITY (Chen et al, 2010)

^d Clashscore is the number of serious steric overlaps (> 0.4) per 1,000 atoms.

Table S2: Primers used for OhyRe mutant construction

name	sequence	feature
OhyRe-fw (for overlap)	5'-GGA GAT ATA CCA TGG GCA GCA-3'	<i>Nco</i> I cutting site (red)
OhyRe-rv (for overlap)	5'-GTG GTG CTC GAG TTA ACG AAA-3'	<i>Xho</i> I cutting site (red)
M77E fw	5'-TTT ATC AAT CGT GGT GGT CGT GAA CTG AAT GAA G-3'	Methionine to glutamic acid (red)
M77E rv	5'-CAC GAT TGA TAA AAC CTG CAT CAT TAC CCA GT-3'	
V393T fw	5'-C AAT GTG CTG CTG AGC ATT ACC GTT CAT CAT C-3'	Valine to threonine (red)
V393T rv	5'-CAG CAG CAC ATT GCT ATC AAC AAA GGT ATT CA-3'	

4. Discussion & Outlook

Scientific publications from the last 20 years have illustrated the great potential of microalgae as a sustainable, green feedstock for many high value compounds⁴². Today, the extraction of those compounds from the microalgae biomass is still problematic and the main challenge to face in the utilization of microalgae biomass. The extraction method of choice has to be economically viable, environmentally friendly, abstain from toxic / harmful solvents, scalable and consistent to common, industrial regulations. The SCCO₂ mediated extraction of hydrophobic compounds from microalgae is one of the most promising methods, since it fits to most of the above mentioned requirements and has already been employed for decades, for example for the extraction of plant oils from seeds⁴⁴, or caffeine from coffee beans⁴⁵. The SCCO₂ extraction of microalgae derived lipids, was already published in 1987 by Choi et al.⁴⁶ for the strain *Scenedesmus obliquus* and the extraction of astaxanthin from *Haematococcus pluvialis*, a green alga from the species Chlorophyta, followed soon after in 1995⁴⁷. Although the extraction of hydrophobic compounds from microalgae has been researched in a laboratory scale for more than 30 years, there are still some obstacles to overcome.

One of the problematic production steps is the preparation of the algae biomass, previous to the extraction procedure. Microalgae are cultivated in water based cultivation media and even if high cell densities are reached with the applied cultivation conditions, the water content of the harvested biomass is very high. Microalgae cells, grown in a newly designed thin-layer cascade reactor, for example, displayed an average daily growth rate of 0.65 d⁻¹, at the applied cultivation conditions, and reached a maximum cell density of 50 g/l (dry cell weight)⁴⁸. This correlates with a water content of 95 wt%. Crampon et al.⁴⁹ showed, that the efficiency of the SCCO₂ extraction of lipids is not affected by a water content of up to 20 wt%, leaving a gap of 75 % water content, which has to be closed. Since suitable filtering techniques are still missing for a scalable application in this area, a drying step is mandatory. This drying step is problematic for the techno economic evaluation of the process, since it is a time and cost intensive procedure. Decreasing these costs should be one of the main objectives for a future process design for the SCCO₂ lipid extraction from microalgae biomass and could be reached by establishing new synergistic routes. For a microalgae cultivation and the following downstream processing, located in Germany, a close proximity to the manufacturing industry could be one interesting option. A lot of branches from this industry, like metal or carbon fiber manufacturing companies, produce high temperature flue gas streams, which could be directly used to dry the harvested biomass. For a cultivation facility located in Germany, the usage of rejected heat could also lower the cultivation costs and allow an efficient cultivation even during winter, by tempering the cultures. Another benefit of the connection between microalgae cultivation and the manufacturing industry could be the supply of the microalgae culture with

surplus CO₂, produced as a waste stream by industrial factories. The usage of the climate-damaging greenhouse gas in the microalgae cultivation leads to an increased growth rate of the culture and would lower the CO₂-footprint of the connected industrial companies.

Another challenging production steps is the physical accessibility of the intracellularly stored microalgae lipids. In comparison to bacteria, microalgae have a very rigid cell wall, representing a strong barrier for the extraction of intracellular compounds⁵⁰. Furthermore, the composition of the cell walls shows a high diversity between the different microalgae species and even among the same species under different cultivation conditions^{51,52}. In the pretests to our study we extracted untreated *Scenedesmus* biomass resulting in a lipid yield of only 60 % w/w (compared to Soxhlet extraction), whereas the extraction of pretreated biomass (high pressure homogenization) yielded approx. 92 % w/w of total lipids. These results clearly showed, that a disruption of the microalgae cells is essential for an efficient lipid extraction and correlate with the results from other groups^{49,53}.

However, the SCCO₂ mediated extraction of lipids and other hydrophobic compounds from microalgae biomass always requires a drying step and cell disruption for an efficient extraction process, as well as the infrastructure of an extraction facility, representing a big investment and relatively high operating costs. For example, the pure costs for a SCCO₂ extraction of 5 t of (dry) biomass under the experimentally identified, optimal conditions (see publication: 12 MPa, 20 °C and a CO₂ to biomass ratio of 100) would be approx. 15 €/kg. These investments can only be afforded for high value compounds, for example for pharmaceuticals or cosmetic products, but not for the bulk extraction of lipids for bio-lubricants or bio-fuels.

For a large scale extraction, approaches that can be realized with less technical effort and / or lower operating costs are mandatory. The search for an efficient extraction technique has been the subject of many full papers and reviews within the last years, but “the” optimal extraction method, regarding economy and ecology, could not be identified at present. In any case, especially two techniques were identified in these reviews to be suitable for large scale lipid extraction, namely steam explosion and microwave assisted extraction^{9,54}. Both techniques prevent an extensive harvesting process, appear to be technically very effective and are scalable at a relatively low energy consumption. The only drawback of both methods is the fact, that the methods are only pretreatments and, unlike for the SCCO₂ extraction, an additional extraction step is necessary. The extraction is in almost all cases performed with organic solvents, like hexane or chloroform-methanol mixtures^{55,56}, which are ecologically problematic. This problem could be solved, or at least extenuated, in the future by the use of “green”, sustainable solvents. These solvents exhibit the same qualities like common organic solvents, but are less or non-toxic substances that are (most preferable) produced based on biological feedstock^{57,58}. Possible candidates would be for example solvents like ethyl acetate,

n-butanol or isopropyl acetate. The substitution of commonly used organic solvents, like hexane, by green solvents could make the solvent based lipid extraction a scalable, environmentally friendly and, if produced from renewable feedstock, sustainable process.

As already stated in the introduction (see 1.3.5 Hydroxy Fatty Acids in Industrial Applications), hydroxy fatty acids are utilized for many different applications in different industries. 12-HSA, originating from castor oil, was also presented to be the most important one and the only hydroxy fatty acid available in industrial relevant amounts. Nevertheless, in 2016 castor oil only represented 0.15 % of the worldwide vegetable oil production ⁵⁹. The castor bean contains approx. 46 – 55 % (w/w) of lipids and the oil is gained by pressing. Ricinoleic acid (12-hydroxy-9-cis-octadecanoic acid) is the main component of castor oil, accounting for approx. 90 % of the extracted lipid fraction ⁶⁰, and serves as the precursor for 12-HSA production.

Although 12-HSA is produced from plant seeds, a green and renewable feedstock, the sustainability of its utilization and a safe future supply are questionable for different reasons. The increasing industrial demand for hydroxy fatty acids and thereby for castor oil, leads to the well-known competition between an industrial and an agricultural use of land. Although castor bean is a relatively robust plant, which can be grown in semiarid regions in tropical and subtropical areas with high salinity ⁶¹, it should always be considered that the cultivation areas could be used for the production of food. India, producing approx. 90 % of the worldwide disposable castor oil, is the second most populous country in the world. Since the population is still growing by approx. 0.5 % per year, the above mentioned conflict between industry and agriculture could intensify in the future. Furthermore, the increasing effects of the climate change could become an additional problem for the future supply with castor oil and 12-HSA, respectively. As approx. 86 % of the Indian castor oil is produced in only one federal state of India (Gujarat), the production might be especially susceptible to local effects of global warming. Today the production of castor oil in India already strongly oscillates between 250,000 and 350,000 metric tons per year ⁵⁹, depending on the weather. Trials to cultivate castor bean in the US, to buffer the fluctuation in castor oil production, were not successful, due to the poor climate adaptability of castor bean. Corresponding to the high fluctuation in the production, also the price for castor oil underlies strong fluctuations, but has been continuously rising in the last decades ⁶¹. In addition, the toxic ricin protein and the labor-intensive harvesting process prohibit the cultivation of castor bean in many countries.

The demonstrated problems in a constant and sustainable supply with castor oil, and thereby with hydroxy fatty acids, show the need for alternative supply chains for hydroxy fatty acids. Since alternatives from common agricultural crops for hydroxy fatty acids are missing and would face similar problems, an optional feedstock needs to be found. In this context, sustainable, bio based oils, originating from microalgae or microorganisms (e.g. yeast), are a

promising alternative. A generally rising industrial interest in these alternative oils could be observed lately, since they are not competing with food production, are biodegradable and unproblematic regarding their CO₂-footprint. Although these bio based oils naturally do not exhibit hydroxy fatty acids in relevant amounts, they contain high amounts of unsaturated fatty acids, which can be enzymatically modified.

One option to replace the commonly used 12-HSA is the enzymatic conversion of oleic acid to 10-HSA, which shows the same chemical properties like 12-HSA. High amounts of oleic acid can for example be found in microalgae of the species *Nannochloris sp.*⁶², or in yeast of the specie *Cutaneotrichosporon oleaginosus*⁶³, with oleic acid accounting for more than 50 % of total lipids, respectively. After the hydrolytic liberation of the FFAs from the glycerol backbone, catalyzed by a lipase, bio based oleic acid can further be enzymatically converted to 10-HSA, by employing an OH (EC 4.2.1.53). Although the reaction catalyzed by OHs is highly regio- and stereospecific, (R)-10-HSA is produced by ≥ 95 %, the production of 10-HSA, to our knowledge, has not been lifted to an industrial scale yet. Todea et al.⁶⁴ stated that OhyA, the OH isolated from *Elizabethkingia meningoseptica*, is not stable, representing the main reason for OHs not being used in industrial scale.

In our study we identified and characterized the OH OhyRe (Protein Data Bank ID: 5ODO), originating from the Gram-positive bacterium *Rhodococcus erythropolis*, which turned out to have a unique feature, compared to other published OHs. This unique feature is the strictly monomeric occurrence of the enzyme in its active form. In contrast to OhyRe, all OHs published until today were found to be homodimers in their active form. The dimerization of the two OH protomers is mainly mediated by residues located in the N- and C-terminal ends of the polypeptide chains. Since OhyRe exhibits only truncated N- and C-terminal ends, no dimer is formed. The monomeric state of the active enzyme leads to a higher stability, compared to dimeric protein complexes, as no protomer dissociation can influence the enzymatic activity.

Since the stability and an “easy handling” of an enzyme are essential for its application in an industrial process, biocatalysts are usually immobilized. Although many different immobilization strategies have been developed, there is no “standard” procedure for enzyme immobilization and the method of choice has usually to be identified experimentally.

So far, the only article dealing with the immobilization of OHs was published by Todea et al.⁶⁴. The techniques tested by the group were adsorption, affinity, ionic binding, cross-linking, covalent binding and sol-gel entrapment. Even though the loading of the protein to the different materials for immobilization was very high, only poor activities of could be recovered. While the sol-gel entrapment did not lead to any recovered activity at all, the covalent binding of the enzyme complex to different carrier materials resulted in the highest recovered activities. Especially the covalent binding to CMP (carboxylated magnetic particles) and AMP-CHT

(chitosan-coated macro particles) were shown to be most effective, although only 19.8 % and 23.7 % of the enzyme activity could be recovered, respectively. Since the monomeric structure of the active OhyRe differs from the homodimeric structure of OhyA, these results are not directly transferable, but might give an indication for techniques to be tested with OhyRe. The immobilization of OhyA by ionic binding onto chitosan resulted in a high level of protein loading, but at the same time very low recovered activity (5.5 %). The protein loading and constant binding to chitosan could probably be even higher for OhyRe than for OhyA, since the calculated net charge of OhyRe is more negative than the net charge of OhyA (OhyRe: $z = -25.32$ at pH 7.2; OhyA: $z = -15.05$ at pH 7.2). The authors did not speculate about the reason for the low activity, but one possible reason could be the dimeric state of OhyA. Unlike LAH, OhyA has not been crystallized together with its substrate (oleic acid). For LAH it was shown, that the homodimeric enzyme undergoes a conformational change in the asymmetric unit, conducted by substrate recognition, so that one unit hydrates the substrate, while the other unit is blocked²⁶. It could be possible, that a related mechanism of conformational changes also takes place in OhyA, which could be hindered by the ionic binding of the homodimer's surface to the supporter material. In this case the monomeric structure of OhyRe could still allow hydration activity while bound to chitosan, since the reaction is independent from other enzyme units. The also tested immobilization by affinity (via His-tag and Ni²⁺NTA-affinity) can directly be excluded for wild type OhyRe. During affinity based protein purification of OhyRe it was shown, that the binding of the FAD cofactor to the enzyme was so weak, that it was completely lost after the purification procedure. Although the activity can be recovered after external addition of FAD, the cofactor will probably not be bound to the enzyme permanently, especially not in a continuous reaction system in an aqueous milieu. For OhyA the immobilization on chitosan coated magnetic particles was shown to be the most efficient method tested. The results achieved by Todea et al. and the high handling qualities of the magnetic particles make this a promising technique for future immobilization tests with OhyRe, although the amino acids, available for covalent binding, are fewer in the amino acid chain of OhyRe.

Depending on the application of the produced 10-HSA, for example as a precursor for the food industry, the usage of a wild type enzyme is mandatory, due to legal regulations. For applications in the formulation of lubricants instead, the disposition of genetically modified enzymes for the production of 10-HSA would not be problematic.

Engleder et al. lately published an article presenting their results of new mutagenesis approaches for the OH OhyA⁶⁵. The group aimed to broaden the substrate acceptance of the enzyme in order to convert different types of oleic acid derivatives. The derivatives tested were composed of a compound selection that mainly differed in the head group of the molecule, which were not or only poorly accepted by the wild type enzyme. It was proposed, that the

entrance of the substrate channel of OhyA does not allow the acceptance of molecules with head groups larger than the carboxylic group of the native substrate (oleic acid). Amino acid exchanges, from single to quadruple variants, were performed, with exchanges from the native amino acids to alanine resulting in the best conversion performance. The exchange to alanine, a small, nonpolar amino acid, widened the entrance of the substrate channel and, together with the low reactivity of the amino acid, thereby allowed the recognition of the non-natural substrates.

The amino acid sequence alignment of OhyRe and 13 other OHs showed that two of the selected amino acids (Gln 265 & His 442) are also detected in OhyRe, whereas the other two amino acids (Thr 436 & Asn 438) are substituted by valine and histidine (Fig. 4). Since the amino acids, mutated in OhyA, are located in equal positions in the three-dimensional structure of OhyRe (Fig. 8), a similar mutagenesis approach for OhyRe would be interesting.

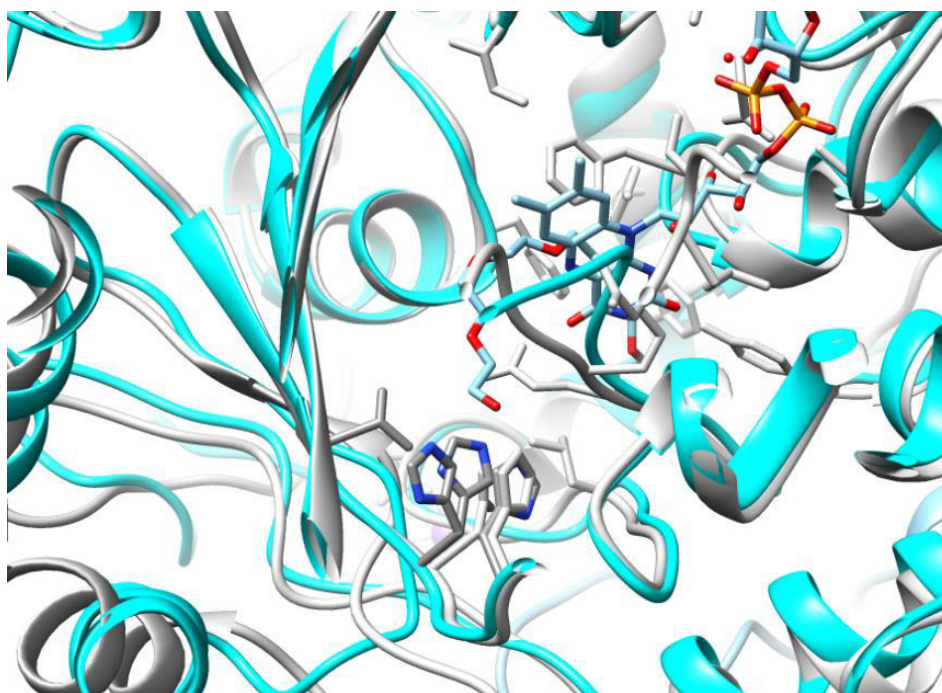


Figure 8: Structural alignment of the substrate channels of OhyRe (cyan) and OhyA (gray), with the four potential target amino acids highlighted (colored: OhyRe; gray: OhyA).

The mutations, performed in the predicted active center of OhyRe (see publication, according to a previous publication of Engleder et al. ²⁷) resulted in drastically reduced activity of the OhyRe mutants. Since it is not clear, if the catalysis of OhyRe is driven by a different mechanism, compared to OhyA, a prediction of the resulting effects for these new mutations would be very speculative. An experimental approach, to evaluate these effects, is therefore mandatory and could provide further insights on the reaction mechanism and the substrate recognition of OhyRe.

The reproduction of the mutagenesis experiments from Engleder et al. are very important to gain a better understanding of the reaction mechanism and the substrate recognition inside

the heterogenic group of OHs. In consequence of the heterogeneity within this group (variable reaction mechanisms, e.g. for OhyA and OhyRe, and substrate recognition, e.g. for OhyA and LAH), it seems to be very difficult to transfer strategies for targeted mutagenesis to the different OH families (Hfam1-11). Therefore, the generation of an extensive mutant library for the OhyRe gene, e.g. by error-prone-PCR, would be the best option to get more information about this intriguing enzyme.

At present, there are three main targets that need to be addressed by future experiments for OhyRe. Firstly, the elucidation of the exact reaction mechanism. Secondly, the identification of the substrate recognition motives, including the ability of the enzyme to hydrate a broader spectrum of (poly-) unsaturated fatty acids. Thirdly, it is essential to improve the affinity of protein scaffold to the FAD cofactor to prevent FAD loss during protein purification and work-up. These objectives can be achieved by using a tailor-made, automated screening process for each of the three targets, in order to generate improvements in terms of information and catalytic flexibility. The screening for residues involved in the catalytic reaction of OhyRe could be tested by a simple activity assay, with oleic acid as the natural substrate. The results of these assays can be compared to the activity of the wild type enzyme and detected changes in the enzymatic activity, increase or decrease, would indicate an involvement of the mutated amino acid(s) in the catalytic mechanism. A similar approach could be applied to facilitate the substrate recognition and the acceptance of different fatty acids. The substrate of interest would be applied for the activity assays and changes in the conversion ability, in comparison to the wild type OH, would show the impact of the mutated amino acid(s) on the substrate recognition or transformation efficiency of “unnatural” substrates, respectively. The detection of an increased ability for cofactor binding could also be realized in an automated process. An automated affinity chromatography, employing the fused hexa-histidine-tag in a Ni²⁺-NTA chromatography, would be applied for protein purification. Subsequently, the FAD binding could easily be monitored in the eluted fractions by detection of the UV-visible absorption spectrum measured from 300 to 600 nm ⁶⁶. Since the wild type enzyme completely loses the FAD cofactor during the purification procedure, the detection of FAD in the eluted fractions would show an increased binding ability of the enzyme to the cofactor. The monitored spectra could furthermore, in correlation to a respective calibration curve, be used to calculate the amount of active enzyme, since every active enzyme is binding only a single FAD molecule. An important point to be mentioned, regarding the screening procedures, is the fact that all three screenings would probably lead to “cross over-results”. A loss in enzymatic activity for example could be caused by the mutation of an amino acid relevant for the catalytic reaction, but also by a mutation avoiding substrate recognition, or the loss of the ability to bind FAD. Therefore, a detailed analysis of detected changes in the conversion activity of the OhyRe mutants would be essential.

Unfortunately, there was not enough time during the project to evaluate the above stated hypotheses, concerning the possible immobilization techniques and mutagenesis experiments for OhyRe. In any case, the field of OHs and especially the (to date) unique OhyRe show great potential for follow-up experiments.

5. List of Publications

Catalytic Decomposition of the Oleaginous Yeast *Cutaneotrichosporon Oleaginosus* and Subsequent Biocatalytic Conversion of Liberated Free Fatty Acids

Martina K. Braun, **Jan Lorenzen**, Mahmoud Masri, Yue Liu, Eszter Baráth, Thomas Brück, and Johannes A. Lercher

ACS Sustainable Chemistry & Engineering **2019** Feb 20 DOI:10.1021/acssuschemeng.8b04795

***Rhodococcus erythropolis* Oleate Hydratase: a New Member in the Oleate Hydratase Family Tree – Biochemical and Structural Studies**

J. Lorenzen, R. Driller, A. Waldow, F. Qoura, B. Loll, T. Brück

ChemCatChem first published **2017** Oct 03, DOI: 10.1002/cctc.201701350; Cover feature 02 / 2018.

Extraction of microalgae derived lipids with supercritical carbon dioxide in an industrial relevant pilot plant

Jan Lorenzen, Nadine Igl, Marlene Tippelt, Andrea Stege, Farah Qoura, Ulrich Sohling, Thomas Brück

Bioprocess Biosyst Eng **2017** Mar 15, DOI: 10.1007/s00449-017-1755-5

Genomics and Transcriptomics Analyses of the Oil-Accumulating Basidiomycete Yeast *Trichosporon oleaginosus*: Insights into Substrate Utilization and Alternative Evolutionary Trajectories of Fungal Mating

Kourist R, Bracharz F, **Lorenzen J**, Kracht ON, Chovatia M, Daum C, Deshpande S, Lipzen A, Nolan M, Ohm RA, Grigoriev IV, Sun S, Heitman J, Brück T, Nowrousian M. *Systems*.

MBio. **2015** Jul 21, DOI: 10.1128/mBio.00918-15

Patent: A process for the cell-free enzymatic production of 10-hydroxystearic acid (10-HSA) from bio-based oils for lubricant formulation

Jan Lorenzen & Thomas Brück

Publication number: WO 2019/063718; publication date 04.04.2019

6. Reprint Permission

1. Extraction of microalgae derived lipids with supercritical carbon dioxide in an industrial relevant pilot plant

SPRINGER NATURE

Title: Extraction of microalgae derived lipids with supercritical carbon dioxide in an industrial relevant pilot plant
Author: Jan Lorenzen, Nadine Igl, Marlene Tippelt et al
Publication: Bioprocess and Biosystems Engineering
Publisher: Springer Nature
Date: Jan 1, 2017
Copyright © 2017, The Author(s)

Creative Commons

This is an open access article distributed under the terms of the [Creative Commons CC BY](#) license, which permits unrestricted use, distribution, and reproduction in any medium, provided the original work is properly cited.

You are not required to obtain permission to reuse this article.

2. *Rhodococcus erythropolis* Oleate Hydratase: a New Member in the Oleate Hydratase Family Tree – Biochemical and Structural Studies

JOHN WILEY AND SONS LICENSE TERMS AND CONDITIONS

May 15, 2019

This Agreement between Jan Lorenzen ("You") and John Wiley and Sons ("John Wiley and Sons") consists of your license details and the terms and conditions provided by John Wiley and Sons and Copyright Clearance Center.

License Number	4590191361152
License date	May 15, 2019
Licensed Content Publisher	John Wiley and Sons
Licensed Content Publication	ChemCatChem
Licensed Content Title	Rhodococcus erythropolis Oleate Hydratase: a New Member in the Oleate Hydratase Family Tree—Biochemical and Structural Studies

Licensed Content Author	Jan Lorenzen, Ronja Driller, Ayk Waldow, et al
Licensed Content Date	Dec 4, 2017
Licensed Content Volume	10
Licensed Content Issue	2
Licensed Content Pages	8
Type of use	Dissertation/Thesis
Requestor type	Author of this Wiley article
Format	Print and electronic
Portion	Full article
Will you be translating?	No
Title of your thesis / dissertation	Enzymatic functionalization of bio based fatty acids and algae based triglycerides.
Expected completion date	Jul 2019
Expected size (number of pages)	70
Requestor Location	Jan Lorenzen Lichtenbergstraße 4 Garching, 85748 Germany Attn: Jan Lorenzen
Publisher Tax ID	EU826007151
Total	0.00 EUR
Terms and Conditions	

TERMS AND CONDITIONS

This copyrighted material is owned by or exclusively licensed to John Wiley & Sons, Inc. or one of its group companies (each a "Wiley Company") or handled on behalf of a society with which a Wiley Company has exclusive publishing rights in relation to a particular work (collectively "WILEY"). By clicking "accept" in connection with completing this licensing transaction, you agree that the following terms and conditions apply to this transaction (along with the billing and payment terms and conditions established by the Copyright Clearance Center Inc., ("CCC's Billing and Payment terms and conditions"), at the time that you opened your RightsLink account (these are available at any time at <http://myaccount.copyright.com>).

Terms and Conditions

- The materials you have requested permission to reproduce or reuse (the "Wiley Materials") are protected by copyright.
- You are hereby granted a personal, non-exclusive, non-sub licensable (on a stand-alone basis), non-transferable, worldwide, limited license to reproduce the Wiley Materials for the purpose specified in the licensing process. This license, **and any CONTENT (PDF or image file) purchased as part of your order**, is for a one-time use only and limited to any maximum distribution number specified in the license. The first instance of republication or reuse granted by this license must be completed within two years of the date of the grant of this license (although copies prepared

before the end date may be distributed thereafter). The Wiley Materials shall not be used in any other manner or for any other purpose, beyond what is granted in the license. Permission is granted subject to an appropriate acknowledgement given to the author, title of the material/book/journal and the publisher. You shall also duplicate the copyright notice that appears in the Wiley publication in your use of the Wiley Material. Permission is also granted on the understanding that nowhere in the text is a previously published source acknowledged for all or part of this Wiley Material. Any third party content is expressly excluded from this permission.

- With respect to the Wiley Materials, all rights are reserved. Except as expressly granted by the terms of the license, no part of the Wiley Materials may be copied, modified, adapted (except for minor reformatting required by the new Publication), translated, reproduced, transferred or distributed, in any form or by any means, and no derivative works may be made based on the Wiley Materials without the prior permission of the respective copyright owner. **For STM Signatory Publishers clearing permission under the terms of the STM Permissions Guidelines only, the terms of the license are extended to include subsequent editions and for editions in other languages, provided such editions are for the work as a whole in situ and does not involve the separate exploitation of the permitted figures or extracts,** You may not alter, remove or suppress in any manner any copyright, trademark or other notices displayed by the Wiley Materials. You may not license, rent, sell, loan, lease, pledge, offer as security, transfer or assign the Wiley Materials on a stand-alone basis, or any of the rights granted to you hereunder to any other person.
- The Wiley Materials and all of the intellectual property rights therein shall at all times remain the exclusive property of John Wiley & Sons Inc, the Wiley Companies, or their respective licensors, and your interest therein is only that of having possession of and the right to reproduce the Wiley Materials pursuant to Section 2 herein during the continuance of this Agreement. You agree that you own no right, title or interest in or to the Wiley Materials or any of the intellectual property rights therein. You shall have no rights hereunder other than the license as provided for above in Section 2. No right, license or interest to any trademark, trade name, service mark or other branding ("Marks") of WILEY or its licensors is granted hereunder, and you agree that you shall not assert any such right, license or interest with respect thereto
- NEITHER WILEY NOR ITS LICENSORS MAKES ANY WARRANTY OR REPRESENTATION OF ANY KIND TO YOU OR ANY THIRD PARTY, EXPRESS, IMPLIED OR STATUTORY, WITH RESPECT TO THE MATERIALS OR THE ACCURACY OF ANY INFORMATION CONTAINED IN THE MATERIALS, INCLUDING, WITHOUT LIMITATION, ANY IMPLIED WARRANTY OF MERCHANTABILITY, ACCURACY, SATISFACTORY QUALITY, FITNESS FOR A PARTICULAR PURPOSE, USABILITY, INTEGRATION OR NON-INFRINGEMENT AND ALL SUCH

WARRANTIES ARE HEREBY EXCLUDED BY WILEY AND ITS LICENSORS AND WAIVED BY YOU.

- WILEY shall have the right to terminate this Agreement immediately upon breach of this Agreement by you.
- You shall indemnify, defend and hold harmless WILEY, its Licensors and their respective directors, officers, agents and employees, from and against any actual or threatened claims, demands, causes of action or proceedings arising from any breach of this Agreement by you.
- IN NO EVENT SHALL WILEY OR ITS LICENSORS BE LIABLE TO YOU OR ANY OTHER PARTY OR ANY OTHER PERSON OR ENTITY FOR ANY SPECIAL, CONSEQUENTIAL, INCIDENTAL, INDIRECT, EXEMPLARY OR PUNITIVE DAMAGES, HOWEVER CAUSED, ARISING OUT OF OR IN CONNECTION WITH THE DOWNLOADING, PROVISIONING, VIEWING OR USE OF THE MATERIALS REGARDLESS OF THE FORM OF ACTION, WHETHER FOR BREACH OF CONTRACT, BREACH OF WARRANTY, TORT, NEGLIGENCE, INFRINGEMENT OR OTHERWISE (INCLUDING, WITHOUT LIMITATION, DAMAGES BASED ON LOSS OF PROFITS, DATA, FILES, USE, BUSINESS OPPORTUNITY OR CLAIMS OF THIRD PARTIES), AND WHETHER OR NOT THE PARTY HAS BEEN ADVISED OF THE POSSIBILITY OF SUCH DAMAGES. THIS LIMITATION SHALL APPLY NOTWITHSTANDING ANY FAILURE OF ESSENTIAL PURPOSE OF ANY LIMITED REMEDY PROVIDED HEREIN.
- Should any provision of this Agreement be held by a court of competent jurisdiction to be illegal, invalid, or unenforceable, that provision shall be deemed amended to achieve as nearly as possible the same economic effect as the original provision, and the legality, validity and enforceability of the remaining provisions of this Agreement shall not be affected or impaired thereby.
- The failure of either party to enforce any term or condition of this Agreement shall not constitute a waiver of either party's right to enforce each and every term and condition of this Agreement. No breach under this agreement shall be deemed waived or excused by either party unless such waiver or consent is in writing signed by the party granting such waiver or consent. The waiver by or consent of a party to a breach of any provision of this Agreement shall not operate or be construed as a waiver of or consent to any other or subsequent breach by such other party.
- This Agreement may not be assigned (including by operation of law or otherwise) by you without WILEY's prior written consent.
- Any fee required for this permission shall be non-refundable after thirty (30) days from receipt by the CCC.
- These terms and conditions together with CCC's Billing and Payment terms and conditions (which are incorporated herein) form the entire agreement between you and WILEY concerning this licensing transaction

and (in the absence of fraud) supersedes all prior agreements and representations of the parties, oral or written. This Agreement may not be amended except in writing signed by both parties. This Agreement shall be binding upon and inure to the benefit of the parties' successors, legal representatives, and authorized assigns.

- In the event of any conflict between your obligations established by these terms and conditions and those established by CCC's Billing and Payment terms and conditions, these terms and conditions shall prevail.
- WILEY expressly reserves all rights not specifically granted in the combination of (i) the license details provided by you and accepted in the course of this licensing transaction, (ii) these terms and conditions and (iii) CCC's Billing and Payment terms and conditions.
- This Agreement will be void if the Type of Use, Format, Circulation, or Requestor Type was misrepresented during the licensing process.
- This Agreement shall be governed by and construed in accordance with the laws of the State of New York, USA, without regards to such state's conflict of law rules. Any legal action, suit or proceeding arising out of or relating to these Terms and Conditions or the breach thereof shall be instituted in a court of competent jurisdiction in New York County in the State of New York in the United States of America and each party hereby consents and submits to the personal jurisdiction of such court, waives any objection to venue in such court and consents to service of process by registered or certified mail, return receipt requested, at the last known address of such party.

WILEY OPEN ACCESS TERMS AND CONDITIONS

Wiley Publishes Open Access Articles in fully Open Access Journals and in Subscription journals offering Online Open. Although most of the fully Open Access journals publish open access articles under the terms of the Creative Commons Attribution (CC BY) License only, the subscription journals and a few of the Open Access Journals offer a choice of Creative Commons Licenses. The license type is clearly identified on the article.

The Creative Commons Attribution License

The Creative Commons Attribution License (CC-BY) allows users to copy, distribute and transmit an article, adapt the article and make commercial use of the article. The CC-BY license permits commercial and non-

Creative Commons Attribution Non-Commercial License

The Creative Commons Attribution Non-Commercial (CC-BY-NC) License permits use, distribution and reproduction in any medium, provided the original work is properly cited and is not used for commercial purposes.(see below)

Creative Commons Attribution-Non-Commercial-NoDerivs License

The Creative Commons Attribution Non-Commercial-NoDerivs License (CC-BY-NC-ND) permits use, distribution and reproduction in any medium, provided the original work is properly cited, is not used for commercial purposes and no modifications or adaptations are made. (see below)

Use by commercial "for-profit" organizations

Use of Wiley Open Access articles for commercial, promotional, or marketing purposes requires further explicit permission from Wiley and will be subject to a fee.

Further details can be found on Wiley Online

Library <http://olabout.wiley.com/WileyCDA/Section/id-410895.html>

Other Terms and Conditions:

v1.10 Last updated September 2015

Questions? customer care@copyright.com or +1-855-239-3415 (toll free in the US) or +1-978-646-2777.



7. Figures & Tables

Figure 1: Schematic diagram of the ABV project, including the main steps of the process chain.	2
Figure 2: Pressure and temperature phase diagram of CO ₂ . K: Kelvin, p: pressure, T: temperature, sc: supercritical, l: liquid, g: gaseous, s: solid. After Nowak et al. ¹	5
Figure 3: Oleate hydratase (OH) reaction scheme.....	7
Figure 4: Sequence alignment of 14 different OHs from <i>Rhodococcus erythropulus</i> (Rre; HFam3), <i>Staphylococcus aureus</i> (Sau; HFam2), <i>Lysinibacillus fusiformis</i> (Lfu; HFam2), <i>Macrococcus caseolyticus</i> (Mca; HFam2), <i>Lactobacillus acidophilus</i> (Lac; HFam2), <i>Ochrobactrum anthropi</i> (Oan; HFam2), <i>Bifidobacterium breve</i> (Bbr; HFam2), <i>Streptococcus pyogenes</i> (Spy; HFam2), <i>Elizabethkingia meningoseptica</i> (Eme; HFam11), <i>Myroides odoratus</i> (Mod; HFam11), <i>Cellulophaga algicola</i> (Cal; HFam11), <i>Stenotrophomonas maltophilia</i> (Sma; HFam2), <i>Corynebacterium kroppenstedtii</i> (Ckr; HFam10) and <i>Chryseobacterium gleum</i> (Cgl; HFam11). The seven crucial amino acids, identified by Engleder at al. are highlighted with boxes. The two differing positions are highlighted with red boxes.....	10
Figure 5: Schematic diagram of the employed extraction pilot plant.	13
Figure 6: GC-chromatograms of the marine oil standard FAMES (A) and a microalgae extract from <i>S. obtusiusculus</i> (B), the corresponding retention times (RT) and fatty acids for the standard are found in Table 1.....	15
Figure 7: GC-MS chromatograms documenting the conversion of oleic acid (OA) to 10-hydroxystearic acid (10-HSA) after 90 min reaction time. A) negative control without oleate hydratase and B) sample after reaction with oleate hydratase.....	17
Figure 8: Structural alignment of the substrate channels of OhyRe (cyan) and OhyA (gray), with the four potential target amino acids highlighted (colored: OhyRe; gray: OhyA).	62
Table 1: Fatty acids included in the marine oil mix with the corresponding retention times (RT), corresponding to Figure 6.....	16
Table 2: Utilized <i>E. coli</i> strains with respective genotypes.	18

8. Literature

- 1 Nowak, S. & Winter, M. The Role of Sub- and Supercritical CO₂ as "Processing Solvent" for the Recycling and Sample Preparation of Lithium Ion Battery Electrolytes. *Molecules* **22**, doi:10.3390/molecules22030403 (2017).
- 2 Lee, Y. Commercial production of microalgae in the Asia-Pacific rim. *Journal of Applied Phycology* **9**, 403-411 (1997).
- 3 Bleakley, S. & Hayes, M. Algal Proteins: Extraction, Application, and Challenges Concerning Production. *Foods* **6**, doi:10.3390/foods6050033 (2017).
- 4 Henriquez, V., Escobar, C., Galarza, J. & Gimpel, J. Carotenoids in Microalgae. *Subcell Biochem* **79**, 219-237, doi:10.1007/978-3-319-39126-7_8 (2016).
- 5 Zhang, D. *et al.* Dynamic modelling of *Haematococcus pluvialis* photoinduction for astaxanthin production in both attached and suspended photobioreactors. *Algal Research* **13**, 69-78, doi:10.1016/j.algal.2015.11.019 (2016).
- 6 Harun, R., Danquah, M. K. & Forde, G. M. Microalgal biomass as a fermentation feedstock for bioethanol production. *Journal of Chemical Technology & Biotechnology*, n/a-n/a, doi:10.1002/jctb.2287 (2009).
- 7 Khozin-Goldberg, I., Leu, S. & Boussiba, S. in *Lipids in Plant and Algae Development* (eds Yuki Nakamura & Yonghua Li-Beisson) 471-510 (Springer International Publishing, 2016).
- 8 Bligh, E. G. & Dyer, W. J. A rapid method of total lipid extraction and purification. *Canadian journal of Biochemistry and Physiology* **37**, 911-917 (1959).
- 9 Kapoore, R. V., Butler, T. O., Pandhal, J. & Vaidyanathan, S. Microwave-Assisted Extraction for Microalgae: From Biofuels to Biorefinery. *Biology (Basel)* **7**, doi:10.3390/biology7010018 (2018).
- 10 Chen, L., Li, R., Ren, X. & Liu, T. Improved aqueous extraction of microalgal lipid by combined enzymatic and thermal lysis from wet biomass of *Nannochloropsis oceanica*. *Bioresour Technol* **214**, 138-143, doi:10.1016/j.biortech.2016.04.031 (2016).
- 11 Yoo, G., Park, W. K., Kim, C. W., Choi, Y. E. & Yang, J. W. Direct lipid extraction from wet *Chlamydomonas reinhardtii* biomass using osmotic shock. *Bioresour Technol* **123**, 717-722, doi:10.1016/j.biortech.2012.07.102 (2012).
- 12 Heald, S. C., Brandao, P. F. B., Hardicre, R. & Bull, A. T. Physiology, biochemistry and taxonomy of deep-sea nitrile metabolising *Rhodococcus* strains. *Antonie van Leeuwenhoek* **80**, doi:10.1023/A:1012227302373 (2001).
- 13 Langdhal, B. R., Bisp, P. & Ingvorsen, K. Nitrile hydrolysis by *Rhodococcus erythropolis* BL1, an acetonitrile-tolerant strain isolated from a marine sediment. *Microbiology* **142**, doi:10.1099/13500872-142-1-145 (1996).
- 14 Whyte, L. G. *et al.* Prevalence of alkane monooxygenase genes in Arctic and Antarctic hydrocarbon-contaminated and pristine soils. *FEMS Microbiology Ecology* **41**, 141-150 (2002).
- 15 Margesin, R., Labbe, D., Schinner, F., Greer, C. W. & Whyte, L. G. Characterization of Hydrocarbon-Degrading Microbial Populations in Contaminated and Pristine Alpine Soils. *Applied and Environmental Microbiology* **69**, 3085-3092, doi:10.1128/aem.69.6.3085-3092.2003 (2003).
- 16 Strnad, H. *et al.* Genome Sequence of *Rhodococcus erythropolis* Strain CCM2595, a Phenol Derivative-Degrading Bacterium. *Genome Announc* **2**, doi:10.1128/genomeA.00208-14 (2014).
- 17 Werf, M. J. v. d., Swarts, H. J. & Bont, J. A. M. d. *Rhodococcus erythropolis* DCL14 Contains a Novel Degradation Pathway for Limonene. *Appl Environ Microbiol* **65**, 2092-2102 (1999).
- 18 Gröger, H. *et al.* Preparative asymmetric reduction of ketones in a biphasic medium with an (S)-alcohol dehydrogenase under *in situ*-cofactor-recycling with a formate dehydrogenase. *Tetrahedron* **60**, 633-640, doi:10.1016/j.tet.2003.11.066 (2004).

- 19 Geize, R. v. d., Hessels, G. I., Gerwen, R. v. d., Meijden, R. v. d. & Dijkhuizen, L. Molecular and functional characterization of kshA and kshB, encoding two components of 3-ketosteroid 9 α -hydroxylase, a class IA monooxygenase, in *Rhodococcus erythropolis* strain SQ1. *Mol Microbiol* **45**, 1007– 1018 (2002).
- 20 Vlugt-Bergmans, C. J. v. d. & Werf, M. J. v. d. Genetic and biochemical characterization of a novel monoterpene epsilon-lactone hydrolase from *Rhodococcus erythropolis* DCL14. *Appl Environ Microbiol* **67**, 733-741, doi:10.1128/AEM.67.2.733-741.2001 (2001).
- 21 Ohshiro, T., Kojima, T., Torii, K., Kawasoe, H. & Izumi, Y. Purification and Characterization of Dibenzothiophene (DBT) Sulfone Monooxygenase, an Enzyme Involved in DBT Desulfurization, from *Rhodococcus erythropolis* D-1. *J Biosci Bioeng* **88**, 610–616 (1999).
- 22 Wallen, L. L., Benedict, R. G. & Jackson, R. W. The microbiological production of 10-hydroxystearic acid from oleic acid. *Archives of Biochemistry and Biophysics* **99**, 205-357 (1962).
- 23 Niehaus, W. G., Jr. and G. J. Schroepfer, Jr. The reversible hydration of oleic acid to 10D-hydroxystearic acid. *Biochem. Biophys. Res. Commun.* **21**, 271-275 (1965).
- 24 Kusic, A., Miura, Y. & Schroepfer, G. J., Jr. Oleate hydratase: studies of substrate specificity. *Lipids* **6**, 541-545, doi:10.1007/bf02531133 (1971).
- 25 Bevers, L. E., Pinkse, M. W., Verhaert, P. D. & Hagen, W. R. Oleate hydratase catalyzes the hydration of a nonactivated carbon-carbon bond. *J Bacteriol* **191**, 5010-5012, doi:10.1128/JB.00306-09 (2009).
- 26 Volkov, A. *et al.* Crystal structure analysis of a fatty acid double-bond hydratase from *Lactobacillus acidophilus*. *Acta Crystallogr D Biol Crystallogr* **69**, 648-657, doi:10.1107/S0907444913000991 (2013).
- 27 Engleder, M. *et al.* Structure-Based Mechanism of Oleate Hydratase from *Elizabethkingia meningoseptica*. *Chembiochem* **16**, 1730-1734, doi:10.1002/cbic.201500269 (2015).
- 28 Park, A. K. *et al.* Crystal structure of oleate hydratase from *Stenotrophomonas* sp. KCTC 12332 reveals conformational plasticity surrounding the FAD binding site. *Biochem Biophys Res Commun* **499**, 772-776, doi:10.1016/j.bbrc.2018.03.220 (2018).
- 29 Elliger, C. A., Guadagni, D. G. & Dunlap, C. E. Thickening Action of Hydroxystearates in Peanut Butter. *Journal of the American Oil Chemists Society* **49**, 536-537 (1972).
- 30 Wache, Y. *et al.* Role of beta-oxidation enzymes in gamma-decalactone production by the yeast *Yarrowia lipolytica*. *Appl Environ Microbiol* **67**, 5700-5704, doi:10.1128/AEM.67.12.5700-5704.2001 (2001).
- 31 Perneti, M., van Malssen, K. F., Flöter, E. & Bot, A. Structuring of edible oils by alternatives to crystalline fat. *Current Opinion in Colloid & Interface Science* **12**, 221-231, doi:10.1016/j.cocis.2007.07.002 (2007).
- 32 Rogers, M. A., Wright, A. J. & Marangoni, A. G. Crystalline stability of self-assembled fibrillar networks of 12-hydroxystearic acid in edible oils. *Food Research International* **41**, 1026-1034, doi:10.1016/j.foodres.2008.07.012 (2008).
- 33 Tantishaiyakul, V. *et al.* A Supramolecular Gel Based on 12-Hydroxystearic Acid/Virgin Coconut Oil for Injectable Drug Delivery. *European Journal of Lipid Science and Technology* **120**, doi:10.1002/ejlt.201800178 (2018).
- 34 Malamet, G., Peltzer, B., Schnell, H. & Niehaus, C. CROSSLINKABLE LACQUER RESINS. US3,541,055 (1970).
- 35 Andrew, M. A. & Backhouse, A. J. SPRAY COATING OF ACRYLIC RESIN COMPRISING POLYMERIC MICROPARTICLES. US4,242,384 (1980).
- 36 Hamaguchi, T. & Mori, A. PLASTICIZER FOR BIODEGRADABLE RESIN. US20060276575A1 (2006).
- 37 Luo, D. *et al.* TRANSFER RESISTANT COSMETIC. US7261877B2 (2007).
- 38 Kobayashi, M., Zavadoski, W., Kalriess, W., Smith, I. & Kishida, S. PIGMENTS AND EXTENDER PIGMENTS WITH ENHANCED SKIN ADHESION FOR COSMETIC PREPARATIONS. USA patent US 6,887,494 B2 (2005).

- 39 Griffiths, M. J., van Hille, R. P. & Harrison, S. T. Selection of direct transesterification as the preferred method for assay of fatty acid content of microalgae. *Lipids* **45**, 1053-1060, doi:10.1007/s11745-010-3468-2 (2010).
- 40 Volkov, A. *et al.* Myosin cross-reactive antigen of *Streptococcus pyogenes* M49 encodes a fatty acid double bond hydratase that plays a role in oleic acid detoxification and bacterial virulence. *J Biol Chem* **285**, 10353-10361, doi:10.1074/jbc.M109.081851 (2010).
- 41 Mendes, R. L., Nobre, B. P., Cardoso, M. T., Pereira, A. P. & Palavra, A. F. Supercritical carbon dioxide extraction of compounds with pharmaceutical importance from microalgae. *Inorganica Chimica Acta* **356**, 328-334, doi:10.1016/s0020-1693(03)00363-3 (2003).
- 42 Yen, H. W., Yang, S. C., Chen, C. H., Jescica & Chang, J. S. Supercritical fluid extraction of valuable compounds from microalgal biomass. *Bioresour Technol* **184**, 291-296, doi:10.1016/j.biortech.2014.10.030 (2015).
- 43 Santana, A., Jesus, S., Larrayoz, M. A. & Filho, R. M. Supercritical Carbon Dioxide Extraction of Algal Lipids for the Biodiesel Production. *Procedia Engineering* **42**, 1755-1761, doi:10.1016/j.proeng.2012.07.569 (2012).
- 44 Bulley, N. R., Fattori, M., Meisen, A. & Moyls, L. Supercritical fluid extraction of vegetable oil seeds. *Journal of the American Oil Chemists' Society* **61**, 1362-1365 (1984).
- 45 Peker, H., Srinivasan, M. P., Smith, J. M. & McCoy, B. J. Caffeine Extraction Rates from Coffee Beans with Supercritical Carbon Dioxide. *AIChE Journal* **38** (1992).
- 46 Choi, K. J., Nakhost, Z., Krukoni, V. J. & Karel, M. Supercritical fluid extraction and characterization of lipids from algae *Scenedesmus obliquus*. *Food Biotechnol* **1**, 263-281, doi:10.1080/08905438709549669 (1987).
- 47 Mendes, R. L. *et al.* Supercritical CO₂ extraction of carotenoids and other lipids from *Chlorella vulgaris*. *Food Chemistry* **53**, 99-103 (1995).
- 48 Apel, A. C. *et al.* Open thin-layer cascade reactors for saline microalgae production evaluated in a physically simulated Mediterranean summer climate. *Algal Research* **25**, 381-390, doi:10.1016/j.algal.2017.06.004 (2017).
- 49 Crampon, C., Mouahid, A., Toudji, S.-A. A., Lépine, O. & Badens, E. Influence of pretreatment on supercritical CO₂ extraction from *Nannochloropsis oculata*. *The Journal of Supercritical Fluids* **79**, 337-344, doi:10.1016/j.supflu.2012.12.022 (2013).
- 50 González-Fernández, C., Sialve, B., Bernet, N. & Steyer, J.-P. Impact of microalgae characteristics on their conversion to biofuel. Part II: Focus on biomethane production. *Biofuels, Bioproducts and Biorefining* **6**, 205-218, doi:10.1002/bbb.337 (2012).
- 51 Beacham, T. A., Bradley, C., White, D. A., Bond, P. & Ali, S. T. Lipid productivity and cell wall ultrastructure of six strains of *Nannochloropsis*: Implications for biofuel production and downstream processing. *Algal Research* **6**, 64-69, doi:10.1016/j.algal.2014.09.003 (2014).
- 52 Brown, M. R. The amino acid and sugar composition of 16 species of microalgae used in mariculture. *J. Exp. Mar. Biol. Ecol.* **145**, 79-99 (1991).
- 53 Lee, S. Y., Cho, J. M., Chang, Y. K. & Oh, Y. K. Cell disruption and lipid extraction for microalgal biorefineries: A review. *Bioresour Technol* **244**, 1317-1328, doi:10.1016/j.biortech.2017.06.038 (2017).
- 54 Al Hattab, M. & Ghaly, A. Microalgae Oil Extraction Pre-treatment Methods: Critical Review and Comparative Analysis. *J Fundam Renewable Energy Appl* **5**, doi:10.4172/20904541.1000172 (2015).
- 55 Lorente, E., Farriol, X. & Salvadó, J. Steam explosion as a fractionation step in biofuel production from microalgae. *Fuel Processing Technology* **131**, 93-98, doi:10.1016/j.fuproc.2014.11.009 (2015).
- 56 Mubarak, M., Shaija, A. & Suchithra, T. V. A review on the extraction of lipid from microalgae for biodiesel production. *Algal Research* **7**, 117-123, doi:10.1016/j.algal.2014.10.008 (2015).

- 57 Byrne, F. P. *et al.* Tools and techniques for solvent selection: green solvent selection guides. *Sustainable Chemical Processes* **4**, doi:10.1186/s40508-016-0051-z (2016).
- 58 Jeevan Kumar, S. P., Vijay Kumar, G., Dash, A., Scholz, P. & Banerjee, R. Sustainable green solvents and techniques for lipid extraction from microalgae: A review. *Algal Research* **21**, 138-147, doi:10.1016/j.algal.2016.11.014 (2017).
- 59 Patel, V. R., Dumancas, G. G., Kasi Viswanath, L. C., Maples, R. & Subong, B. J. Castor Oil: Properties, Uses, and Optimization of Processing Parameters in Commercial Production. *Lipid Insights* **9**, 1-12, doi:10.4137/LPI.S40233 (2016).
- 60 Alwaseem, H., Donahue, C. J. & Marincean, S. Catalytic Transfer Hydrogenation of Castor Oil. *Journal of Chemical Education* **91**, 575-578, doi:10.1021/ed300476u (2014).
- 61 Severino, L. S. *et al.* A Review on the Challenges for Increased Production of Castor. *Agronomy Journal* **104**, doi:10.2134/agronj2011.0210 (2012).
- 62 Viso, A.-C. & Marty, J.-C. FATTY ACIDS FROM 28 MARINE MICROALGAE. *Phytochemistry* **34**, 1521-1533 (1993).
- 63 Görner, C. *et al.* Genetic engineering and production of modified fatty acids by the non-conventional oleaginous yeast *Trichosporon oleaginosus* ATCC 20509. *Green Chem.* **18**, 2037-2046, doi:10.1039/c5gc01767j (2016).
- 64 Todea, A. *et al.* Increase of stability of oleate hydratase by appropriate immobilization technique and conditions. *Journal of Molecular Catalysis B: Enzymatic* **119**, 40-47, doi:10.1016/j.molcatb.2015.05.012 (2015).
- 65 Engleder, M. *et al.* Evolving the Promiscuity of *Elizabethkingia meningoseptica* Oleate Hydratase for the Regio- and Stereoselective Hydration of Oleic Acid Derivatives. *Angew Chem Int Ed Engl*, doi:10.1002/anie.201901462 (2019).
- 66 Joo, Y. C. *et al.* Biochemical characterization and FAD-binding analysis of oleate hydratase from *Macrococcus caseolyticus*. *Biochimie* **94**, 907-915, doi:10.1016/j.biochi.2011.12.011 (2012).